Spatiotemporal Characterization of Stochastic Bacterial Growth in Biofilm Environment

Sung-Ho Paek

Dissertation submitted to the faculty of the Virginia Polytechnic Institute and State University in partial fulfillment of the requirements for the degree of

Doctor of Philosophy
In
Biological Systems Engineering

Warren C. Ruder, Chair
Yi-Heng Percival Zhang
Justin Barone
Pablo Sobrado

April 25th 2017
Blacksburg, Virginia

Keywords: synthetic biology, biofilms, stochastic gene expression, stochastic phenotypic expression, microfluidics, quorum sensing, genetic toggle switch, droplet-microfluidics, biomimetic

Spatiotemporal Characterization of
Stochastic Bacterial Growth in Biofilm Environment

Sung-Ho Paek

ACADEMIC ABSTRACT

Research on bacteria in their biofilm form is limited by the ability to artificially culture bacterial biofilms in a system that permits the visualization of individual cells. The experiments comprising this thesis research are on-going investigations of bacterial culture systems engineered to provide an environment that mimics biofilms while enabling real-time microscopy. Specifically, the microfluidic systems developed and assessed as part of this thesis permit the visualization of individual bacteria cells within consortia growing within a narrow space provided by a microfluidic device. This research demonstrates the versatility of these microfluidic systems across potentially high-throughput microbiological experiments utilizing genetically engineered *Escherichia coli*.

Before demonstrating the efficacy of these systems, the development of the field of synthetic biology over the past half century is reviewed, focusing on synthetic genetic circuits and their applications (Chapter 2). The first and main microfluidic device explored in this research was developed to mimic the nutrient-deficient conditions within biofilms by forcing media to enter the culture area through a narrow, torturous channel. The microfluidic channel was thin enough (0.97 μm) to prevent the motility of 1-μm-wide *E. coli* cells, enabling visualization of individual cells. The bacteria cultured in the device contained either a simple P_{lux}-driven quorum sensing receiver (Chapters 3 and 5) or a LacI- and TetR-driven genetic toggle switch (Chapter 4). Under the culture conditions, the quorum sensing reporter signal was detected even without addition of the signaling molecule (Chapter 3). The genetic toggle switch was stable when the system began in the high-LacI expression state, but after 5 days of culture, >5% of high-TetR expression cells began to consistently express the high-LacI state (Chapter 4). This system was also employed to track lineages of cells using real-time microscopy, which successfully characterized the inheritance of aberrant, enlarged cell phenotypes under stress (Chapter 5).

Another microfluidic device, a droplet bioreactor, was also developed to culture small numbers of cells in an aqueous bubble suspended in oil (Chapter 6). Quorum sensing receiver cells were cultured in this device, demonstrating that it is well suited for testing the effects of compounds on biofilms within water-in-oil droplets.

Spatiotemporal Characterization of
Stochastic Bacterial Growth in Biofilm Environment

Sung-Ho Paek

GENERAL AUDIENCE ABSTRACT

Bacteria are the most abundant organisms globally, yet relatively little is understood about the basic biology of biofilms, one of the most common natural states of bacteria. Biofilms are ubiquitous consortia of individual microbial cells that send and received chemical signals from one another to carry out group behaviors such as quorum sensing. The impacts of biofilms range from the contamination of food processing equipment to antibiotic resistant bacterial infections. The vast majority of microbiological research has been conducted on bacteria in their planktonic state as individual cells cultured in a liquid medium. This form of culture does not permit the types of research that can help address the impacts of biofilms on human health and economic activities, never mind examine the biological mechanism of random gene and morphological expression within bacterial biofilm.

This thesis presents research utilizing two microfluidic devices that will enable further large-scale studies to unravel the mechanisms that create biofilms as well as permit high-throughput testing of chemical compounds to control the growth and development of biofilms. Moreover, these devices permit the use of real-time microscopy to track cells and their growth over time. The first microfluidic device utilized in this research mimics the nutrient-limiting conditions of biofilms. This biofilm-mimicking device was used to culture a common research bacteria, *Escherichia coli*, with one of two engineered genetic circuits (reviewed in Chapter 2): a quorum sensing receiver (Chapters 3 and 5) or genetic toggle switch (Chapter 4). Both of these genetic circuits demonstrated stochasticity in their gene expression states under the culture conditions in the biofilm-mimicking device. The second microfluidic device successfully permitted the culture of small numbers of isolated cells within a small bubble of bacterial media suspended in oil (Chapter 6). Additionally, this device enabled the addition of chemical compounds to influence the growth and metabolism of the trapped cells. Collectively, these microfluidic devices provide the ability to effectively study both the mechanisms underlying

random gene expression within biofilms as well as explore the chemical factors that can be used to control and mitigate biofilm formation and growth.

ACKNOWLEDGEMENTS

The authors gratefully acknowledge support from Virginia Tech Institute for Critical Technology and Applied Science's Graduate Research Scholarship Program. The authors additionally acknowledge support from award FA9550-13-1-0108 from the Air Force Office of Scientific Research of the USA and also awards N00014-17-12306 and N00014-15-1-2502 (to W.C.R.) from the Office of Naval Research of the USA.

TABLE OF CONTENTS

LIST OF FIGURES AND TABLES

LIST OF ABBREVIATIONS

autoinducer 1 (CAI-1)

autoinducer 2 (AI-2)

anhydrotetracycline (aTc)

carbenicillin (Cb)

cholera toxin (CT)

differential interference contrast (DIC)

Escherichia coli (*E. coli*)

extracellular polymeric substances (EPS)

green fluorescence protein (GFP)

invasin (inv)

isopropyl ß-D-1-thiogalactopyranoside (IPTG)

listeriolysin (LLO)

Luria–Bertani (LB)

mitogen activated protein kinase (MAPK)

N-acyl homoserine lactone (AHL)

phosphate-buffered saline (PBS)

polydimethylsiloxane (PDMS)

secreted alkaline phosphatase (SEAP)

short hairpin RNA (shRNA)

CHAPTER 1

INTRODUCTION

1.1. Organization of the Thesis

This doctoral thesis comprises seven chapters, consisting of one review chapter and four specific research results, each of which was published, submitted to a journal, or has been prepared for submission.

The overall organization of this thesis is presented in Figure 1.1. The main structure for this investigation of bacterial biofilm characterization systems can be divided into two parts: (1) application of a biofilm-mimicking microfluidic channel as an approach utilizing a well-defined component to characterize the behavior of complex microbial populations (Chapters 3 to 5) and (2) application of a water-in-oil droplet bioreactor for a multiplexed biofilm assay, as a useful approach for saving time and labor in, for example, chemical screening (Chapters 6). These bioengineering studies utilized synthetic biology-based signal transduction technology (e.g., gene circuits; see an overview in Chapter 2). These tools were used to translate individual cellular responses to a local environmental change to visible, quantifiable signals (e.g., fluorescence). The signals indicated the current biochemical and physiological statuses of the bacterial cells grown within the bioreactor, which enabled the evaluation and optimization of the microfluidic system.

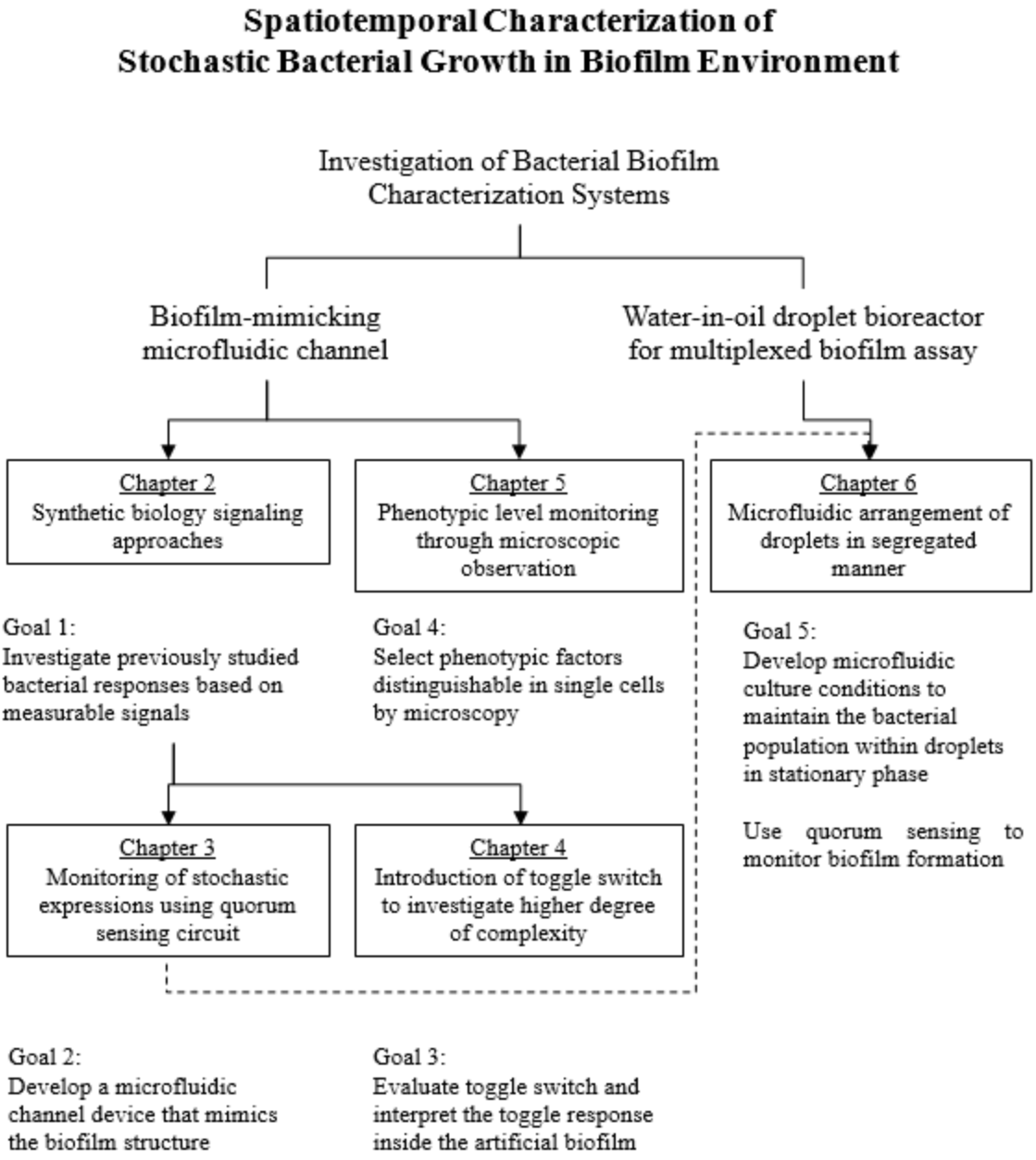

Figure 1.1. Organizational chart summarizing the thesis structure.

1.2. Objective and Significance

Studies in this thesis are part of on-going investigations for the engineering of bacterial culture systems that provide conditions similar to natural environments suitable for biofilm formation, thus enabling the characterization of a bacterial consortium under defined conditions. The main research objective is to investigate microfluidic channel devices that simplify the complexity of biofilm developmental and stress response processes in combination with synthetic biology signaling techniques for manipulating and observing cell signaling. We expect that the application of these systems will further our understanding of the protective mechanisms within biofilms against chemical substances, such as antibiotics. We hope to contribute to the eventual identification of new methods for targeting biofilm colonies and, furthermore, for the disruption of their functions.

Many challenges related to biofilms remain, e.g., the pervasive effects on human health, water quality, corrosion, power generation efficiency, deterioration of dental surfaces, and contamination in the food processing industry [1-4], owing to a lack of information pertaining to the hundreds of genes that are differentially expressed during biofilm development, including stress-associated genes [5]. It is well known that gene expression differs between biofilm bacteria and planktonic bacteria [6]. These differences in gene expression have several implications. One example is related to the development of antibiotics [7]. These drugs have traditionally been developed to kill planktonic bacteria. We now know that planktonic bacteria are more susceptible to antimicrobial agents than biofilm bacteria. Traditional antibiotics target bacterial cells in a relatively unprotected state [8]. Moving forward, it will be necessary to develop new classes of antibiotics that target bacteria within the biofilm structure.

Figure 1.2 illustrates some of the hypothesized mechanisms of biofilm protection against antimicrobial agents. First, as shown in panel a, free-floating cells utilize nutrients in the surrounding environment, but lack sufficient metabolic activity to utilize all substrates in their vicinity. In contrast, the collective metabolic activity of cells in a biofilm leads to concentration gradients in the chemical substrate as well as localized chemical microenvironments. As a result, reduced metabolic activity may result in a lower susceptibility to antimicrobials. Second, as

depicted in panel b, free-floating cells harbor genes involved in many protective stress responses. Planktonic cells, however, are overwhelmed by strong antimicrobial challenges and die before stress responses can be activated. In contrast, stress responses are effectively implemented in some cells within a biofilm at the expense of other cells. Last, as shown in panel c, free-floating cells generate protected persister cells. However, under abundant growth conditions in planktonic cultures, persisters rapidly revert to a susceptible state. In contrast, persister cells accumulate in biofilms because they revert less readily and are physically retained within the biofilm matrix [9].

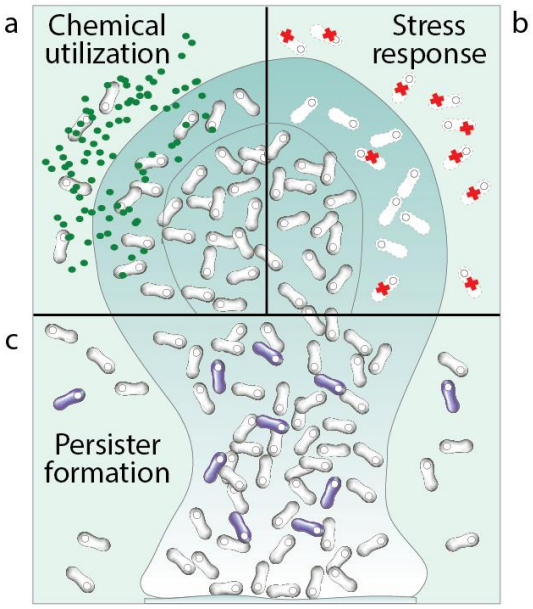

Figure 1.2. Biofilm behavioral mechanisms that exert protective effects: (a) chemical utilization; green dots represent chemicals, such as antibiotics, in the vicinity of the biofilm. (b) stress response; planktonic cells are overwhelmed by antimicrobial challenges and die before activating stress responses, and (c) persister cells are physically retained within the biofilm structure.

To better understand the nuances of biofilm protective effects, we proposed to utilize recombinant gene circuits, i.e., a quorum sensing circuit and a toggle switch, as synthetic biology tools to translate microbial responses to physically measurable signals. We intend to simplify the complexity of the biofilm developmental and stress response processes by utilizing well-characterized components and further deploying cells within the biomimetic biofilm channel.

We describe our hypotheses and specific aims, including possible approaches, in the next section. Furthermore, experimental designs for microfluidic systems and synthetic biological methodologies used in this study are presented.

1.3. Specific Goals

Despite the pervasive effects of biofilms in various fields, including human health, research is limited by a lack of information on the complex gene networks associated with biofilm formation and the individual responses of single cells to local environmental changes. To simplify the complexity of biofilm-associated processes and response mechanisms, in this thesis, we developed sophisticated engineered microfluidic devices mimicking or carrying biofilm structures and cultivated cells within the devices to analyze the microbial community. We further propose to utilize recombinant gene circuits as synthetic biology tools for the translation of microbial responses to local environmental changes to quantifiable signals. This integrative approach combining synthetic biological tools with microfluidic channel technology may facilitate progress in various areas of biofilm research, for example, the nuances of the biofilm protective effect.

As described in Figure 1.1, we have investigated novel approaches with (1) a biomimetic system that can provide information on unique biofilm characteristics, such as resistance to chemicals, and (2) a micro-droplet bioreactor suitable for multiplexed biofilm assays, unlike conventional methods. We proposed and eventually obtained empirical support for the following three hypotheses.

HYPOTHESIS 1:

The microfluidic device designed to allow a mass transport gradient from the main flow channel to the inner regions of the channel can provide an environment for bacterial cell growth that mimics natural biofilms.

HYPOTHESIS 2:

If the first hypothesis is true, cells residing in remote areas of the channel device will show a heterogeneous stress response which will be observable at the single-cell level.

HYPOTHESIS 3:

A segregated water-in-oil droplet used for the cultivation of bacterial cells in the aqueous core can be maintained to form a biofilm at the liquid–liquid interface.

We have established specific goals corresponding to the overall objective to obtain experimental support for the proposed hypotheses as follows (refer to Figure 1.1):

1. Investigate indicators of bacterial responses that can be translated to measurable signals through a literature survey; develop signal transduction technologies and design gene circuits (e.g., a quorum sensing circuit and toggle switch) that produce fluorescence as an indicator of bacterial responses to environmental changes.

2. Design and construct a microfluidic channel device mimicking a biofilm structure, which results in nutrient shortage within the deeper regions of the channel, and monitor the growth status of bacterial cells within the device using a synthetic gene circuit.

3. Introduce a toggle switch to test a higher degree of complexity by the evaluation of gene induction and repression and analyses of the toggle response to stochastic environments within the artificial biofilm.

4. Select a phenotypic factor that is distinguishable in single cells using a microscope; specifically, introduce an elastic bacteria (e.g., *Escherichia coli,* [*E. coli*]) in the culture and selectively capture cells with morphological changes (e.g., swollen cells) at predetermined sites in the device.

5. Develop a microfluidic device for micro-droplet formation, droplet segregation and the maintenance of cells in stationary phase for long-term monitoring utilizing quorum sensing signaling.

1.4. Experimental Design

The experimental design used to test the three hypotheses is summarized in Figure 1.3. As mentioned above, we have developed two different systems that can be used to characterize biofilm microbial populations: a biomimetic microchannel and micro-droplet bioreactor. The biomimetic system is a simplified, artificial version of biofilm structures comprising complex extracellular polymeric substances. It was constructed using microfluidic technology to show a mass transport gradient for nutrient supply from the main flow to peripheral regions. The droplet bioreactor uses a water-in-oil configuration and bacterial cells are cultured in the aqueous core, providing a high potential for biofilm formation at the hydrophobic interface.

We have tested the first two hypotheses using the artificial biofilm, and the droplet bioreactor was required to test the third hypothesis. We selected the following procedure for the design and execution of the experiments to investigate the systems: (1) introduce two gene circuits, a quorum sensing circuit and toggle switch as stress indicators separately into the bacterial genome, (2) validate the performance of the biomimetic microfluidic device by culturing the recombinant cells within the device (hypothesis 1), (3) obtain additional stochastic information for biofilm characterization, such as morphological changes, at the single-cell level (hypothesis 2), and (4) develop a water-in-oil droplet bioreactor and culture the encapsulated cells in stationary phase for biofilm formation (hypothesis 3).

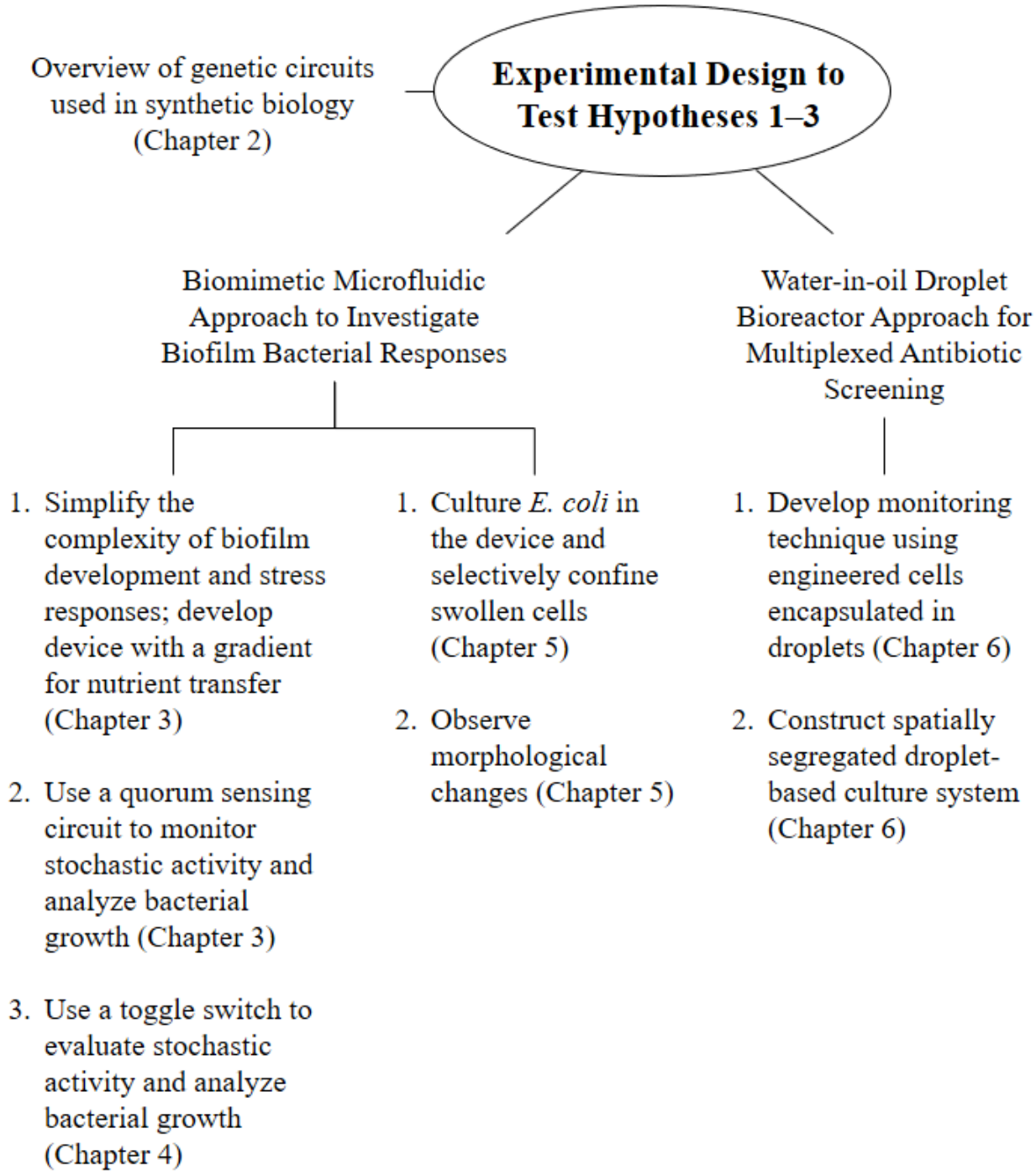

Figure 1.3. Experimental design for tests of the three hypotheses.

1.4.1. Biomimetic Microfluidic-channel Approach

The biomimetic microfluidic strategy using a nutrient transport-limiting model mimicking the biofilm structure is described in Figure 1.4. An *E. coli* strain will be engineered to contain recombinant gene circuits producing signals in response to a local environmental change (Figure 1.4, top) and further seeded into the biomimetic biofilm channel (Figure 1.4, middle). We will characterize the circuit upon stress induction, such as nutrient shortage and/or space scarcity, to observe adaptive responses within the biofilm community (Figure 1.4, bottom).

Engineering of an artificial biofilm. The biofilm structure consisting of different extracellular polymeric matrices is extremely complex and difficult to control, limiting the ability to obtain reproducible responses from the microbial community to environmental changes (refer to Chapter 3 for details). Therefore, the use of an engineered biomimetic system is highly valuable for the simplification of conditions to investigate the mechanism underlying, for example, the biofilm protective effect. We here designed an artificial biofilm model in a geometry that offers a medium gradient that determines the nutrient transfer rate from the main flow channel to peripheral tortuous locations (Figure 1.4, middle). Furthermore, such well-characterized components enable us to analyze biofilm developmental and stress response processes by integrating the system with recombinant cells, which are able to generate signals, from synthetic biology (see the next subsection).

To this end, we designed and constructed a microfluidic channel device mimicking biofilms (Goal 2) by (a) simplifying the complexity of the biofilm structure, (b) manufacturing a microfluidic device in a geometry offering medium transfer gradient, and (c) analyzing the growth status of bacterial cells within the device by monitoring signals emitted from gene circuits (see below; Chapter 3).

Bacterial response via gene circuits. The responses of *E. coli* cells grown within the microfluidic device can be quantified using synthetic gene networks that express green fluorescent protein in the presence of an inducer, e.g., the quorum signal. This technology is capable of promoting the growth of cells that stochastically expresses the quorum sensing reporter gene,

without the addition of inducer. Thus, this engineered gene construct used in our biomimetic biofilm device allows us to study gene expression dynamics for quorum sensing (Chapters 3 and 6).

We first investigated a quorum sensing indicator to translate bacterial responses to measurable signals (Goal 1) through (a) a literature survey of signal transduction technologies and (b) the design of gene circuits producing fluorescence as an indicator of bacterial responses to environmental change (Chapter 3). The introduction of a toggle switch was then examined to test a higher degree of complexity in the biofilm (Goal 3) by (a) evaluating the toggle with respect to gene induction and repression, (b) deploying recombinant cells in the biomimetic system, and (c) interpreting the toggle response with respect to stochastic activity (Chapter 4).

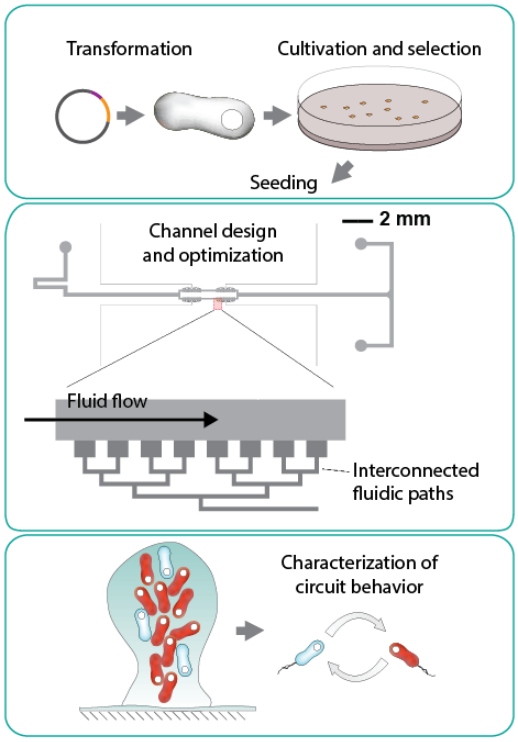

Figure 1.4. Summary of the biomimetic microfluidic channel approach.

Heterogeneous stochastic activity. An elastic bacteria (e.g., *E. coli*) cultivated in the biofilm-mimicking microfluidic device may provide insights into single-cell growth and division

under stochastic growth conditions. We monitored cellular behavior based on morphological changes of bacterial cells by microscopy to minimize the intrinsic noise in biological processes. Genetic variability of single cells may result in cell size expansion as an indicator of clonal adaptation to a stressful environment.

We selected a phenotypic factor distinguishable in single cells using a microscope (Goal 4) by the following procedure: (a) introducing an elastic bacteria (e.g., *E. coli*) to the culture, (b) cultivating the cells in the microfluidic device, selectively confining swollen cells, (c) microscopically observing target cells with respect to growth and division, and (d) determining whether the observed morphologic changes reflect epigenetic mechanisms (Chapter 5).

1.4.2. Micro-droplet Bioreactor

A water-in-oil micro-droplet bioreactor that carries bacterial cells in the aqueous core can be maintained to allow biofilm formation at the hydrophobic interface. As shown in Figure 1.5, a microfluidic channel device can be used to run the droplet-based culture in a spatially segregated manner, readily providing the necessary settings for biofilm formation (Figure 1.5, right). Under optimal conditions, the cells retaining the quorum-sensing gene circuit (Figure 1.5, left) are grown in the stationary phase, which allows biofilm formation to be monitored by microscopy. As the microfluidic device is manufactured with multiple channels, biofilm characterization can be conducted in parallel during long-term cultivation.

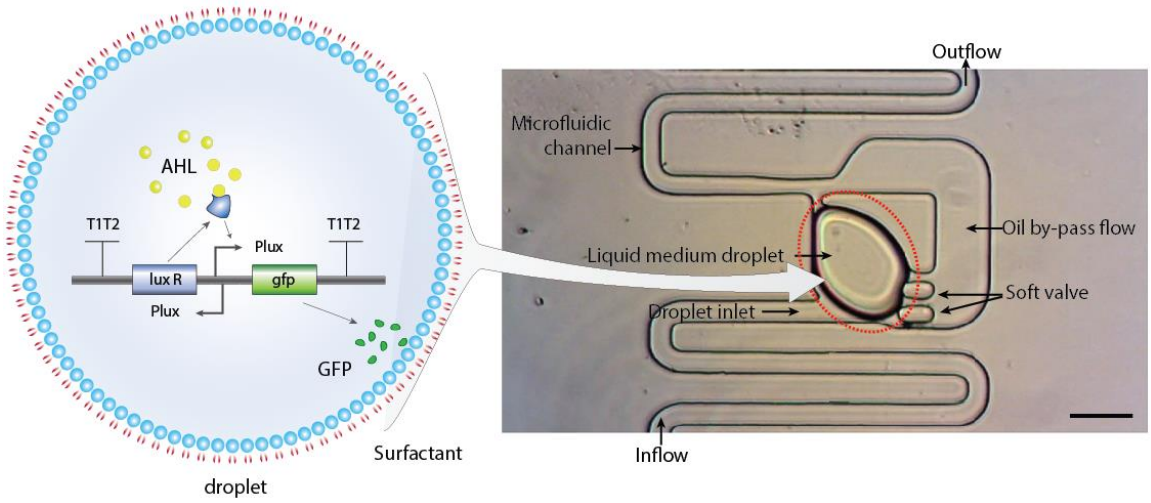

Figure 1.5. Microfluidic device for the maintenance of a micro-droplet bioreactor in a spatially segregated manner.

To this end, we investigated microfluidic culture conditions necessary to maintain the bacterial population in a droplet at the stationary phase. The approach can be summarized as follows: (a) develop microfluidic technologies for micro-droplet formation and droplet segregation, (b) establish bacterial population monitoring techniques, and (c) maintain biofilm cells for long periods.

CHAPTER 2

OVERVIEW OF SYNTHETIC CIRCUITS IN SYNTHETIC BIOLOGY

2.1. The Initial Development of Synthetic Biology

Approaches that change the cellular composition of the body through the introduction of new cellular constituents have proved to be dramatically successful as medical interventions over the past century. Ranging from the transplant of bone marrow stem cells to treat leukemia beginning in the 1950's to the transplant of gut flora to fight *Clostridium difficile* infection in recent decades, the manipulation of the body's cellular composition through cell therapy has uniquely complemented pharmaceutical and surgical approaches to disease treatment. As a result, the underlying biological signaling pathways and cellular interactions that control successful cell therapies are of significant interest. In particular, it would be ideal if these pathways and interactions could be synthetically tuned to enhance cellular therapy [10]. Fortunately, the years since 2000 have been marked by the development of synthetic biology as a field that specializes in reengineering cellular behaviors with synthetic networks [11]. Borrowing inspiration from electrical engineering, synthetic biologists have developed engineered gene and protein circuits in microbial and mammalian cells. Furthermore, they have harnessed and reengineered novel phenotypes from across the phylogenic kingdoms to provide cells with new capabilities. Together, these initial novel circuits and capabilities have allowed biomedical scientists and engineers to create enhanced cellular therapies. For example, synthetic circuits and capabilities have been used to develop bacteria that invade cancer as well as bacteria that disrupt cholera infection [12-13]. At the same time, new synthetic circuits have been developed in mammalian cells that allow the regulation of blood glucose and the proliferation of T-cells [14-15]. Ultimately, these efforts to combine synthetic biology with cellular therapy are poised to make significant breakthroughs in the coming decade.

As a first step toward exploring the current and future impact of synthetic biology in cellular therapy, it will be important to review developments in each field that are particularly amenable to integration. Given the engineering undercurrent of synthetic biology, this definition will include both research thrusts where living cells are reengineered, as well as efforts to construct cell-like encapsulations of biological networks and functions. Synthetic networks can be constructed to control functions in both living cells and liposomal pseudo-cells. Furthermore, although many synthetic networks can be constructed *in vivo*, cell-free synthetic biology has an important role in the optimization of synthetic pathways for cell therapy. The genome-scale engineering tools are certain to be useful in expanding these initial, synthetically enabled therapies in the future. However, initial efforts in synthetic biology in general, and specifically in cell therapy, have focused on the development of individual, fundamental control modules that create new phenotypes. Ideally, at some future point, genome-scale techniques will allow diverse combinations of these synthetic circuits to be deployed in enhanced therapies.

As a result, this chapter will focus on the synthetic components and circuits that have thrust synthetic biology to the forefront of new bioengineering disciplines as well as how they can enhance cell therapy. Over a decade ago, the creation of two engineered gene networks – a toggle switch [16] and an oscillator [17] – began the rapid advance of synthetic biology as a field. In the years that followed, increasingly complex synthetic circuits were developed that enabled fundamental engineering control processes in cellular networks. These synthetic biological devices were inspired by electrical circuits as well as natural biomolecular networks, and include timers, counters, clocks, logic processors, pattern detectors, and intercellular communication modules [18-25]. As shown in Figure 2.1, these DNA-encoded synthetic circuits are typically uploaded into cells, enhancing them with new abilities that have been externally programmed by the circuit's designer. In the case of cell therapies, upon infusion or implantation, the programmed networks can then interface with endogenous physiological networks to correct aberrant conditions *in vivo*.

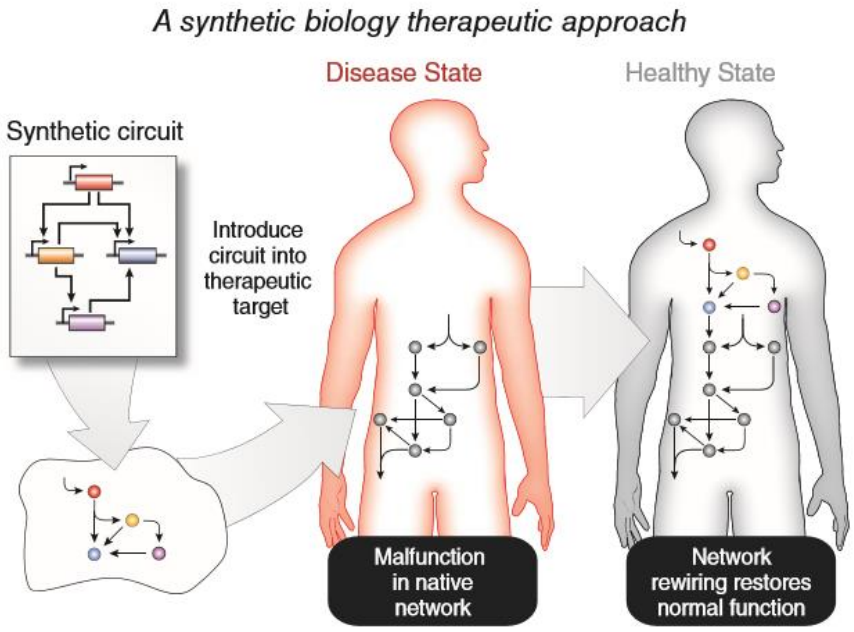

Figure 2.1. Creating new cell therapies with synthetic circuits. A synthetic circuit design is engineered in a therapeutic cell. The cell is then transplanted into the body, interfacing with endogenous networks, causing a transition from a disease state to a healthy state.

New approaches using synthetic networks for cell therapy are critical, because in many cases the creation of new medical treatments has stalled. Many technical hurdles need to be overcome. For example, efforts to regenerate tissues are slowly progressing [26]. Furthermore, many treatments for cancer such as chemotherapy and radiation have limitations that include incomplete tumor targeting, inadequate tissue penetration, and toxicity towards normal cells [27]. Ultimately, we need new therapies that can be customized to patients, and that go beyond mainstream medical approaches. Synthetic biology is beginning to use its approaches and platforms to fill this void and transform biomedicine into an engineering science. Thus, key synthetic biological discoveries and developments will be described, following by a detailed description of new technologies that are revolutionizing cell therapy using synthetic approaches.

2.2. Synthetic Circuits

Synthetic circuits are one of the core technologies available in synthetic biology. They are critical for reprogramming cellular phenotypes to enhance therapies. As noted previously, the development of synthetic circuits has spurred the growth of synthetic biology as a field. The discussion that follows will outline design approaches in synthetic circuit construction as well as provide a review of robust gene and protein circuits that have been successfully constructed. Synthetic biology and its revolutionizing approaches to cellular engineering have already shown the potential to impact cell therapies by altering their internal signaling networks. Whenever attempting to engineer cellular signaling cascades, care must be taken to ensure robust design and predictable cell behavior, along with repeatable and precise expression of critical genetic outputs. Biological systems naturally incorporate all of these requirements in their internal programming.

As previously mentioned, the development of two synthetic circuits, the toggle switch and an oscillator deemed "the repressilator," inspired the field of synthetic biology in 2000 [16-17]. Instead of open-loop control of gene expression, these circuits used feedback to provide an additional level of complexity in the precision control of phenotype. In the years following these developments, new circuits have been developed that leverage components from a range of different organisms. Synthetic circuit design has also expanded beyond these initial circuits that were based on DNA-protein interactions and now includes circuits based on protein-protein interactions as well [28-29]. In both cases, new computational algorithms and software programs have been created to speed the engineering of synthetic biological circuits [30-33]. These research thrusts have built a foundation for synthetic biology as a complete discipline.

2.2.1. Engineering Synthetic Gene Circuits

In order to develop the first synthetic circuits, several molecular biological components and control structures had to be available. In the last decades of the 20th century, investigators began to develop control elements for each step in the cascade of events between gene transcription and protein translation. Each of these processes is regulated by biophysical interactions, such as the docking of transcription factors and RNA polymerase to operator sites on promoters, or the binding of ribosomes to messenger RNA (mRNA) transcripts. Synthetic biology components that control and manipulate all of these interactions have been created. These biological components

can be combined to form modules for the design and construction of synthetic circuits. Biological circuits consist of modules of interacting genes and proteins, and synthetic biology seeks to rewire these modules to create new circuits and new phenotypes. Several other components have been created that leverage the interactions between RNA molecules themselves [34-35], RNA molecules and small chemical molecules [15, 36-39], and recombinases with DNA templates [20, 40].

For example, new engineered promoters [41] were critical in the design of networks like the aforementioned toggle switch developed in the laboratory of James Collins [16]. As shown in Figure 2.2a the toggle consists of two mutually repressible genetic operons, and when the strength of each repression event is balanced, a bistable switch is formed. Over multiple generations of cell division, the toggle will remain in either an ON or OFF state, regardless of the presence of a corresponding inducer. In this network topology, the ability of each operon to repress the other must be balanced, and these repressing interactions are governed by several factors, such as the strength of each operon's promoter as well as the strength of the ribosome binding sites (RBS) associated with each repressor's mRNA transcript. By carefully altering the nucleic acid bases in each promoter and RBS, the switching properties of the toggle switch can be manipulated.

Other synthetic networks illustrated the potential for digital logic gate behavior in synthetic circuits [22, 40, 42-44]. In one of the first examples, Anderson et al. created a synthetic AND-gate in bacteria as shown in Figure 2.2b. This AND-gate switching behavior, mimicking the gates enabled by integrated circuits in Electrical Engineering, used an engineered viral RNA polymerase with a slight defect (an amber – UAG – stop codon) in the middle of its transcript [44]. As a result, when one input (such as salicylate) was provided, only a partial polymerase was expressed. With the addition of a second input, such as arabinose, transcription of a small RNA was initiated, and this small molecule worked to suppress the defect. As a result, the fully translated viral polymerase was able to activate its viral promoter. In another study, the Voigt group engineered communities of bacteria to produce NOR-gate behavior [43]. This is especially important as NOR-gates are *Boolean complete*, and therefore can be combined to form any other type of logic gate. As a result, this work suggests that with enough discrete bacterial colonies, significantly more complexity in digital behavior computing could be possible. Alternately, other applications could require analog

signals. To this end, work in the laboratory of Timothy Lu has recently resulted in the creation of sophisticated analog circuits in single bacteria cells [45].

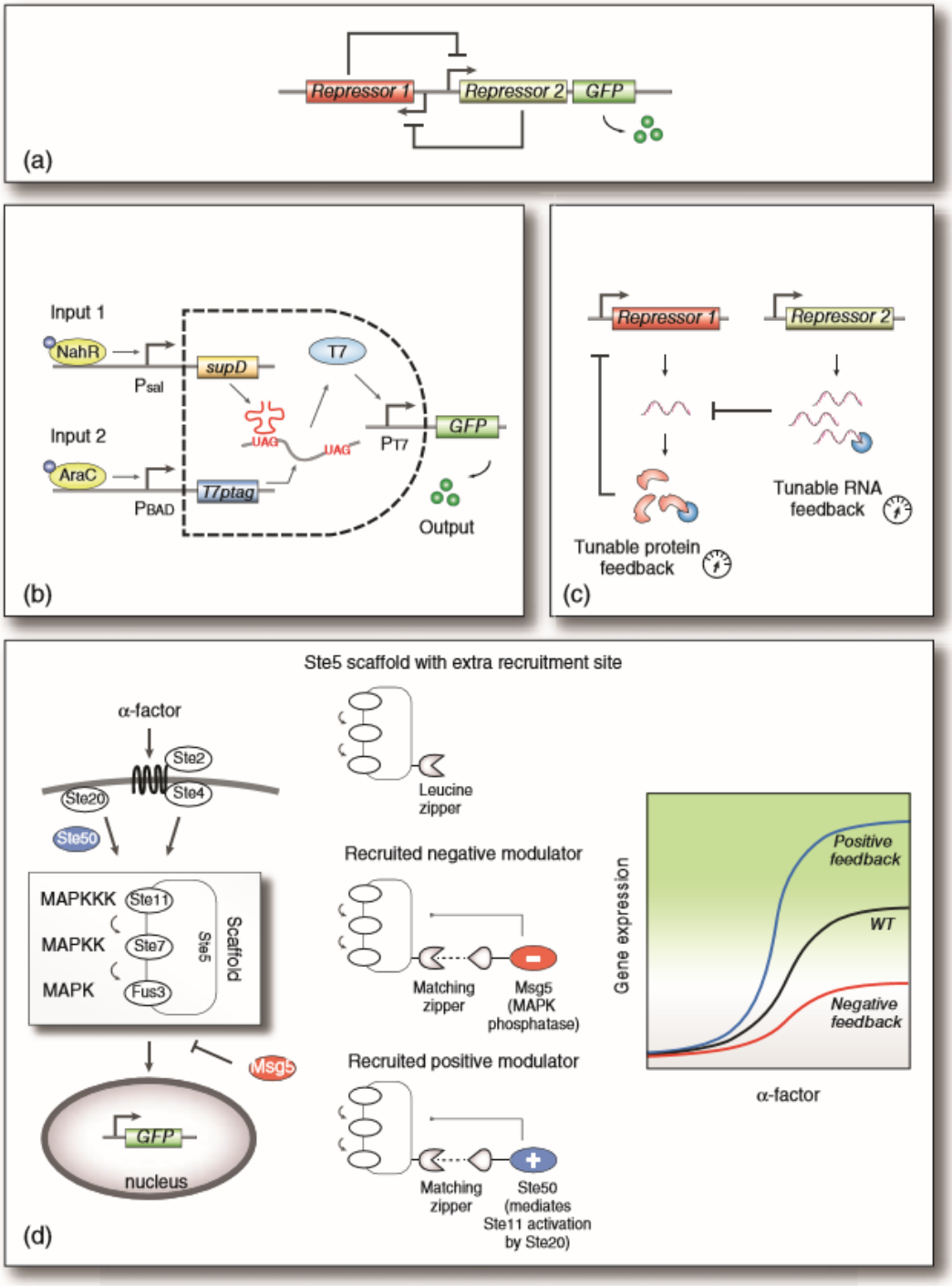

Figure 2.2. A broad range of synthetic components and control structures exist. (a) Synthetic components can be combined to create control structures such as memory. Two mutually

repressing operons can be used to create a bistable toggle switch; (b) Alternately, logic behavior such as a digital AND-gate can be created. Two engineered, synthetically activated operons alternately drive the expression of a faulty viral polymerase transcript or an RNA element that corrects the resulting translation errors. When expressed together, the resulting translated viral polymerase can activate the expression of an output gene; (c) Filter characteristics can be modified by tuning the degradation of protein or RNA regulators; (d) A synthetic scaffold can be rewired to control the mitogen activated protein kinase (MAPK) cascade in eukaryotes. By engineering docking sites for positive and negative effector proteins using leucine zippers, synthetic circuits can be created that control the MAPK cascade.

Other synthetic control behaviors are also possible, such as the genetic timers created by Collins and colleagues. These timers, deployed in yeast, allowing flocculation to be precisely timed [19], and therefore can control the fermentation process. In an another interesting study, Stricker et al. showed that a minimal set of components could create an oscillator much more robust than the repressilator [46]. In fact, several oscillators have been developed since the original repressilator in both bacterial and mammalian systems [17, 21, 46-49]. These oscillator enhancements mirror efforts to improve the efficiency of other basic control modules that have been built into synthetic gene circuits. Other studies also have demonstrated that signal filtering can be created in auto-regulated, negative-feedback circuits by tuning the degradation level of repressor elements as shown in Figure 2.2c [50-53]. More relevant to cell therapy, each could allow unique, precise types of signaling behaviors to drive the therapeutic function of cellular therapeutics.

2.2.2. Engineering Synthetic Protein Circuits

Although engineering circuits that rely on DNA-protein interactions has been a major thrust in synthetic biology, another key thrust that could be even more critical in leveraging synthetic biology in cell therapy has been the development of protein-protein signaling circuits. Just as genetic components allowed the development of diverse, tunable synthetic gene circuits, engineered protein signaling components have allowed for new synthetic circuit designs as well. These engineered proteins interactions have been important in two key ways. First, many of these new components interface with the previously described genetic circuits providing enhanced

features. Second, other aspects of these components allow for robust, speedy protein-protein interaction circuits. In fact, a key advantage of these protein-based circuits is the opportunity to take advantage of the speed at which proteins interact. In comparison to gene expression, enzyme-mediated single phosphorylation signals are evident in cellular phenotype on the order of seconds, whereas gene expression events frequently require minutes or longer to emerge in a cell's phenotype.

Several exciting examples of these protein-protein components have been developed in the past few years. For example, synthetic biology has significantly impacted the field of optogenetics. In early work, a light sensor was created by fusing a cyanobacterial photoreceptor to an *E. coli* intracellular histidine kinase domain to control gene expression [28]. This work has now been expanded to allow activation by multiple different wavelengths along with multiple applications in a significant expansion the components available to synthetic biologists [14, 54-56]. In a particularly interesting advance, June Medford's laboratory developed a plant signaling receptor that allows plants to detect TNT. Using this synthetic component, her group engineered sensitive Arabidopsis plants that turn white in the presence of TNT explosives [57]. Beyond components, protein-protein interactions have formed the basis of synthetic circuits as well. Some of the most interesting work along these lines has come from the laboratory of Wendell Lim [29, 58-60]. For example as shown in Figure 2.2d, Lim and colleagues showed that positive and negative feedback loops could be engineered by anchoring synthetic protein signaling components directly to an engineered protein scaffold using leucine zippers [29].

2.2.3. Deploying Circuits in Mammalian Cells

The initial circuit modules developed in microbes like bacteria and yeast have been expanded in higher order eukaryotes, and several synthetic circuits are now available that robustly control gene expression in mammalian cells. This precise control of specific genes will be critical for effective cell therapies. As an example of these mammalian circuits, Deans et al. developed a tunable, modular mammalian genetic switch [61]. This synthetic gene network coupled repressors with an RNAi design involving shRNA. Gene expression was turned on by the addition of an inducer, which controlled the transcription of a repressor, and simultaneously turned off the

generation of the RNAi component. Thus, this synthetic module allowed the transcript to be retained and translated (Figure 2.3Aa). This construct offered >99% repression, along with an ability to tune gene expression. This modular component can allow for the regulation of any gene, and was validated in both mouse and human cells.

Another synthetic control module – the toggle switch – has also been developed in mammalian cells as shown in Figure 2.3b. In multicellular systems such as the tissues of humans, cell identity is regulated by epigenetic networks that determine which genes become part of each cell's transcriptome. By combining two repressors, which control each other's expression, Kramer et al. developed a mammalian epigenetic circuitry that exhibited genetic toggle behavior and could be switched using two different drugs. These researchers used the toggle to regulate expression profiles of a human glycoprotein in engineered Chinese hamster ovary cells, and these cells also functioned after microencapsulation and implantation into mice. Just like previous bacterial toggles, switching dynamics and expression could be predicted with mathematical models [62].

While these synthetic networks show the usefulness of synthetic control in mammalian cells, the engineering of synthetic networks in mammalian cells is significantly more challenging that developing circuits in bacteria or yeast. Bacteria and yeast are much more tractable as model organisms for the design and tuning of synthetic circuits, as they are more easily genetically engineered. Ideally, mammalian circuits could be first developed in simple eukaryotes like yeast in a way that would allow their behavior in mammalian cells to be easily predicted upon transfer. Thus, for cell therapy applications, once a clinician determines the mammalian cellular behavior needed to treat a disease, the corresponding synthetic circuits could be rapidly developed in yeast. Synthetic biologists could generate a diverse library of functional circuits (e.g., though approaches such as site-directed mutagenesis), each with predictable function in human cells. This library would then provide the clinician with a spectrum of synthetically engineered cell therapies to prescribe.

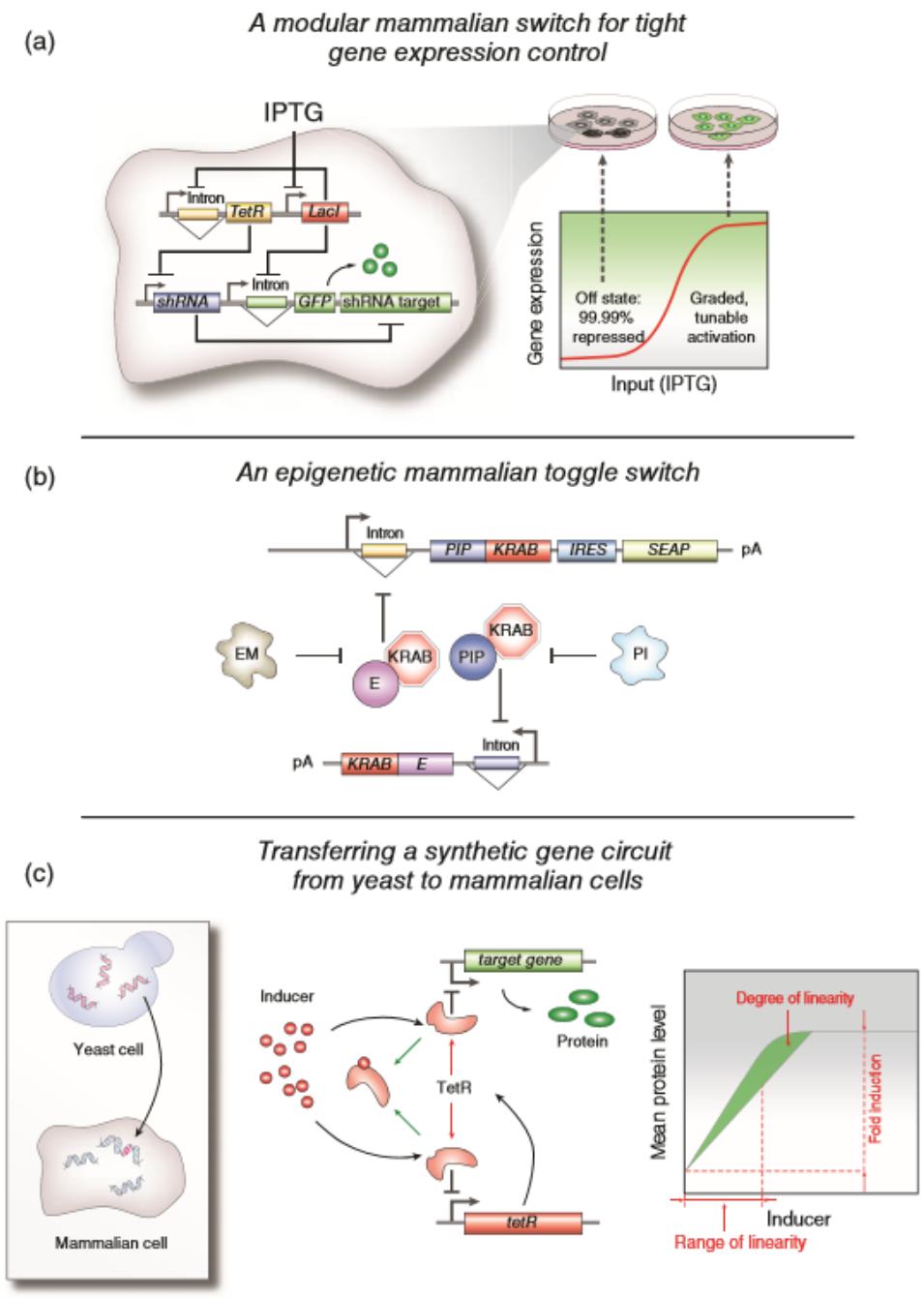

Figure 2.3. Synthetic circuits for the control of mammalian cells. (a) Tight control of specific genes will be critical for effective cell therapies. Here, a tunable, modular mammalian genetic switch was created that couples repressor proteins with an RNAi design involving shRNA. The switch is controlled by an inducer, which activates repressor expression, while simultaneously turning off RNAi components, allowing the output gene to be translated; (b) Genetic toggle switches can also be created in mammalian cells. By combining engineered streptogramin and

macrolide-inducible promoters to drive the expression of their respective engineered repressors, the mammalian output gene secreted alkaline phosphatase (SEAP) can be stably toggled by pulsing the system with erythromycin (E) or pristinamycin I (PI); (c) Synthetic circuits can be constructed in yeast with predictable behavior upon transfer to mammalian cells. Here, a linearizer gene circuit was created using the TetR repressor and an arbitrary target gene, both controlled by the same promoter. In the absence of inducer, the TetR protein blocks transcription from both promoters. When an inducer is added to cause de-repression, protein levels increase until TetR synthesis exceeds inducer influx, at which point TetR blocks both promoters once again. By using analytical and computational modeling, investigators were able to accurately predict the behavior of the circuit in mammalian cells after recording its behavior in yeast.

As a step toward predictably transferring synthetic circuits from yeast to mammalian cells, the group of Gabor Balazi constructed a mammalian version of a negative feedback-based "linearizer" gene circuit (Figure 2.3c). The work version from yeast was at first non-functional in mammalian cells. However, computational modeling suggested that function could be recovered by improving nuances gene expression and protein localization. As a result, after rationally developing and combining new synthetic parts, as suggested by the model, the circuit regained function in human cells. Investigators were able to tune and target gene expression linearly and precisely, just as they had been able to do in yeast. This approach should be relevant in transferring many gene circuits of interest from yeast to mammalian cells and will be critical for quickly developing therapies in the future [63].

2.3. Utilities of Engineered Bacteria

The above-described collection of engineered gene networks forms the foundation of a large synthetic biology toolkit that is now available for the creation of new applications such as cell therapies and cellular signal transduction. These synthetic components and circuits – which have been developed in both microbial and mammalian cells – form the basis of several approaches that have shown promise in regulating organismic physiology. A selection of these new approaches

towards synthetically enabled cell therapy and, in direct relevance to this thesis research, cellular signal transduction is described in the following sections.

2.3.1. Cell Therapy

As discussed previously, the cells regulating human physiology include both the body's human cells as well as the collection of all the microorganisms associated with the body (i.e., the microbiome). As these commensal organisms are well tolerated, they provide an ideal platform for launching synthetic networks in the body. With this approach in mind, Duan and March recently engineered a commensal strain of *E. coli* to prevent cholera infection by creating a synthetic interaction between gut microbes [13]. Cholera infection is marked by the secretion of virulence factors by *Vibrio cholerae*. At low population density, these virulence factors include cholera toxin (CT). In order to assess its own density, *V. cholerae* uses quorum sensing, a process in which it secretes and detects autoinducer signaling molecules. Specifically, *V. cholerae* detects cholera autoinducer 1 (CAI-1) and autoinducer 2 (AI-2). When both autoinducers are high, it ceases expression of virulence factors. Duan and March leveraged this mechanism by engineering *E. coli* – that already produced AI-2 – to also secrete CAI-1 (Figure 2.4). They found that when infant mice ingested the engineered *E. coli* eight hours prior to *V. cholerae* ingestion, their survival rate increased dramatically. Furthermore, cholera toxin intestinal binding was reduced by 80%.

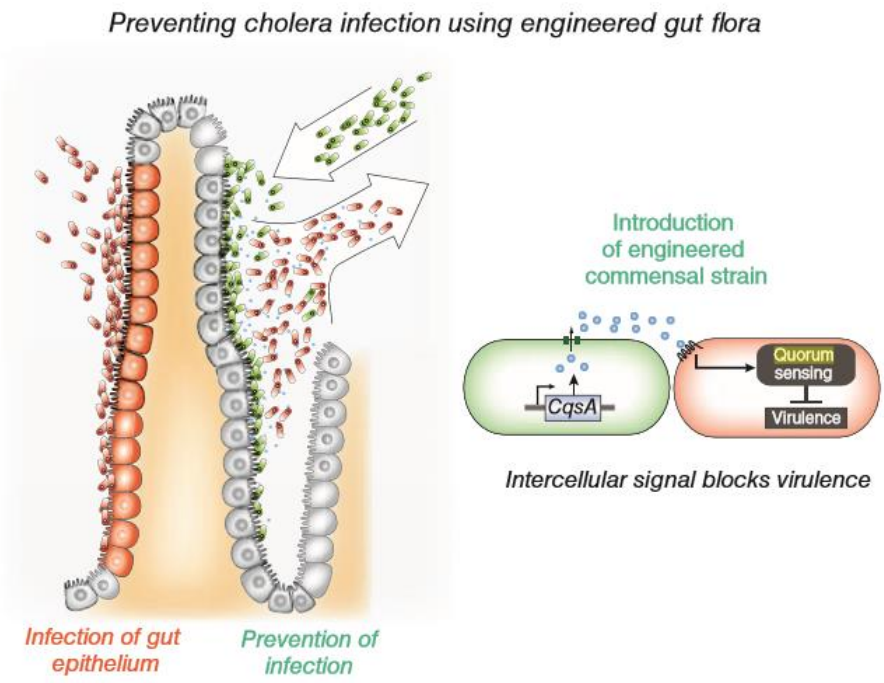

Figure 2.4. The gut microbiome can be synthetically reprogrammed by adding new members to the gut ecosystem. Probiotic, commensal *E. coli* were engineered to secrete the molecular signal cholera autoinducer (CAI-1), which leads to inhibition of *V. cholerae* virulence. In mice infected with cholera, survival rates were dramatically increased for mice that had consumed the engineered probiotic several hours prior to ingesting *V. cholerae*.

In addition to using engineered microbes to deter infection by other microbial species, engineered microbes could be added to a patient's microbe to secrete therapeutic molecules directly to the body. Along these lines, commensal bacteria have been engineered to secrete molecules for the treatment of several diseases. These molecules include insulinotropic proteins for diabetes [64], an HIV fusion inhibitor peptide for prevention of HIV infection [65], and interleukin-2 for immunotherapy [66]. Although these studied showed effective expression of the therapeutically relevant molecules, the addition of synthetic circuits could allow these therapies to be more precisely tuned to a patient's physiology. For example, for effective cell therapy, gene expression could be turned on only when the prescribed molecular interventions are needed. This increased control would reduce metabolic load on the bacteria and increase their ability to assimilate into the microbiome.

Another approach toward using engineered bacteria to treat disease has been explored by synthetic biologists who have created bacteria that seek and destroy cancer. Although it is not entirely clear how these engineered microbes should come into contact with tumors occurring distal to host locations where microbes normally reside, these engineered microbes use an interesting approach to cancer treatment. In one of these studies, Voigt and colleagues created bacteria that invaded cancer cells only in the hypoxic environments that frequently are indicative of tumor tissue, as well as bacteria that used quorum sensing components from other species to amplify their invasion response [12]. As shown in Figure 2.5a, *E. coli* were engineered to invade by causing them to express invasin (*inv*), an adhesion protein from *Yersinia Pseudotuberculosis*, which tightly binds mammalian β1 integrin receptors and induces uptake. Invasin expression was driven by the LuxI/LuxR quorum-sensing genes, allowing *E. coli* to produce an autoinducer that amplified invasin expression as the colony grew. Of course, using bacteria to treat cancer could come with a risk of infection from the bacteria themselves.

However, in another study, Li and colleagues intravenously delivered engineered, cancer-invading bacteria to target a tumorigenic pathway *in vivo* [67]. They used RNA interference (RNAi) to create bacterial invaders that knocked down expression of *CTNNB1* (encoding β-1 catenin), a gene that initiates many colon cancers upon its overexpression or oncogenic mutation (Figure 2.5b). The engineered bacteria generated short hairpin RNA (shRNA) segments that bound to *CTNNB1* mRNA transcripts and induced mRNA cleavage. In addition to shRNA and invasin, the synthetic system also produced lysteriolysin O (encoded by the *hylA* gene). Lysteriolysin enables molecular transport out of vesicles potentially through entry vesicle disruption. When engineered bacteria were intravenously delivered into immune-deficient deficient mice with subcutaneously xenografted human colon cancer cells, the investigators observed significant knockdown of the gene in tumor cells.

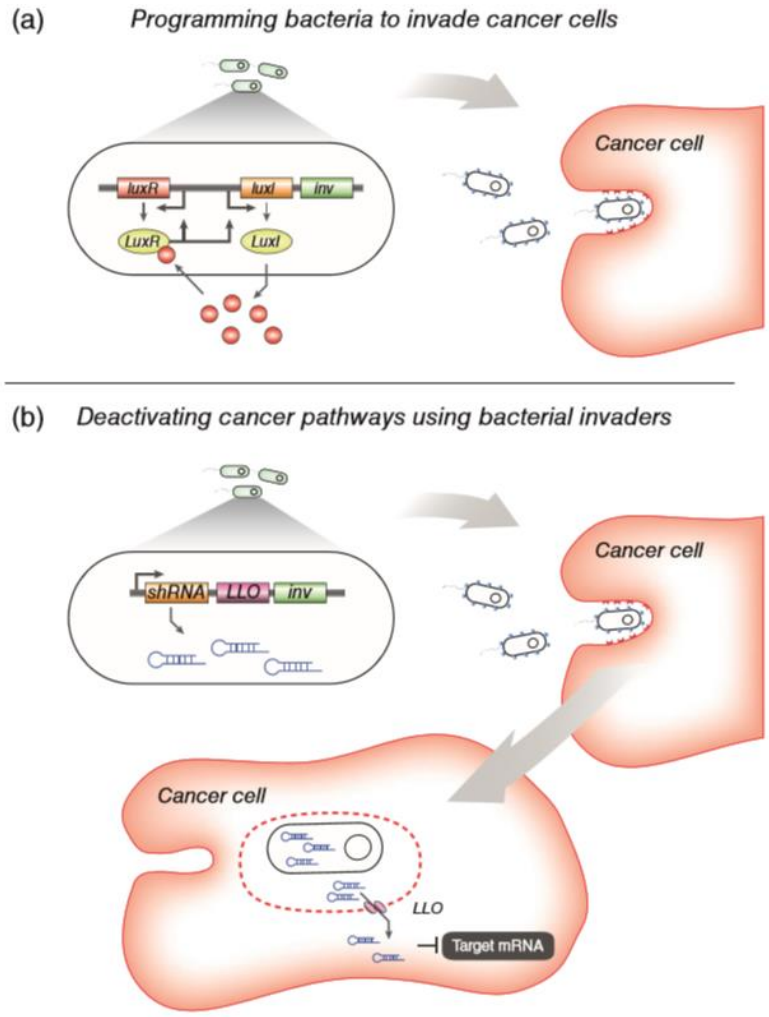

Figure 2.5. Bacteria can be synthetically programmed to invade cancer. (a) A population-density-dependent invasion of cancer cells can be created in bacteria. *E. coli* was engineered to express invasin (inv) at high population densities by borrowing the LuxI/LuxR quorum-sensing apparatus. Invasin binds β1-integrin receptors and induces uptake by targeted cells; (b) Intravenously delivered engineered bacteria were created that express invasin while also suppressing oncogene expression. By expressing a catenin β-1-specific short hairpin RNA (shRNA), oncogene expression was knocked down as listeriolysin (LLO) expression allowed escape from the phagosome.

2.3.2. Cellular Signal Transduction

As introduced in the preceding section, although cell therapy is a widely used medical intervention with many successes, it also has the potential for use as a tool for creating synthetic biological constructs and circuits. While approaches that have leveraged synthetic biology to engineer therapies have shown promise [68], many technical challenges remain. In the meantime, the same technologies can be applied to the monitoring and control of microbial populations, in particular, bacterial biofilms that have pervasive implications on, for example, human health as well as water and food quality. Most of these challenges have not been successfully overcome owing to a lack of information about the hundreds of genes that interact during the biofilm development process, including stress-associated genes. The research presented in this thesis utilized engineered bacteria with synthetic gene circuits (e.g., a quorum sensing receiver construct and a toggle switch) for bacterial signal transduction in order to better understand the mechanisms underlying genetic variation in biofilms.

Quorum sensing receiver cell line. The vast majority of microbiological studies have examined bacteria in their planktonic state rather than their biofilm state. Bacterial biofilms normally exhibit complex, heterogeneous structures, which vary widely in their mechanical properties, chemical compositions, and morphologies. In general, the local cell densities of biofilms are substantially higher than of planktonic bacterial cultures, as are the concentrations of metabolic by-products, secondary metabolites, and other secretory microbial factors. Of these, intercellular signaling and quorum sensing molecules are particularly important microbiological factors, as they link individual bacterial cells to the formation or dissolution of the biofilm community.

Environmentally sensitive bacterial cells, referred to as “receiver” cells - that generate visible signals upon induction with *N*-acyl homoserine lactone (AHL) can be constructed to better understand stochastic expression of quorum sensing signaling within biofilms (refer to Chapter 3 for details). The receiver contains a genetic construct with the *luxR* transcription factor and a green fluorescence protein (GFP) gene encoded by a bidirectional P_{lux} promoter. Quorum sensing is activated by the production and release of AHL, thereby signaling the local cell density to neighboring bacterial cells, which in turn express quorum signaling on their own. This type of signal transduction to a visibly measurable signal can be used to monitor bacterial growth within

bioreactors as shown in Chapter 6. Furthermore, quorum sensing can also be triggered in model bacteria systems like *E. coli* in the absence of AHL; bacteria with an identical gene circuit construct was examined to monitor induction of stochastic quorum signaling within the biofilm-mimicking microfluidic structure in the research presented in Chapters 3,5 and 6.

Toggle switch circuit-integrated bacteria. Bacteria endowed with a bistable toggle switch have been fully characterized as described earlier and can be utilized to study stochasticity in microenvironments, such as biofilms. A toggle switch is a circuit that can switch between two stable states, ON and OFF. Consequently, such a switch possesses a form of memory. The toggle switch consists of two transcriptional repressors, each repressing the other (refer to Chapter 4 for further details). The switch uses two small molecule-responsive transcriptional repressors—TetR, which is inhibited when it binds anhydrotetracycline (aTc), and LacI, which is inhibited when it binds isopropyl β-D-1-thiogalactopyranoside (IPTG). The introduction of aTc into a bacterial culture inactivates the ability of TetR to repress the P_{LtetO} promoter, thereby switching the system into a state with high expression of LacI, which then continually maintains a low concentration of TetR. Conversely, addition of IPTG inactivates LacI from repressing the P_{trc-2} promoter, switching the system into a high-TetR expression state, which then maintains a low concentration of LacI. The function of the toggle switch depends on the relative expression levels of its component transcriptional repressors. Additionally, this system can be utilized to drive the expression of reporter molecules, such as GFP and mCherry, in order to visualize the toggle switch state within a culture. We show in Chapter 4 that stochastic gene expression revealed in relatively simple inducible genetic systems also appears in the bistable genetic toggle switch system. This approach permits the study of stochastic gene expression with a higher degree of complexity.

CHAPTER 3.

STOCHASTICALLY INDUCED QUORUM SENSING

3.1. Abstract

We have investigated a microfluidic environment that can be used to monitor stochastic activities within a microbial consortium. The layout of microfluidic channels in a device was designed to regulate the growth of bacterial communities by confining bacterial cells while maintaining nutrient availability for survival, permitting cells to populate the region. Similar to naturally occurring biofilms, such engineered environment can exhibit different local growth rates as a function of distance from the bulk flow media. To demonstrate this phenomenon, we developed a microfluidic bioreactor (a maximum 0.97-μm height) containing two distinct regions for cell growth that differ in diffusion path length from the main fluid channel (12-μm height). This reactor was then populated with *Escherichia coli* engineered to retain a quorum sensing (P_{lux}-driven) circuit. The cells that were 225-μm distance away from the bulk-flow channel exhibited a strong GFP signal, our proxy for quorum, even in the absence of the quorum sensing signaling molecule. This finding suggests quorum sensing pathways may be de-repressed as a stress response in nutrient and space scarce environments. This new mode of quorum sensing activated by a starvation-induced stress response can be used to study quorum sensing in the laboratory.

3.2 Introduction

Throughout its life cycle, bacteria can exist in both planktonic and sessile states. The latter state is often associated with the formation of stationary, multicellular communities known as biofilms. Nearly all microbes can occur as biofilms in aqueous environments. Under such

conditions, biofilms are formed by the attachment of bacteria to submerged macro-surfaces, micro-particles, also to one another [69-71]. Biofilms can form along a surprisingly wide variety of surfaces, including metals, plastics, medical implants, and organic surfaces such as plant and animal tissues [72]. While biofilm communities within laboratories are often comprised of a single bacterial strain, naturally occurring biofilms can be composed of a broad array of bacterial, fungal, algal, and protozoan species among other microorganisms [9, 73]. For example, human dental plaque biofilms can consist of over five hundred bacterial species [74]. Furthermore, these communities are often bound together with sugar-rich molecular strands, collectively referred to as extracellular polymeric substances (EPS) [75]. Taken together, even a simple biofilm can be composed of a complex, heterogeneous network of spatial and genetic variations. Additionally, the biofilm development process involves temporally varying regulated of many genes, a large portion of which are stress-induced. The complex network of structure and responses makes it difficult for scientists to recapitulate, and controllably observe and study, biofilms within a laboratory setting [76-78].

Biofilms are formed through bacterial aggregation and subsequent self-secretion of EPS. Both of these processes are associated with a suite of phenotypic and physiological processes, such as altered gene transcription [79], changes in nutrients accessibility and preference [80], and an increased resistance to external stresses [81]. The complexity of biofilm formation and the related changes creates challenges in clinical and industrial settings, including human infections, biofouling, clogs in flow systems and pipelines, and bactericide efficacy [71].

An enormous body of research has examined the planktonic state of bacteria, while technological challenges have limited the number and scope of studies examining bacteria in their sessile state (i.e., biofilm state) [82]. These challenges arises from the complex, heterogeneous structures of biofilms, which vary widely in mechanical properties, chemical composition, and morphology [71, 83]. In general, the local cell densities of biofilms are much higher than those of free-floating planktonic cell cultures [84]. Consequently, the concentrations of metabolic by-products, secondary metabolites, and other secretory microbial factors are much higher within the interior of biofilm structures [85]. Of these, intercellular signaling and quorum sensing molecules are

particularly important factors in the biology of microbes, as they link individual bacterium to the formation or dissolution of the biofilm community.

When planktonic bacteria cells encounter a submerged surface, they quickly adhere to the surface [86]. Once attached, the cells begin to produce EPS and colonize the surface [6]. EPS production allows the emerging biofilm community to develop a complex, three-dimensional structure [87]. These biofilm communities develop within hours and propagate to new surfaces over time through detachment of small or large clumps of cells [88]. Later stages of detachment allow bacteria to propagate to wider surface areas or to a location downstream of the original community [79]. Though the physiological process of attachment–growth–detachment process is well described in the literature [89], the chemical signaling dynamics associated with biofilm quorum sensing has not yet been fully investigated [90].

In addition to cell-produced signaling chemicals, biofilms are influenced by internal small-molecule and nutrient gradients (Figure 1.2). These phenomena play a critical role in the cellular physiology of pathogens [91]. Near the fluid interface of biofilms, mass transport is high, providing bacteria with the nutrients necessary for robust growth [92]. In contrast, nutrient concentrations are low within the biofilm interior. This lack of resources within the biofilm interior slows growth and causes starvation-induced stress responses, potentially activating protective metabolic states [93]. These key features can be modeled using microfluidic channels, allowing the induction of a biofilm-like structure to study stochastically expressed quorum sensing signals.

Biofilm quorum sensing mechanisms are difficult to study due to technical challenges in examining bacterial aggregates over appropriate spatiotemporal scales. Additionally, the mechanics of EPS and flow interactions pose a make modeling and studying quorum sensing chemical transport non-trivial. However, microfluidic techniques have emerged as a promising approach for many applications owing to their low cost and ease of use [94-97]. Early research efforts that utilized microfluidics to study biology focused on biochemical assays containing small concentrations of DNA and proteins [94-95]. Over the past fifteen years, microfluidic devices have become significantly more complex. For example, Hasty et al. used microfluidic chambers to observe and track individual cells within a single focal plane under various environmental

conditions [94, 98-99]. Extensions of this work in an artificial biofilm structure could produce novel insights made possible by controlled observations. For this reason, microfluidic devices have been designed to mimic physical conditions that resemble natural cellular habitats, thus enabling the investigation of complex physiological states such as biofilms [100].

However, researchers have yet to develop microfluidic systems that mimic the biophysics of natural biofilm structures and while also enabling researchers to monitor cells in a planktonic state. Here, we describe the development of a novel microfluidic device that enables monitoring sessile, biofilm-like state cells and planktonic-like state cells together. This system allows researchers to investigate cellular and community physiology while monitoring single-cell phenotypic responses. Together, this allows researchers to study phenomena such as stochastic gene regulation in a single cell, while observing the phenomena's effect within a larger biofilm community, all on a single microfluidic device. The microfluidic device developed herein, referred to as a biomimetic biofilm, utilizes a unique design that mimics the key features of natural biofilm, while allowing researchers to take advantage of a well-characterized, controllable environment. This microfluidic tool can be used in combination with synthetic gene networks in *E. coli* that express GFP upon induction with AHL, the quorum signal produced by *Vibrio cholerae* [101]. Taken together, this engineered gene construct and our biomimetic biofilm device allows us to study gene expression dynamics for quorum sensing at a scale and time period not previously possible.

3.3 Materials and Methods

3.3.1. Manufacture of microfluidic device

Master mold fabrication. All master molds were fabricated in the Virginia Tech Micro & Nano Fabrication Laboratory (MICRON). Photomasks were drawn in AutoCAD (Autodesk, San Rafael, CA, USA), printed onto transparency film by CAD/Art Services, Inc. (Output City, Poway, CA, USA), and mounted onto glass plates (McMaster-Carr, Los Angeles, CA, USA). The first layer of the master mold was created by first spin-coating with SU-8 2000 negative photoresist (MicroChem Corp., Newton, MA, USA) onto clean silicon wafers to 0.96 µm in height using a

WS-650-8B programmable spinner (Laurell Technologies Corp., North Wales, PA, USA) and then using a MA/BA6 UV contact mask aligner (MicroTec, Garching, Germany) for subsequent UV exposure. After being exposed to UV radiation, the unexposed photoresist was rinsed away using developer (MicroChem Corp.). For the second layer, the SU-8 2010 negative photoresist was spin-coated on top of the first layer to achieve a height of 10 μm. Again, the MA/BA6 UV contact mask aligner was used for UV exposure, and the unexposed photoresist was rinsed away using the same process described above.

PDMS device fabrication. Replica molds were created from master molds by mixing polydimethylsiloxane (PDMS)/Sylgard 184 (Dow Corning, Midland, MI, USA) with a 10:1 ratio of the elastomer base to curing agent, degassing in a vacuum desiccator for 1 h, and curing in an oven at 90°C for 2 h. Following removal of the PDMS, devices were cut, holes were punched for ports, and the cell was cleaned with filtered DI water and then permanently bonded to clean coverslips (Thermo Fisher Scientific, Waltham, MA, USA) via exposure to O_2 plasma for 1 min in a PDC-32G plasma cleaner (Harrick Scientific, Ithaca, NY, USA).

3.3.2. Construction and characterization of the quorum sensing receiver circuit

Cloning details. The receiver circuit (pSP035) used in this study was constructed using six components, pKE1-MCS as the vector, P_{lux}, luxR T1T2, rbs027 and GFPmut3b as inserts (Figure 3.1). The desired restriction sites were added to the 5′ and 3′ ends of each construct using overhang PCR (Table 3.1). For each insertion, both the insert construct and vector were uniquely double digested using appropriate enzymes. Followed by gel purification, the fragments were then ligated and transformed, and the resulting clones were screened against carbenicillin (Cb) resistance.

Induction conditions. To characterize the performance of the receiver circuit we conducted a series of experiments. The cells were first grown overnight in Luria–Bertani (LB) media with 100 μg/ml Cb from a frozen stock. At the beginning of the experiment, overnight grown cells were diluted 1:1000 in fresh LB media and once again grown and kept at exponential growth density. The receiver cells were then induced with of AHL to yield final concentrations of 0.001, 0.01, 0.1 and 1 mM. The fluorescent intensity was measured at given times by diluting each

sample 1000-fold using phosphate-buffered saline (PBS) and collecting 10 000 events per replicate using a BD Accuri™ C6 (BD Bioscience, Piscataway, NJ, USA). Cell were maintained at 37°C before flow cytometry analysis.

3.3.3. Maintenance and monitoring of cell growth in microfluidic channels

Microfluidic cell culture. The recombinant *E. coli* cells were loaded into the trapping channels of the microfluidic device by directing the flow in the direction from the cell port to the waste port. Upon trapping a few cells in each region, the flow was reversed and slowed to steadily supply the cells with fresh nutrients from the media port through a combination of diffusion and advection. The cells were maintained at 22°C and grown to fill the chamber over a duration of 6–10 h.

Cell microscopy. Cell images were acquired using an inverted epifluorescent microscope (Ti-E; Nikon Instruments Inc., Tokyo, Japan). Differential interference contrast (DIC) and fluorescent images were captured every 15 min, and focus was maintained automatically using Nikon Elements software.

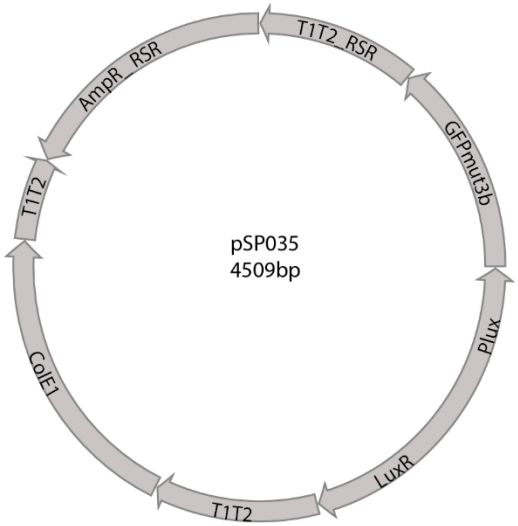

Figure 3.1. The receiver circuit (pSP035) used in this study was constructed using six components, pKE1-MCS as the vector, P_{lux}, luxR T1T2, rbs027 and GFPmut3b as inserts [102]. Insert rbs027 was first extended to GFPmut3b using overlap extension PCR and all other segments were amplified

using a standard PCR protocol using plasmids mentioned elsewhere (Table 3.1) [102]. Each component was sequentially transformed into NEB turbo strain (New England Biolabs) and the final pSP035 plasmid was transformed into *E. coli* K-12 wild type (MG1655) strain (CGSC6300).

Table 3.1. Primers used in this study.

Components	Plasmid	Primer sequence
Fwd T1T2	pKLi028	GCCGTCCCCGGGTTTGTAGAAACGCAAAAAGG
Rvs T1T2	pKLi028	ATTAATAACATATGGCTAGAGGCATCAAATAAAACGAAAG
Fwd luxR	pKLi049	GCCTCTAGCCATATGTTATTAATTTTTAAAGTATGGGC
Rvs luxR	pKLi049	GTAAGGATAAAGAGATGGGTATGAAAAACATAAATGCCGA
Fwd P_{lux}	pKLi055	TCGGCATTTATGTTTTTCAT ACCCATCTCTTTATCCTTAC
Rvs P_{lux}	pKLi055	CGATAGTTAATACT CTTAAGATTCGACTATAACAAACCAT
rbs027 (ext2)	pKLi071	ATGGTTTGTTATAGTCGAATCTTAAGAGTATTAACTATCG
rbs027 (ext1)	pKLi071	CTTAAG AGTATTAACTATCGTTCAACTGATAGGGA
Fwd GFPmut3b	pKLi071	TCAACTGATAGGGAGAGCTCATGCGTAAAGGAGAAGAACT
Rvs GFPmut3b	pKLi071	GCGTTTCTACAAAGCTAGCTTATTTGTATAGTTCATCCA
Fwd T1T2	pKLi028	ATACAAATAAGCTAGCTTTGTAGAAACGCAAAAAGG
Rvs T1T2	pKLi028	GGTCTAATAAGTCGACGCTAGAGGCATCAAATAAAACG

3.4. Results and Discussion

3.4.1. Validation of a quorum sensing receiver cell line

To monitor stochastic quorum signaling within the biofilm-like structure, we constructed an environmentally sensitive bacterial cell, defamed a “receiver”, that generates visible signals upon induction with AHL. The receiver contained the transcription factor *luxR* and a GFP gene encoded by a bidirectional P_{lux} promoter [103] (Figure 3.2b and 3.2c). Quorum sensing is activated by the production and release of AHL, thereby signaling the cell density to neighboring bacterial

community members and in turn expressing the GFP reporter in the following experiments [104] (Figure 3.2d). However, quorum sensing can also be triggered in the absence of AHL (Figure 3.2e); in this situation, the P_{lux} promoter is activated without the presence of AHL. This activation could be the result of de-repression, a consequence of cell density or nutrient deprivation.

In order to validate the receiver circuitry that we used in subsequent experiments, we first verified the GFP expression of the receiver cell when induced by AHL supplemented with LB media containing 50 μg/mL Cb. By varying the AHL concentrations over an induction period of 5 h, changes in fluorescence were observed using a flow cytometer. In the absence of AHL, GFP was not expressed (Figure 3.2f). The GFP signal reached saturation at a 1 mM AHL concentration, while intermediate concentrations produced intermediate expression (Figure 3.2f). A comparison between the 0- and 1-mM AHL treatments clearly shows that the receiver cells were not induced in the absence of AHL (Figure 3.2f).

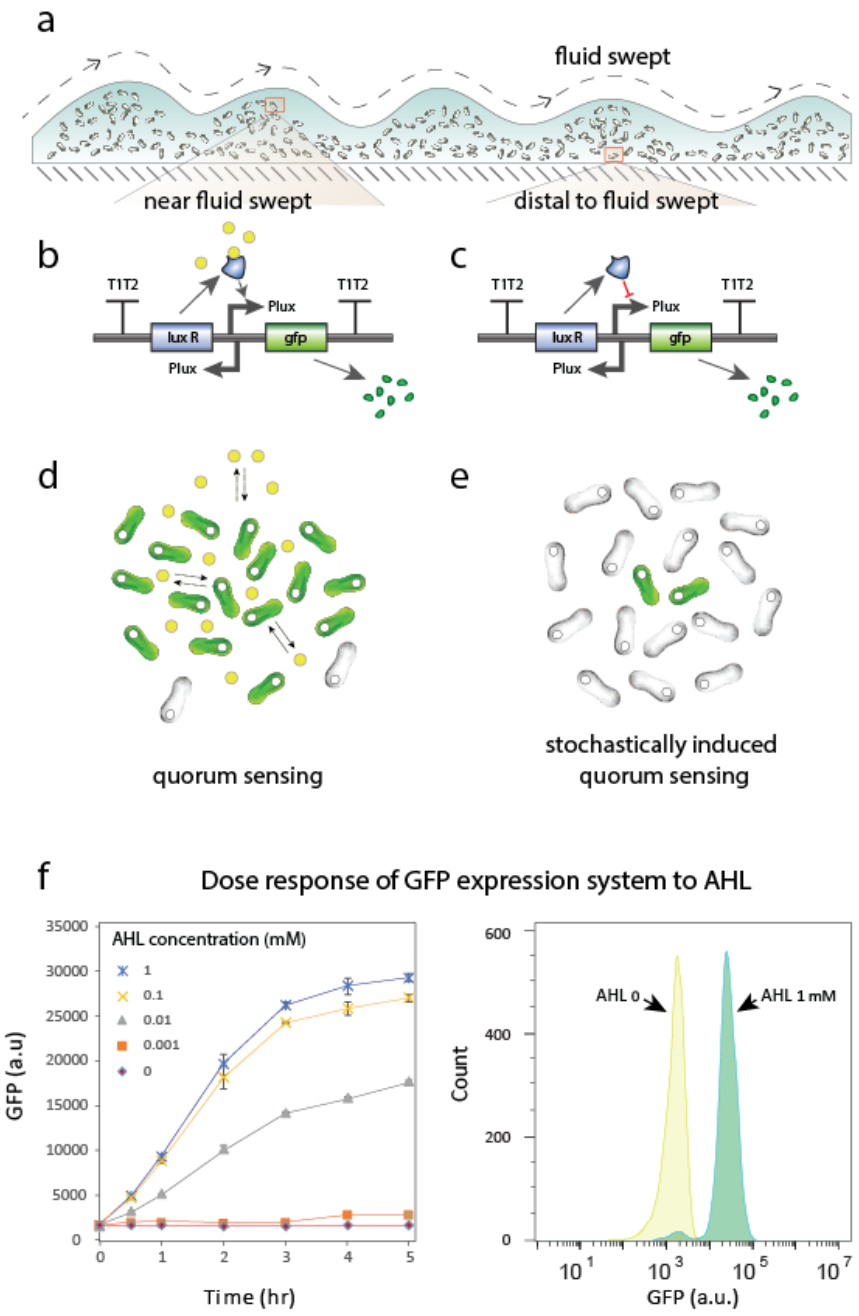

Figure 3.2. Understanding quorum sensing for biofilm consortia. (a) Within a microbial consortium, different states of bacterial cells exist. Part of these differences are a function of the distance the bacteria cells are from the source of flow. (b) Normal quorum sensing system. Upon reaching a certain threshold population density, the quorum sensing genes are induced, and the cells GFP. (c) Stochastically induced quorum sensing system. Even without the signal molecule (i.e., AHL), the quorum sensing gene circuit is triggered in certain cells within the microbial population. This can occur from a shortage of LuxR production or an inability for LuxR to repress

the P_{lux} promoter site. (d) Characterization of receiver cells using a flow cytometer. (d) The receiver cells were exposed to different concentrations of AHL in the culture medium, and GFP expression levels were measured continuously over 5 h. The fluorescence signal increased in proportion to the inducer concentration between 0.001 and 1 mM over the 5-h time period. The receiver cells were only responsive in the presence of AHL.

3.4.2. Biomimetic biofilm

To explore the spatiotemporal dynamics of quorum sensing within biofilms, we developed a three-port microfluidic device that mimics the key transport phenomena in biofilm colonies. The device consists of two regions on opposite side of the main flow channel in parallel: rectangular chambers independent of one another and identical chamber regions connected via convolutions resembling an inverted dichotomously branching tree of channels. Both chambers are open to the flow of the medium. Along the direction of the flow, the convolutions converged into a single path and ultimately came to a closed end (Figure 3.3a-c). The cell chamber region and convoluted pathway both have a channel height of 0.97 μm. Since *E. coli* cells have a ~1 μm diameter, the height of the trapping region allowed linearized observation of confined cells (Figure 3.4b). The device was also designed to continuously discharge cells from the device through the main flow channel (12 μm in height). In this biofilm-like structure, the PDMS structures of the microfluidic device captured and accumulated the extracellular matrix within structures constrained to resemble biofilms (Figure 3.4a and 3.4b). Additionally, we designed the device to have a well-characterized ability to transport media throughout the biofilm-like structure.

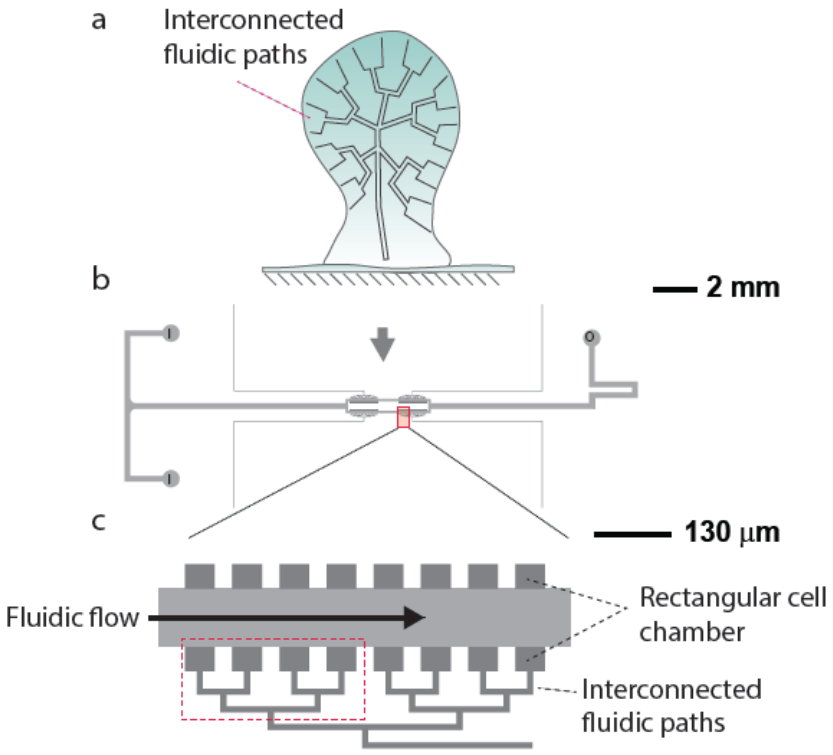

Figure 3.3. Design of the microfluidic device that mimics biofilm structures. (a) A diagram of a typical biofilm structure and the interconnected fluid paths from which the bacterial colonies are able to grow. (b) Overall design of the microfluidic device used in this study. Gray circles indicate two inputs on the left (I) and an output (O) on the right side of the channel. The two inputs supply microbial cells and culture medium, respectively, while the output permits the outflow of waste. (c) The interconnected region of the device, mimicking the biofilm, contained rectangular cell chambers adjacent to the central flow channel.

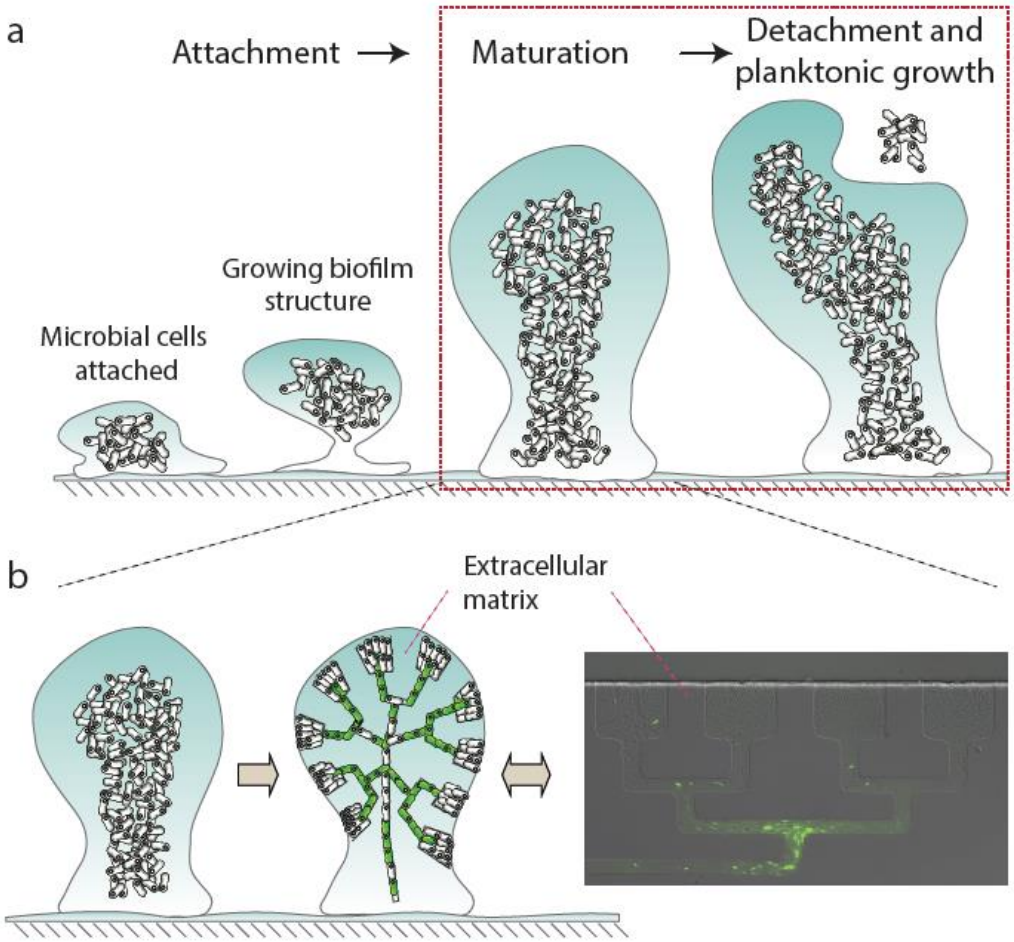

Figure 3.4. Biofilm developmental process and the design of a biofilm-like structure using microfluidic channels. (a) Microbial cells are attached to solid surfaces and grow to form biofilm-like structures. The outer cells are ultimately detached from the biofilm structure and return to individual planktonic states. (b) To investigate spatiotemporal characteristics of quorum sensing mechanisms within a microbial consortium, we have designed a device that mimics the key features of a biofilm structure. The microfluidic device is constructed to retain microbial colonies within interconnected fluidic paths. The device design limits growth areas in deeper regions of the device by constraining space while imparting a nutrient gradient.

3.4.3. Stochastically expressed quorum sensing GFP reporter in batch culture

The effects of nutrient availability on the diversity of phenotypes in our tightly regulated receiver colonies were also apparent in experiments lacking AHL within batch cultures in test tubes. We conducted two experiments in parallel. The first maintained cells in the exponential

phase while the second maintained cells in the stationary phase over a 4-day duration. For the exponential phase cultures, the media and cells were periodically diluted with a fresh batch of LB supplemented with Cb in order to provide optimal nutrients and growth conditions. At each observation point throughout the full duration of the experiment, the exponential phase cells showed minimal GFP expression (Figure 3.5, Exponential, quadrant 2 [Q2] in each panel). On day 2, there was a slight overall shift (of only 0.27%) towards the high GFP expression state; however, this increase was temporary, and the expression later returned to basal levels for the remainder of the experiment (Figure 3.5, Exponential, days 3 and 4).

While exponentially maintained receiver cells did not exhibit an increase in stochastic quorum signaling over time, we did observe an increase in stochastic behavior for receiver cells held at stationary phase. For this trial, receiver cells were held in stationary phase, without being supplemented with fresh nutrients after the inoculation. As above, we monitored for cells that were expressing GFP stochastically without AHL induction. As shown in Figure 3.5, we were able to observe a gradual increase of the cell population in the high GFP state, with day 4 showing the most stochastic events (1.51%). We replotted our observations from the Q2 sections, respectively, from the exponential and stationary phase cultured cells, in order to compare the course of stochasticity over the 4-day period (Figure 3.5, far right panels). We were able to see a distinct difference between the two culture phases; over time, the stationary phase receiver cells showed a 10-fold increase in cells transitioning to a high GFP expression state.

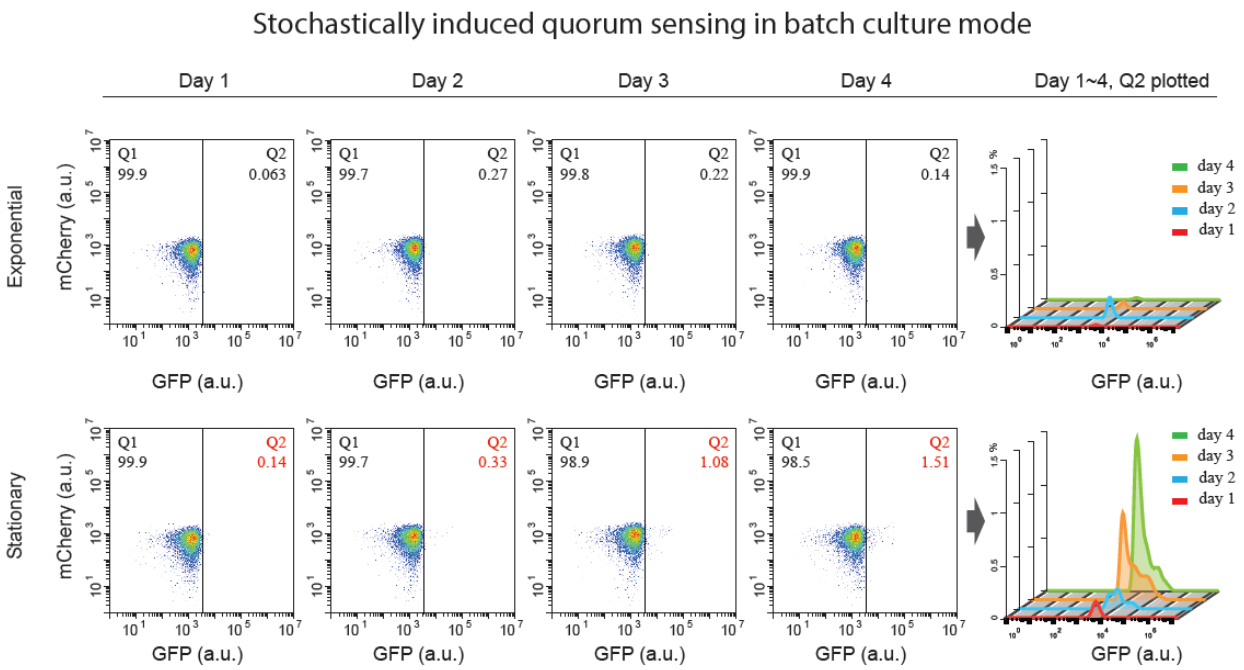

Figure 3.5. Comparison of gene expression between exponential and stationary phase cultures of quorum sensing receiver cells in batch cultures. All batches were carefully maintained in respective culture conditions and measured across 10,000 events through the flow cytometer at established times over 4 days. Cumulative data from quadrant 2 (Q2) for each of the 4 days are plotted in the far right line graphs.

3.4.4. Stochastic quorum sensing expression in biomimetic biofilm channels

After confirming that the receiver cells trigger quorum signals (i.e., exhibit GFP expression) dependent on the local environment, we further sought to observe and analyze these effects in our microfluidic device. Receiver cells were seeded into the biofilm-like channel of the device for long-term observations. The initial seeding was conducted by applying pressure to syringes containing an inoculum through the inlet ports (Figure 3.3) in order to direct the cells towards the main fluid flow channel and also to expand the capture region of the device. Once the device was seeded, the inlets were connected to syringes containing fresh LB/Cb media and monitored over time using a fluorescent microscope. While receiver colonies were successfully seeded into the biofilm-like channel, the height (0.97 μm) of the channels partially restricted the

ability of *E*. *coli* to swim, especially within deeper regions of the microfluidic structure where the flow velocity is low. In these constricted environments, bacterial dispersal throughout the channel is driven by growth and division of parental cells rather than motility Sequential images of a typical experimental run are presented in Figure 3.7. Initially, a few isolated colonies began to grow and subsequently merged into a large monolayer that filled the chamber (Figure 3.7, 20 h). Doubling times are shown in Figure 3-6. Once the chamber areas of the channels were fully occupied by 20 h, a localized burst of GFP expression began to occur within the deeper regions of the convoluted channel (in a localized area of stochastic bursting) as depicted in the red box in Figure 3.7. This region of stochastic bursting, approximately 200–250 μm away from the flow main channel, exhibits stochasticity as a result of several factors including a lack of nutrients and cell crowding. By the conclusion of the full experiment over a duration of 60 h, these localized regions showed an accumulation and intensification of quorum signaling cells.

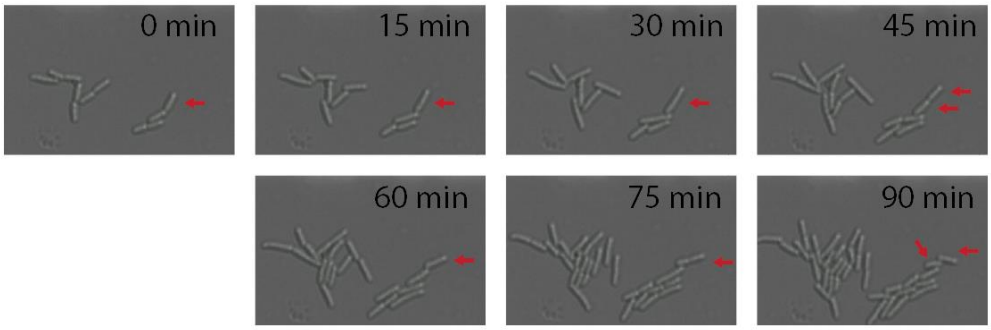

Figure 3.6. Motility and doubling time of the quorum sensing cells within the biomimetic biofilm channel. Red arrows are for tracking purposes. Single red arrows within a frame show the parental cell. At approximately 45 min, the parental cell divides, generating two daughter cells. The second cycle of division is shown in subsequent frames. The cell located on the top in the 45-min image was tracked for an additional division cycle. All experiments were conducted at 22°C. Sequential snapshots of a typical experiment are presented. Initially, we observed a few isolated receiver colonies. Over time, the colonies subsequently merged into a larger monolayer that filled the chamber.

We further compared these findings to colonies that were grown in independent rectangular chambers (Figure 3.3). The rectangular chambers were located directly in parallel to the biofilm-like channel (Movie 2). Owing to the difference in nutrient transport levels and growth

environments, stochastically triggered quorum sensing (i.e., GFP expression) was only observed in the biofilm-like channels. These findings are also consistent with the results obtained previously in batch culture modes (Figure 3.5).

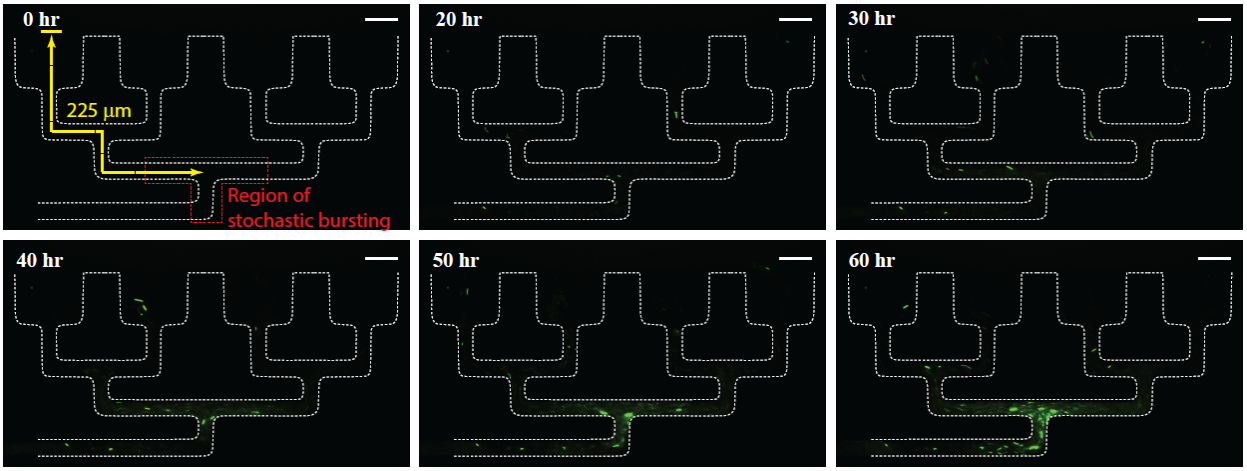

Figure 3.7. Stochastically expressed quorum signaling within the biomimetic biofilm channel. Quorum sensing colonies were seeded in the microfluidic channels, and GFP expression was monitored over time. The red dotted line indicates localized areas of stochastic bursting of the quorum sensing cell line. The yellow dotted line shows the path from the main fluid flow to the center of the region of stochastic bursting. The total duration of the experiment was 60 h, with time-lapse images obtained every 15 min. All scale bars indicate 25 µm.

3.5. Conclusion

In this work, we examine how quorum sensing can be triggered stochastically within communities of *E. coli* cells. We developed an artificial biofilm-like structure that facilitates lateral observations of microbial community structures. This enabled us to directly visualize phenomena occurring within the core of these structures at the scale of individual cells. Moreover, the structure induced expression of the GFP reporter, indicating the stochastic induction of quorum sensing. The effects of quorum sensing within biofilms in the environmentally relevant context were made possible by the design of our microfluidic device.

In nature, dense microbial groups, such as bacterial biofilms, commonly contain diverse cell types and species due to local fitness advantages [105]. Even within even isogenic cell populations, some cells exhibit genetic mutations and stochastic gene expression [106-107], producing fluctuations in transcription and translation as well as aberrant gene products. Our microfluidic device is able to stochastically trigger quorum sensing within microbial communities that are densely packed and lack sufficient nutrients, allowing us to study such mutations in a well-controlled environment.

Recent research has shown that novel genotypes within biofilm structures can arise through both mutation and recombination [107-108]. These stress-induced genetic changes have been primarily attributed to changes in the colony morphology following biofilm growth. In addition, as shown in our study, subpopulations within biofilm colonies can exhibit distinct differences in gene expression in a stochastic manner, leading to phenotypic heterogeneity. There are several examples in which microenvironmental heterogeneity within biofilms leads to stochastic gene expression and potential adaptive group behaviors. For example, a heterogeneous bacterial population created as a result of stochastic gene expression may be able to adapt more efficiently to sudden changes in environmental conditions, benefiting the entire biofilm structure [109].

The described microfluidics device provides a unique opportunity for the study of the complex phenomenon of quorum sensing. This system vastly simplifies any *E. coli* assays that require steady, reproducible populations of sessile cells in their biofilm state. There are three major advantages over similar platforms. First, the microfluidics device induces quorum sensing pathways without the use of signaling molecules such as AHL. In other words, the structure and flow characteristics serve as appropriate environmental stimuli to induce quorum sensing in *E. coli*, a major system for the study of biofilms. Second, the linearized channels of the microfluidics device make it possible to visually isolate single *E. coli* cells. In this way, individual cells can be visualized continuously. This capability may be combined with other visual reporter assays in order to examine other genetic factors both downstream and upstream of the GFP reporter construct as well as any small or environmental stimuli that can be applied through the apparatus. Third, the design of the microfluidics device allows the parallel culture of cells exhibiting

stochastically induced quorum sensing in its convoluted chambers with cells cultured in the independent rectangular chambers exhibiting no such phenotype. This parallel structure enables a clear control treatment in any experimental design without any modification.

The microfluidic cell design is somewhat specific to *E. coli* cells; the channels in the device were just sufficient in height (0.97 μm) to accommodate individual *E. coli* cells (1 μm). However, similar systems could be designed to precisely accommodate other species of quorum sensing bacteria. These organisms interact with many of the same environmental stresses in biofilm formation [76-77], indicating the potential for similar induction, especially in an autoinducer species capable of producing their own AHL.

The field of microbiology has long had a limited understanding of the mechanism by which biofilms maintain these diverse cell populations and communities. This biomimetic biofilm structure enables the visualization of phenotypic diversity within biofilm structures, thus providing exciting new opportunities in the study of quorum sensing. Our results suggest that resource levels as well as population density are keys to understanding heterogeneity in microbial communities.

CHAPTER 4.

TOGGLE SWITCH STABILITY IN BIOFILM STRUCTURES

4.1. Abstract

Biofilm bacteria and planktonic bacteria exhibit substantially different gene expression patterns; these differences are not only important for understanding biofilm biology, but also have practical implications for antibiotic development and food processing technology, for example. To better understand biofilm formation, we considered a toggle system in which inducers can be used to switch a gene expression marker between two states. High LacI expression was induced by aTc and indicated by high GFP levels, and high TetR expression was induced by IPTG and indicated by high mCherry levels. We tracked expression under stressful biofilm-like conditions in our previously developed microfluidic device to characterize the stochasticity of gene expression. After induction with aTc, cells showed stable expression of GFP throughout the experiment. After induction with IPTG, cells mainly expressed mCherry, but cells stochastically expressing GFP increased over time. In a more detailed analysis, we demonstrated that this stochastic GFP expression originated from deep regions within the channel and eventually expanded further into the microfluidic device. These results demonstrate the utility of the toggle system and microfluidic device to understand the dynamics of simple regulatory networks in biofilm environments.

4.2. Introduction

Biofilms, aggregated consortia of bacteria that inhabit a wide array of surfaces, have been studied in many different contexts, including the characterization of their pervasive effects on human health, water quality, corrosion, dental health, and contamination of food processing

equipment [1-4]. Many of the challenges presented by biofilms in these contexts come from a lack of information pertaining to the functions of the hundreds of genes that are involved in the biofilm development process, including stress-associated genes in particular [5].

Bacteria comprising biofilms exhibit vastly different gene expression patterns compared to those of planktonic bacteria of the same species. There are several implications of this difference in gene expression, including the development of antibiotics [7]. Most antibiotics have traditionally been developed to kill planktonic bacteria. However, planktonic bacteria are more susceptible to antimicrobial compounds than bacteria in biofilms, and traditional antibiotics have been developed to target bacterial cells in their relatively unprotected planktonic state [8]. Accordingly, modern medicine will require new classes of antibiotics that target bacteria within biofilm structures. Understanding the mechanism underlying the phenotypic variation of biofilms and the genetic underpinnings of biofilm formation will help reveal new ways to target biofilm cells and further disrupt their functions.

Microbiologists have also developed a comprehensive set of genetic engineering tools [110], including genetic circuits such as genetic toggle switches for bacteria [111] that have potential applications in synthetic regulatory networks for synthetic biology (McDaniel & Weiss 2005; [101, 112-113]. However, these genetic toolboxes also may provide insight into the naturally occurring complex genetic regulatory mechanisms that give rise to complex traits like biofilm formation [114-115] and quorum sensing [116-117].

Gardner et al. (2000) developed the first synthetic genetic toggle switch as a simple, two-element bistable gene-regulatory network in *E. coli*. This genetic toggle switch system utilized two mutually inhibitory genetic elements in which the promoter of the first element regulated the expression of a repressor of the second element, and vice versa. With the addition of a specific signaling molecule that interferes with the function of either the first or second repressor protein, the bacterial cell systems would continue to constitutively express the alternate repressor element, thereby deterministically maintaining the cell in one of the two states until a new signal molecule induces a change.

In this toggle switch system developed by Gardner et al. (2000), LacI binds to the promoter of TetR, thereby repressing the expression of the TetR. Similarly, TetR binds to the promoter of LacI, thereby repressing the expression of LacI (Figure 4.1). Each of these promoters can also be used to drive the expression of reporter molecules—such as GFP or mCherry-in order to visualize the state of the toggle switch. Most importantly, the bistability of the simple genetic feedback loop can be initially overcome by the introduction of the small signaling molecules aTc and IPTG, which inhibit the ability of TetR and LacI proteins, respectively, to bind to each other's promoter. Once aTc or IPTG is introduced into a cell culture, the feedback through the simple regulatory network perpetuates the LacI or TetR expression state, respectively, as well as the expression state of any of the proteins that share their promoters.

While the development of these toggle switches has typically assumed a deterministic model of the toggle switch, stochasticity may alter the long-term state of these systems in subpopulations of cells [118-119]. Transitions to the alternate state under a genetic toggle system may come both from the introduction of new stimuli as well as the inherent noise in all biological systems [118]. Moreover, theoretical models predict that cell metabolic parameters such as the rates of protein synthesis and spontaneous unbinding of protein from DNA underlie the robustness of genetic toggle switches [120]. As cells endure stress and begin to exhibit stress responses associated with biofilm formation, these basic metabolic factors may be influenced in such a way that the toggle switch state stochastically switches to the alternate state.

The present study consisted of a series of experiments utilizing a genetic toggle switch to better understand the nuances of biofilm formation. The expression of the toggle-determined alternate GFP and mCherry reporter constructs under the stressful biofilm-like conditions in our microfluidic device provide insight into the stochasticity of gene expression in complex systems. The simplicity of this two-state toggle permits the examination of stochasticity in the simplest regulatory network.

4.3. Materials and Methods

4.3.1. Manufacture of microfluidic device

Master mold fabrication. All master molds were fabricated in the MICRON facility. Photomasks were drawn in AutoCAD (Autodesk, San Rafael, CA, USA), printed onto transparency film by CAD/Art Services, Inc. (Output City, Poway, CA, USA), and mounted onto glass plates (McMaster-Carr, Los Angeles, CA, USA). The first layer of the master mold was created by first spin-coating with SU-8 2000 negative photoresist (MicroChem Corp., Newton, MA, USA) onto clean silicon wafers to 0.96 μm in height using a WS-650-8B programmable spinner (Laurell Technologies Corp., North Wales, PA, USA) and then using a MA/BA6 UV contact mask aligner (MicroTec, Garching, Germany) for subsequent UV exposure. After being exposed to UV radiation, the unexposed photoresist was rinsed away using developer (MicroChem Corp.). For the second layer, the SU-8 2010 negative photoresist was spin-coated on top of the first layer to achieve a height of 10 μm. Again, the MA/BA6 UV contact mask aligner was used for UV exposure, and the unexposed photoresist was rinsed away using the same process described above.

PDMS device fabrication. Replica molds were created from master molds by mixing PDMS/Sylgard 184 (Dow Corning, Midland, MI, USA) with a 10:1 ratio of the elastomer base to curing agent, degassing in a vacuum desiccator for 1 h, and curing in an oven at 90°C for 2 h. Following removal of the PDMS, devices were cut, holes were punched for ports, and the cell was cleaned with filtered DI water and then permanently bonded to clean coverslips (Thermo Fisher Scientific, Waltham, MA, USA) via exposure to O_2 plasma for 1 min in a PDC-32G plasma cleaner (Harrick Scientific, Ithaca, NY, USA).

4.3.2. Characterization of the toggle

Exponential batch culture. To characterize the performance of the toggle circuit we conducted a series of experiments. The cells were first grown overnight in LB media with 100 μg/ml Cb from a frozen stock. At the beginning of the experiment, overnight grown cells were diluted 1:200 in fresh M9 media with 100 μg/ml Cb including aTc (final concentration of 10 ng/ml) or IPTG (final concentration of 1 mM) and once again grown and kept at exponential growth. Once

the toggle was induced to either state, the inducers were removed by providing fresh media to the culture after centrifugation and removal of the supernatant. The fluorescent intensity was measured at given times by diluting each sample 1000-fold using phosphate-buffered saline (PBS) and collecting 10 000 events per replicate using a BD Accuri™ C6 (BD Bioscience, Piscataway, NJ, USA).

Stationary batch culture. All experiment conditions were identical to the exponential batch culture procedure. However, in this case, the cells were maintained in stationary phase after providing fresh media to the culture after centrifugation and removal of the supernatant. Cell were also maintained at 37°C before flow cytometry analysis.

4.3.3. Maintenance and monitoring of cell growth in microfluidic channels

Microfluidic cell culture. The recombinant *E. coli* cells were loaded into the trapping channels of the microfluidic device by directing the flow in the direction from the cell port to the waste port. Upon trapping a few cells in each region, the flow was reversed and slowed to steadily supply the cells with fresh nutrients from the media port through a combination of diffusion and advection. The cells were maintained at 22°C and grown to fill the chamber over a duration of 20–30 h.

Cell microscopy. Cell images were acquired using an inverted epifluorescent microscope (Ti-E; Nikon Instruments Inc., Tokyo, Japan). DIC and fluorescent images were captured every 15 min, and focus was maintained automatically using Nikon Elements software.

4.4. Results and Discussion

4.4.1. Evaluation of stochastic gene expression in microenvironments utilizing the toggle switch

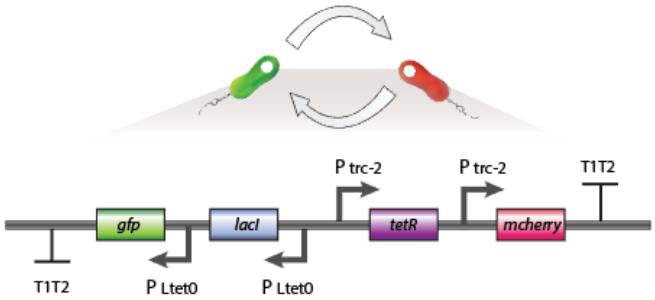

Figure 4.1. Schematic of the toggle switch circuit. A genetic toggle switch was used to examine stochastic gene expression in a system with a marginally higher degree of complexity. The toggle consists of two different proteins with mutually repressive effects, LacI and TetR, driven by two independent promoters, P_{LtetO} and $P_{trc\text{-}2}$, respectively. In this system, LacI and TetR repress each other's expression by binding to the other protein's promoter and thereby inhibiting expression. The toggle used in this study remains bistable when bacterial cultures are continually maintained in the exponential phase.

Previously, we have reported stochastic gene expression in biofilm-like microenvironments using bacterial cells harboring a *gfp* gene driven by a Plux promoter [68]. We showed that the receiver component of the quorum sensing circuit could be stochastically triggered in the absence of the inducer chemical. In this research, we further discuss stochasticity in identical microenvironments using the same microfluidic device described previously. However, in this study, by utilizing bacteria containing a bistable switch (Figure 4.1), we were able to study stochastic gene expression with a higher degree of complexity. The behavior of the toggle-containing *E. coli* has been fully characterized in a previous study [102]. A toggle switch is a circuit that can switch between two stable states, ON and OFF (Figure 4.1). This toggle utilizes the TetR and LacI transcriptional repressors, which bind aTc and IPTG, respectively; the toggle is activated in different directions by the addition of aTc or IPTG. The addition of aTc inactivates TetR from the P_{LtetO} promoter and thus drives high levels of LacI expression, indicated by high GFP, thereby maintaining low TetR protein concentrations. The toggle can also be flipped to the opposite side

by adding IPTG; when supplemented with IPTG, LacI is inactivated from the P_{trc-2} promoter, which toggles the system towards high levels of TetR expression, indicated by high mCherry, and thus reinforces low LacI concentrations (Figure 4.2, in which aTc and IPTG are induced overnight). This toggle was used to examine stochastic gene expression more fully. As each of the elements of the toggle regulates the other, the complex gene circuit was deemed to be an informative experimental subject for stochastic gene expression under growth-limiting conditions.

4.4.2. Evaluating the toggle under exponential batch culture

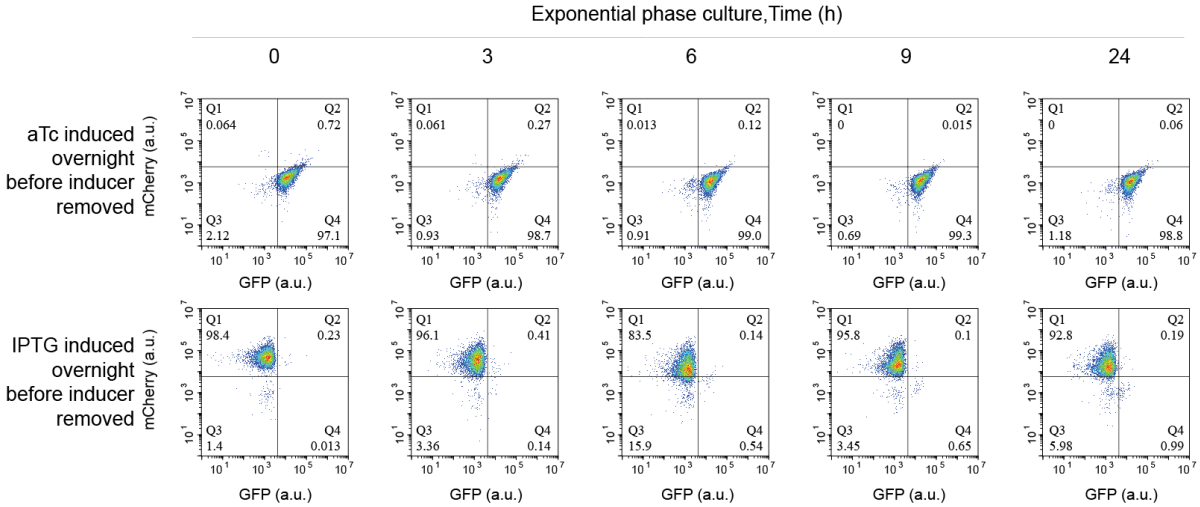

Figure 4.2. Schematic of a balanced toggle under exponential batch culture, the traditional approach for evaluating a toggle circuit. Once the toggle-harboring *E. coli* cells were induced to either state of the circuit, using supplemental aTc or IPTG, the inducers were removed and cells were exponentially cultured in M9 media over a 24-h period. The four quadrants (Q1–Q4) indicate high-mCherry, high-GFP and mCherry, no fluorescent expression, and high-GFP, respectively.

Many studies have evaluated the stability of this toggle and similar systems [111, 121]. Here, we report results that support those of previous studies. In this research we did not use LB media because it contains lactose, which can affect the P_{trc-2} promoter; instead, we utilized M9 media containing 0.2% glycerol and 0.2% casamino acids. First, the bacteria cells were inoculated into test tubes with M9 media and induced overnight by the addition of aTc or IPTG (10 ng/mL and 1 mM, respectively). Once the toggle was induced to either state, we removed both inducers by providing fresh media to the culture after centrifugation and removal of the supernatant and

fluorescent expression levels were recorded using a flow cytometer at a 1:1000 dilution. During the 24-h culture, the cells were manually diluted with fresh M9 media and maintained in exponential growth. The flow cytometry analysis revealed that the cells maintained their initial state, depending on aTc or IPTG induction, throughout, as evidenced by cell counts in quadrant 4 or 1, representing high-GFP or high-mCherry expression states, respectively, consistent with previous results [102] (Figure 4.2).

4.4.3. Evaluating the toggle under stationary batch culture

In stationary batch cultures, as stochastic quorum sensing has been shown in previous studies utilizing the receiver circuit [68], we also expected to observe stochasticity within the bacterial colonies influencing the toggle switch. Additionally, the toggle introduced a higher degree of complexity, compared to the relatively simple receiver circuit, because this system consisted of two proteins that regulate each other via their effects on the promoter upstream of each protein. By utilizing different sets of proteins that repress functionality, we sought to further evaluate the maintenance of protein functionality in a stressful environment, beyond the stochastic expression of the protein itself.

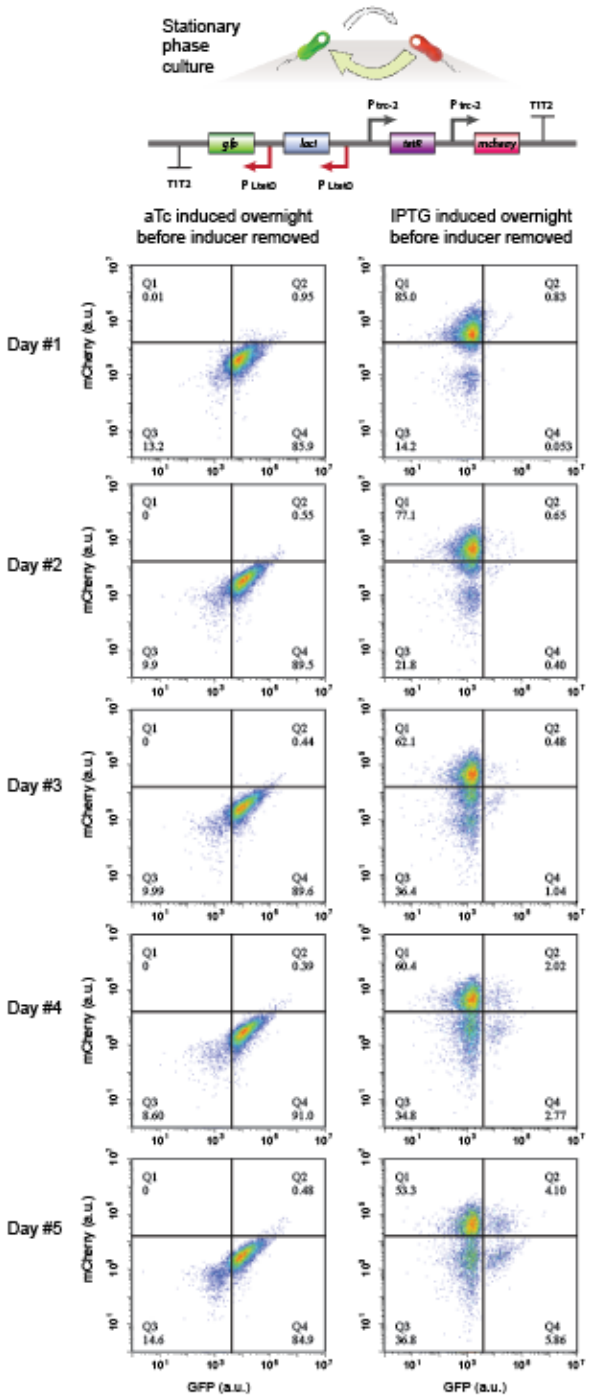

Figure 4.3. The toggle-containing *E. coli* cells cultured in stationary phase in batch cultures over a 5-day period. The cells were first induced to either side of the toggle prior to the experiment and inducer compounds were removed on day 1. Cells that were induced with aTc showed stable expression of the GFP state over the duration of the experiment (Q1; left panels). However, cells that were induced with IPTG showed a relatively high degree of biased expression of mCherry

(Q1; right panels) to GFP (Q4). The four quadrants (Q1–Q4) indicate high-mCherry, high-GFP and mCherry, no fluorescent expression, and high-GFP, respectively.

First, cells containing the toggle circuit were inoculated into M9 media containing either aTc or IPTG. Once the cells reached exponential growth, the cells were removed from the inducer via centrifugation and replacement of the supernatant with fresh M9 media containing antibiotics. During the 5-day experiment, deionized water was added to account for evaporation and maintain a constant final volume. The initial cell state was measured as described above. The cells that were induced with aTc steadily expressed GFP throughout the 5-day experiment (Figure 4.3, left panels). More than 85% of the population maintained the GFP expression state in Q4, with less than 0.01% reverting to the alternate state indicated by mCherry expression in Q1. On the other hand, cells that were induced with IPTG showed an incomplete reversal of expression towards the opposite toggle state (i.e., the GFP expression state) throughout the 5-day experiment (Figure 4.3, right panels). Initially, 85% of these cells expressed mCherry (Q1) on the first day of the experiment. However, the number of cells that exhibited GFP expression (Q4) increased from 0.053% on day 1 to 5.86% on day 5, representing a dramatic increase in the biased gene expression throughout the duration of the experiment. We thought that the increase in GFP expression could be primarily explained by the stochastic bursting of the P_{LtetO} promoter. As discussed in previous reports, cells kept under stress conditions with minimum nutrients can exhibit changes in the regulation of transcription and translation [68]. We later discuss why only one of the promoters exhibited this change over time.

4.4.4. Characterization of the toggle under biomimetic biofilm channel culture

After confirming that the toggle circuit cells had a bias towards the GFP-expression state when grown in stationary cultures, we further sought to assess these effects in our biofilm-like microfluidic device. As described using receiver cells in previous reports [68], the toggle circuit cells were inoculated into the biofilm-like channel for long-term observations. The height of the biofilm-like channel (0.97 μm) partially restricted cell motility and allowed the observation of the state of individual cells over the course of the experiment. Stochastic burst-like expression of a quorum-sensing gene without a signaling molecule had been previously observed based on GFP

expression within the deeper regions of the biofilm-like channel, approximately 250 µm from the main flow channel [68]. In the context of this experiment, stochastic events may be defined as the expression and accumulation of the fluorescent protein in the absence of an inducer. We may also monitor stochastic events in terms of how the cells with a toggle switch maintained a stable balance of bidirectional gene expression patterns when maintained in localized environments within the microfluidic channel.

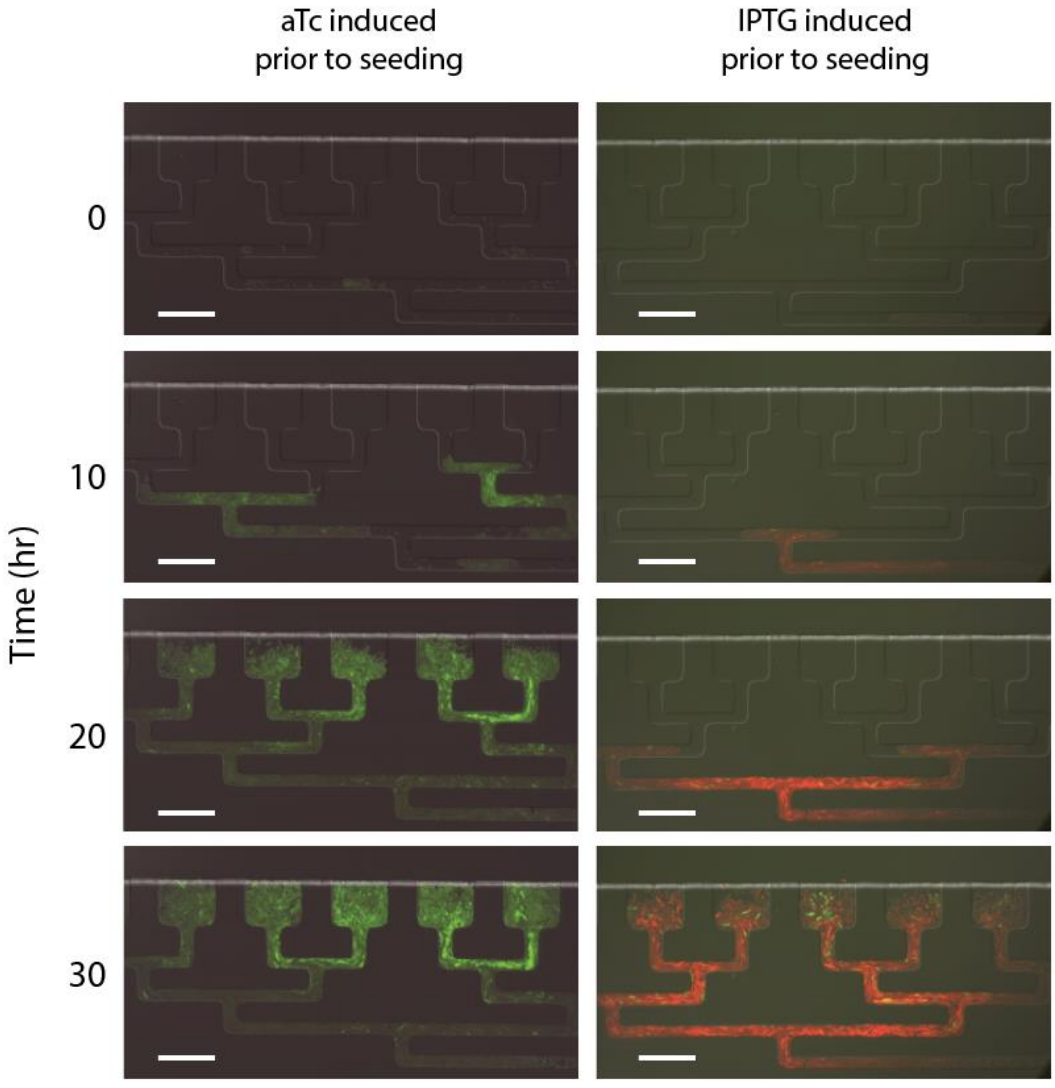

Figure 4.4. Cells with the toggle circuit cultured inside a biomimetic biofilm channel after induction to either toggle state. Cells that were initially induced with aTc showed stable GFP expression throughout the duration of the experiment. However, cells that were induced with IPTG

showed initially uniform mCherry expression and stochastic GFP expression originating from deeper regions within the channel. The cells were observed over a 30-h time period. All scale bars indicate 50 μm.

First, aTc-induced cells were inoculated into the microfluidic channel, and a few isolated colonies began to grow, subsequently merging into a large monolayer that filled the entire chamber. The entire chamber regions were fully occupied after 20 h, and higher levels of GFP expression were observed approximately 120 μm from the main flow channel (Figure 4.4, 20 h in left panels). When comparing these results to previous studies using receiver cells [68], the main flow media used in each experiment must be fully considered. In this set of experiments, M9 media was used, which contains considerably lower levels of nutrients, and thus may thus explain discrepancies between the results of the two studies. For example, under nutrient-deficient conditions, such as those occurring in cultures using M9 media, the heterogeneous stochastic burst-like expression and changes in the toggle state may be more common within the biofilm-like channel. However, higher levels of GFP expression were observed in localized regions of the microfluidic device, and cells consistently maintained a high-LacI expression state, as demonstrated by the visualization of GFP-expressing cells both proximately to the main flow channel (Figure 4.4, 30 h in left panels, arrow).

In contrast, a portion of the IPTG-induced cells expressed the alternate toggle state, i.e., more than 5% of cells stochastically expressed GFP, rather than mCherry (Figure 4.4, IPTG induced, 30 h). Though most of the chamber regions were dominated by mCherry-expressing cells, not all of the cells stably maintained the high-TetR expression state, i.e., the mCherry expression state. This heterogeneity may have been a consequence of the nutrient-deficient conditions, which may have consequences on the stability of genetic toggle switches [120]. We observed a small population of cells that flipped towards the opposite toggle state and thus began to express GFP. This phenomenon was initially detected in the deeper regions of the chambers (Figure 4.4, 20 h in right panels) and gradually dispersed within the microfluidic channel as the subpopulation of stochastically triggered GFP cells generated daughter cells, which maintained their altered expression state (Figure 4.4, 30 h in right panels). These findings were consistent with previous batch culture results. As reported previously [68], biofilm colonies can also have distinct differences

in gene expression owing to transport-dependent signaling states. In other words, there is high nutrient availability and removal of cellular waste products at the biofilm–flow interface, which provides bacteria with the appropriate conditions for robust growth and thus stabilizes gene expression patterns. In contrast, within inner parts of the biofilm channel, where nutrient concentrations are lowest, a lack of nutrients can cause starvation-induced stress responses, i.e., stochastic GFP expression in high-TetR state cells.

We also sought to understand the stochasticity of high-TetR-expressing cells. This requires the consideration of additional factors, such as regulatory networks within *E. coli* that may influence the state of the toggle. Our results suggest that the toggle is biased towards a high-LacI state owing to the P_{trc-2} promoter originating from a chimeric lacUV5 and trp promoter, both of which were isolated from *E. coli* [122], as well as the P_{LtetO} promoter originated from an Enterobacteria phage λ [123]. Elements from the *E. coli* genome will have a regulatory effect on a promoter isolated from *E. coli*; however, we hypothesize that *E. coli* regulatory networks will have a minimal effect on a promoter originating from a viral source. In this way, stochasticity of high-LacI-expressing cells will be triggered in conditions in which nutrient levels are low, causing starvation-induced stress responses.

4.5. Conclusion

Stochastic gene expression revealed in relatively simple inducible genetic systems also appears in the bistable genetic toggle switch system examined in the present study. Previous research revealed that cell culture in the biofilm-mimicking microfluidic device could drive expression of genes generally associated with biofilm formation, as demonstrated by patterns of GFP expression in the device [68]. In the current toggle switch system in the same culture device (though with M9 medium instead of LB medium), stochasticity was also observed, though it was asymmetric between the two toggle switch states. Specifically, induction of the genetic toggle with aTc consistently drove GFP expression in the culture. Neither spurious expression of the mCherry reporter nor stochastic switching of the genetic toggle switch was observed when cells were induced with aTc. Less than 0.01% of GFP-expressing cells expressed mCherry. However, the

long-term effect of IPTG induction was not as consistent. When induced with IPTG, cells within the microfluidic device overwhelmingly expressed mCherry on day 1, with only 0.053% of cells expressing GFP. By day 5, many more cells (5.86% of those observed) expressed mCherry instead of GFP. Moreover, this reverted expression state was inherited by daughter cells, as confirmed by continuous microscopic observation, which was enabled by the design of the microfluidic device.

The current study differed from previous research using this biofilm-mimicking microfluidic device in one key factor—the medium used. Here, M9 medium was used instead of LB medium for the bacterial culture in order to ensure the genetic toggle switch functioned properly. (LB medium can interfere with LacI, a repressor protein element of the toggle switch.) Accordingly, previous experiments should be repeated using M9 medium instead of LB medium to ensure that the observed differences were not caused by the difference in media. It is likely that using M9 medium instead of the more nutrient-rich LB medium will result in an increased level of stochastic burst-like expression observed in previous experiments. As stochasticity in toggle switches may be an important factor in both synthetic biological applications as well as understanding naturally occurring genetic regulatory networks, future research should examine robustness of these systems by examining gradients of stress stimuli.

CHAPTER 5.

STOCHASTIC PHENOTYPIC EXPRESSION OF SINGLE BACTERIAL CELLS CONFINED IN A MICROFLUIDIC CHANNEL

5.1. Abstract

Bacterial growth in harsh environments, including environments with spatial and nutrient limitations, has been a focus of research owing to the obvious and wide biological and human health implications. However, it is difficult to distinguish noise (i.e., statistical and measurement error) from individual among-cell variation under conventional culture methods. In order to characterize individual cell properties, we studied the stochastic growth of *E. coli* cultured in a biofilm-mimicking microfluidic device. Utilizing the narrow device aperture (determined by the diameter of *E. coli* cells), target cells were selectively isolated from a mixed population, and their morphological properties, growth, and fission were observed by microscopy at a fine timescale. This system enabled the tracking of cells of interest (i.e., large cells) and the observation of characteristic patterns of growth and aging, including an increased volume prior to cell division and eventual apoptosis. Additionally, this behavior was associated with changes in cell wall properties after a limited number of divisions, yielding daughter cells with relatively short lifespans. Furthermore, we observed variation among target cells in morphology and survival (e.g., one cell survived the full study period). These findings demonstrate the suitability of the microfluidic device for characterizing the responses of single cells and microbial populations to various environmental conditions and stimuli.

5.2. Introduction

In clonal bacterial cultures, a small inoculum can multiply into hundreds of millions of cells that are assumed to be essentially identical in general. Bacteria, however, often persistently retain individual characteristics, as each cell may evolve from ancestors with distinct genetic characteristics [124]. This individualism is readily observed by measuring morphological changes in single cells under microscopy in real time. Selection among such individual bacterial cells endows populations with the ability to survive through adaptive evolution even within particularly hostile environments, for example, under limitations in nutrition and space [68]. Under nutritional imbalance, a bacterial culture reaches stationary phase, at which the metabolism of cells can become dormant, thus maintaining a constant or stationary cell density, which may further involve genetic switches [68]. In many natural habitats, bacteria live in spaces of less than a micrometer in width; bacterial growth and motility under such restrictions are highly relevant to research in diverse fields including soil microbiology, water purification, and many biomedical disciplines [125]. Although there is an essential need to understand the effects of bacterial growth under severe constraints, such studies have been uncommon. Many basic questions about the law describing bacterial growth under constraint, i.e., the function describing the size of an individual cell over time, remain; it is also unknown whether cells specifically react to their own size, age, or particular molecular features to initiate cell division [126].

Soft-photolithography is a technology with the potential to construct artificial bacterial habitats that mimic the natural constrained habitats in which individual cells grow and divide [68]. The growth and division of individual cells are fundamental events underlying many biological processes, including the development of organisms and tumors as well as pathogen–host interactions [126]. Some important aspects of microfluidic cell culture systems have previously been reviewed in detail, including the effect of surface modification on cellular behavior, cell biology, cell culture models, cellular analysis, cellular microenvironments, cell secretion, and more [127]. With microfluidic devices, researchers can closely mimic a cell's natural microenvironment, for example, by continuous perfusion culture or by creating chemical gradients. Specifically, a microfluidic device that mimics bacterial biofilm environments has been previously constructed to observe bacterial growth under stochastic conditions [68]. Such microfluidic techniques may

further facilitate studies of the characteristics of small numbers of cells or single cells at high temporal and/or spatial resolution via automation, parallelization, on-chip analyses, or direct coupling to downstream analytical chemistry platforms [127]. At the same time, this approach offers benefits including the reduced consumption of reagents, limited contamination risk, and efficient high-throughput experimentation. Recently, the quantitative study of single cells under consistent physiological conditions has been conducted through a unique combination of measurement and analysis technologies together with mathematical modeling [126]. Microfluidic technology may be used to provide bioreactors that closely resemble natural habitats and thus reveal the interplay between critical cell culture parameters and micro-environmental conditions [128].

Certain analytical methods may be necessary for accurately characterizing the behaviors of single cells grown in microfluidic devices, including phenotypic changes and cell division. Studies that require isolation of cells according to phenotype, for instance, to study cell aging, have relied on laborious processes for sorting and manipulating cells. In one notable study, a microfluidics-based cell culture device was used to facilitate cell isolation based on phenotypic markers such as cell size, permitting real-time microscopic observation [126]. In this technique, single cells of different sizes, i.e., ranging from normal cells to expanded or swollen cells, were separately confined within PDMS chambers to demonstrate that these morphological changes were not only maintained across generations, but also had a unique role in the timing of the processes of aging and cellular apoptosis. Another study used time-lapse fluorescent microscopy to show that bacteria exhibit morphological adaptations within sub-micron-diameter pores and cavities that were unexpectedly productive bacterial habitats [125]. Adaptive potential was observed in *E. coli* cells that, despite their considerable restriction, still grew and divided within the narrow channels. The plasticity of these *E. coli* cells was substantially enabled by their thin cell walls, measuring only approximately 3 nm in thickness [129].

We have studied the stochastic growth of an elastic bacteria (i.e., *E. coli*) cultivated in a biofilm-mimicking microfluidic device that permits detailed analyses of single-cell growth and division, which might otherwise be impractical owing to the intrinsic noise of biological processes. This analytical limitation was overcome by monitoring cellular behavior and morphological changes of bacterial cells using real-time microscopic observation. The ability of individual cells

to metabolically adapt and produce similarly adapted daughter cells may have many different effects. For example, daughter cells may exhibit size expansions that indicate successful metabolic adaptation to the stressful environments individual cells experience. The target cells were observed by selectively isolating them from a mixed population and confining them in place under conditions that allowed subsequent viability and potential clonal expansion. To achieve this end, we developed a microfluidic device comprising cell chambers and convoluted paths with a limited aperture that is slightly narrower than the diameter of *E. coli* cells (approximately 1 μm). As the adapted single cells exhibited increased cytoplasmic volume, they were constrained between the bottom and top walls of the channel with normal cells simultaneously exiting into the main channel. This confinement technique enabled the real-time microscopic observation of morphological changes of each individual cell, with images continuously captured to follow growth and division at predetermined time points.

5.3. Materials and Methods

5.3.1. Manufacture of microfluidic device

Master mold fabrication. All master molds were fabricated in the MICRON facility. Photomasks were drawn in AutoCAD (Autodesk, San Rafael, CA, USA), printed onto transparency film by CAD/Art Services, Inc. (Output City, Poway, CA, USA), and mounted onto glass plates (McMaster-Carr, Los Angeles, CA, USA). The first layer of the master mold was created by first spin-coating with SU-8 2000 negative photoresist (MicroChem Corp., Newton, MA, USA) onto clean silicon wafers to 0.96 μm in height using a WS-650-8B programmable spinner (Laurell Technologies Corp., North Wales, PA, USA) and then using a MA/BA6 UV contact mask aligner (MicroTec, Garching, Germany) for subsequent UV exposure. After being exposed to UV radiation, the unexposed photoresist was rinsed away using developer (MicroChem Corp.). For the second layer, the SU-8 2010 negative photoresist was spin-coated on top of the first layer to achieve a height of 10 μm. Again, the MA/BA6 UV contact mask aligner was used for UV exposure, and the unexposed photoresist was rinsed away using the same process described above.

PDMS device fabrication. Replica molds were created from master molds by mixing PDMS/Sylgard 184 (Dow Corning, Midland, MI, USA) with a 10:1 ratio of the elastomer base to curing agent, degassing in a vacuum desiccator for 1 h, and curing in an oven at 90°C for 2 h. Following removal of the PDMS, devices were cut, holes were punched for ports, and the cell was cleaned with filtered DI water and then permanently bonded to clean coverslips (Thermo Fisher Scientific, Waltham, MA, USA) via exposure to O_2 plasma for 1 min in a PDC-32G plasma cleaner (Harrick Scientific, Ithaca, NY, USA).

5.3.2. Maintenance and monitoring of cell growth in microfluidic channels

Microfluidic cell culture. The recombinant *E. coli* cells were loaded into the trapping channels of the microfluidic device by directing the flow in the direction from the cell port to the waste port. Upon trapping a few cells in each region, the flow was reversed and slowed to steadily supply the cells with fresh nutrients from the media port through a combination of diffusion and advection. The cells were maintained at 22°C and grown to fill the chamber over a duration of 20-30 h.

Cell microscopy. Cell images were acquired using an inverted epifluorescent microscope (Ti-E; Nikon Instruments Inc., Tokyo, Japan). DIC and fluorescent images were captured every 15 min, and focus was maintained automatically using Nikon Elements software.

5.4. Results and Discussion

5.4.1. Stochastic growth of single cells under spatial limitation

We manufactured a microfluidic device that mimics the type of biofilm structure that typically forms during adaptation to hostile environments. The biomimetic device consisted of a three-port microfluidic channel with two inlets and one outlet (Figure 5.1a). The main observation

region of the device contained two elements: a series of distinct rectangular cell chambers and a convoluted path connecting the series of chambers (Figure 5.1b). The interior side of the chamber elements opened to the main flow of the medium. The convoluted pathways, however, progressively converged into a single channel, eventually leading to a closed end. The cell chamber region and convoluted pathway both had a maximum height of 0.97 μm. Since *E. coli* cells have a diameter of approximately 1 μm, the height of the trapping region permitted linearized observations of confined cells. The device was also designed to discharge cells from the device continuously through the main flow channel (12-μm height).

Since the convoluted pathways were constructed to maintain a limited height not exceeding the dimensions of bacteria under cultivation, the conditions, i.e., the spatial limitation, could be unfavorable to cells. Cell growth within the narrow channel may further generate a stressful environment and eventually exhibit stochasticity caused by the spatial limitation and nutritional imbalance. This was demonstrated in our previous study showing stochastic burst-like expression of genes within deep regions of the channel using the same device [68]. We further propose in this study that such stochastic conditions can result in phenotypic variation, such as morphological changes, as seen in individually confined bacterial cells [125]. This can occur when individual cells uniquely recognize the hostile surrounding environment, resulting in stochastic morphological changes in single cells via genetic switches, epimutation, or even extraordinarily rare mutations (Figure 5.1c). The shape may vary depending on the confined spatial geometry of a particular culture device [130]. Although cells may divide and grow in hostile surroundings, the culture may not be sustainable compared to normal culture conditions.

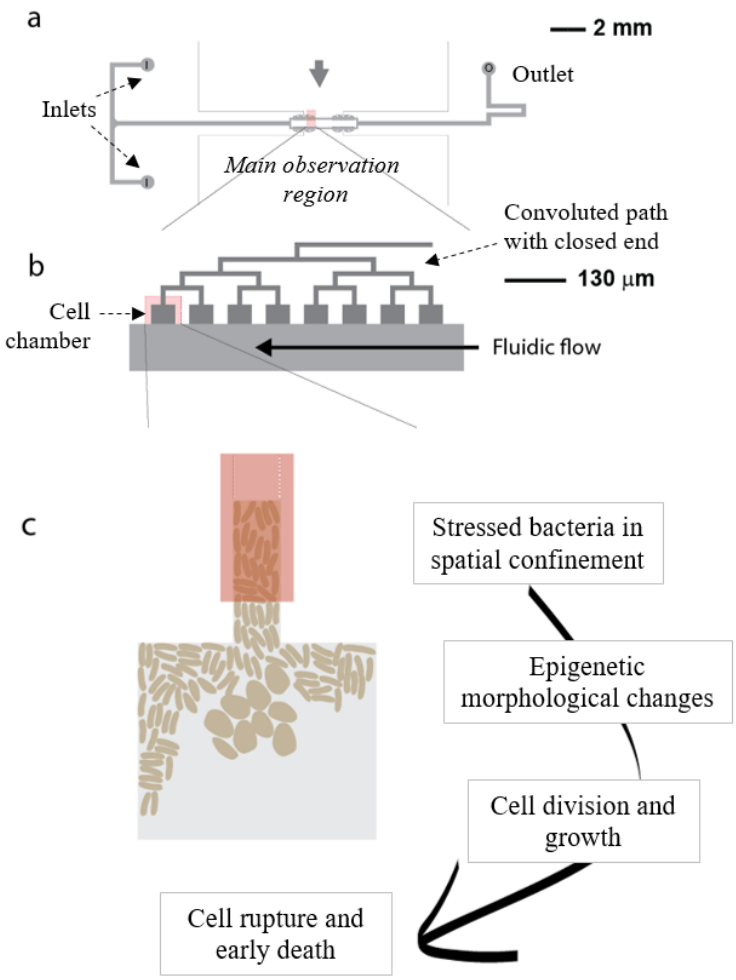

Figure 5.1. A diagram of the device's structure, which mimics a typical biofilm structure, and the interconnected fluid paths from which bacterial colonies are able to grow. (a) The design of the microfluidic device used in this study. Gray circles indicate two inputs on the left and an output on the right side of the channel. The two inputs supply microbial cells and culture medium, while the output permits the disposal of waste. (b) The interconnected region of the device, which mimics biofilm structure, contains rectangular cell chambers adjacent to the central flow channel. (c) The cell chambers are each limited to a height of 0.97 μm, which imposes limited growth conditions on the bacteria (shown as oblongs).

To trigger the stochastic phenotypic change, we cultured quorum-sensing recombinant cells within the biofilm-mimicking microfluidic device and then observed the morphological changes of certain subpopulations in comparison with neighboring normal cells.

5.4.2. Microfluidic environment for individual cell growth

A synthetic receiver circuit (P_{lux}-driven) has been previously designed to assess stochastic quorum sensing [68]. *E. coli* transformed with the receiver plasmid GFP upon chemical induction or induction via environmental stimuli [68]. The cells were inoculated in the biomimetic biofilm channel device and maintained at 22°C. During the observation (Figure 5.2), the cell divisions of parental cells were tracked, as indicated by the red arrow at 0 min. After 45 min, the cells divided and generated two daughter cells. The second cycle of division was also detected within the subsequent 45-min period, indicating a doubling time of the cells of approximately 45 min under the culture conditions.

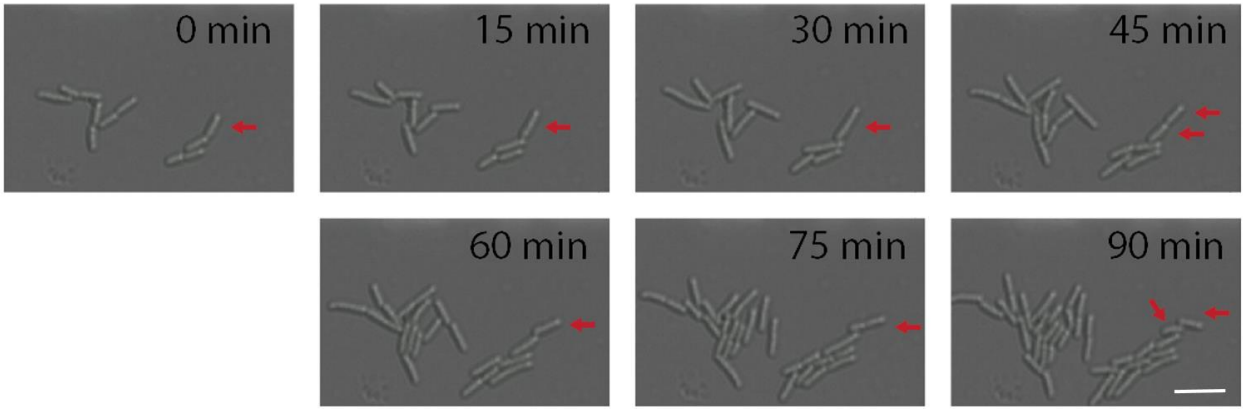

Figure 5.2. Growth kinetics of the quorum-sensing cells within the biomimetic biofilm channel. Single red arrows within a frame show the parental cell. At approximately 45 min, the parental cell divided into two daughter cells. The second cycle of division is shown in the subsequent frames. The cell located on the top of the frame at 45 min was tracked for an additional division cycle, shown occurring over the same time interval. All experiments were conducted at 22°C, and sequential snapshots of a typical experiment are presented.

Long-term morphological changes of bacterial cells grown within the microfluidic device were then monitored by microscopy (Figure 5.3). A few receiver cells as inoculum were detected at the beginning of cultivation (0 h) and subsequently grew over time into a large mono-layer of colonies that filled the microfluidic chamber (typically after 10 h). During the first 30 h, no individual cells showed significant morphological changes. However, after 30 h, a cell population

with a distinct appearance from that of normal cells, i.e., with a typically swollen exterior shape, was found in the observation chamber (Figure 5.3, dotted circle in 40-h image). The population size of the swollen cells varied during the cultivation period up to 72 h, indicating that the morphologically unusual cells grew and also ultimately underwent death by cell rupture (see the cells indicated by red arrows in the images at 50 h and 60 h). This revealed that the life span of these cells decreased under these stressed conditions, which may appear to be inherited by daughter cells (see below for further discussion).

We propose that this swollen and expanded cell morphology may have originated from a single bacterial cell under stressed conditions that developed a mutation or triggered a stochastic genetic switch. As mentioned earlier, two typical constraints, spatial confinement and nutritional deficiency, affected the bacteria grown in the biofilm-mimetic microfluidic device. These conditions may trigger stochastic conditions that promote such changes, as observed of individual cells growing in deeper regions of the channel. Such stress can typically cause morphological changes, such as swelling resulting from defects in the cell wall structure [125, 131]. Identical experimental conditions can also result in stochastic burst-like gene expression, as previously reported by our research group.

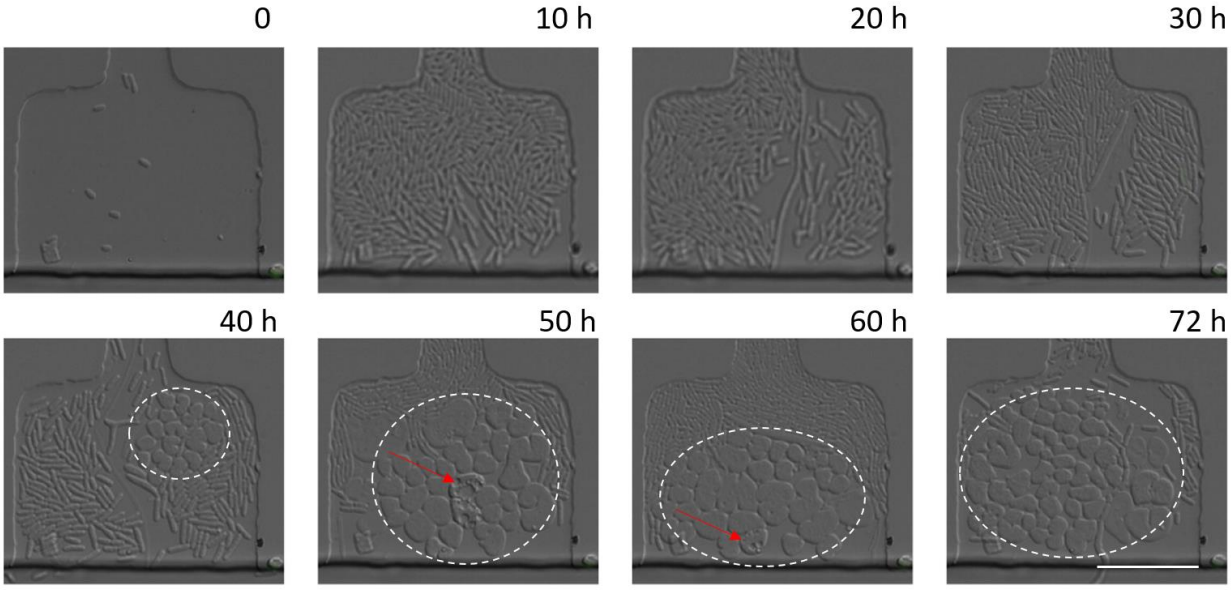

Figure 5.3. Structural changes of single cells maintained within the biomimetic biofilm channel over a long-term period of 72 h. Scale bar indicates 25 μm.

To characterize the stochastic growth, we closely observed the morphological changes of single cells cultured in the microfluidic channel by capturing a time series of cell images at a fine temporal scale. The cells were further monitored to determine whether the changes were maintained by observing the division and death of altered cells, as described in the following sections.

5.4.3. Morphological changes induced by stochastic growth

As the prominent morphological change was observed between 30 and 40 h, as shown in Figure 5.3, cell images throughout this period were captured at a high frequency (Figure 5.4). Among those cells within the observation chamber, two single cells were identified in the image captured at 34 h 52 min (see the cells surrounded by white circles). These cells resembled other cells in the chamber, suggesting they typically appeared uniform under identical environmental conditions, or they were derived from the same parental cells. After exactly 45 min, each single cell divided into two daughter cells (refer to the image at 35 h 37 min), which also exhibited identical characteristics to those of the parental cells, as presented in Figure 5.2. However, over the next 45 min (i.e., at 36 h 22 min), the cells did not divide, but instead expanded substantially in volume. Moreover, this phenotype was generally maintained afterward and through subsequent cell divisions 35 min after the shape change was completed (see the image at 37 h 7 min; also refer to the next section for further discussion).

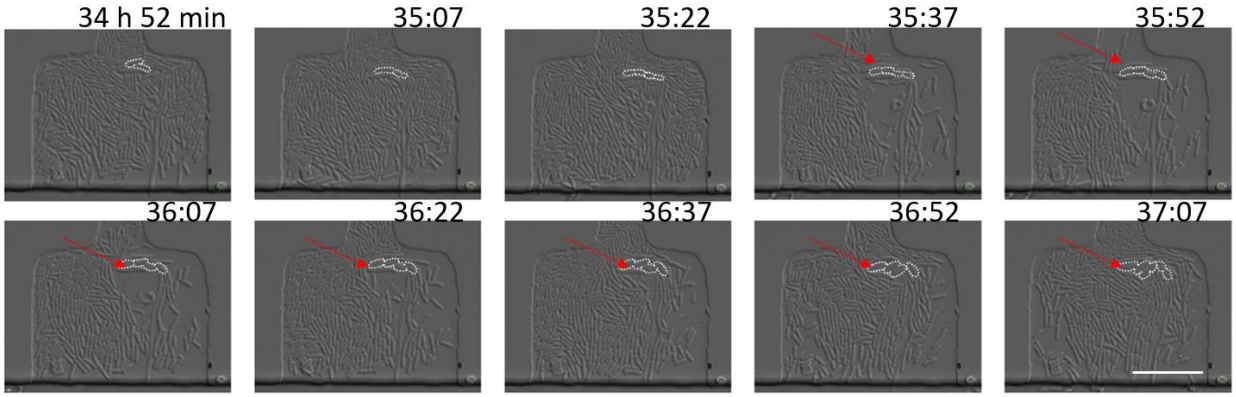

Figure 5.4. Monitoring of the morphology of single cells grown in the microfluidic chamber at a fine timescale. (Cell boundaries in the images have been enhanced for clarity.) Scale bar indicates 25 μm.

Even in clonal bacterial cultures, morphological changes can emerge from individual recombinant *E. coli* as a product of substantial stochastic variation [124]. The sophisticated microfluidic devices described in this study could be useful for probing the responses of individual cells to environmental cues. The device mimicked typical biofilm structure such that microbial cells were not only subjected to spatial limitation within the chamber, but also to irregular nutritional availability. Both factors could be sufficient to induce stochastic growth. Although the initial cultures were assumed to contain essentially identical cells, bacteria often exhibit high levels of among-individual variation [130]. We indeed were able to observe the individual cell behavior in this environment by measuring morphological changes using real-time microscopy. A similar study showed that stochastic variation in gene expression among single cells can lead to strikingly different phenotypes, even among genetically identical cells grown under constant conditions [132]. Usually, these stochastic differences can be attributed to complex multi-stable signal transduction networks that settle into different patterns as a result of small changes in initial conditions [133]. Phenotypic variability may be an important strategy for bacterial survival in an unpredictable environment [134-135].

Microscopic observation of phenotypic changes at the single-cell level could be essential to measure variation in individual cell size over time [126]. Bulk culture measurements are necessarily averaged over large numbers of cells, which can conceal cell-to-cell variability in division times, sizes at division, growth rates, and other properties [136]. Using a unique combination of microfluidic technologies, it has been shown that the sizes of individual cells increase exponentially over time [126]. In a minimal stochastic model based on an autocatalytic cycle, cells divided upon reaching a critical multiple of their initial sizes (approximately 1.8×), rather than an absolute size [137]. Indeed, we also observed that motile bacterial cells were captured within the microfluidic chamber geometry.

5.4.3. Distinct aging characteristics of cells under stochastic growth

After about 40 h from starting the culture, some individual bacterial cells appeared that were substantially larger than the other, normal cells within the microfluidic chamber (see Figure 5.3). The cells of interest in the mixed populations were fixed within the biofilm-like structures by the limited height of the chamber and were distinct from other cells based on their relative cell size. We subsequently investigated cellular behavior across generations, particularly cell aging, by continual microscope observations over time.

We extensively monitored the growth and death of cells with altered phenotypes by analyzing images captured every 15 min over a defined time scale (Figure 5.5). Six cells exhibiting morphological changes (indicated within the colored circles in Figure 5.5) were targeted for the purpose of monitoring over a period of 3 h 45 min (Figure 5.5; 46 h 53 min after inoculation). Cell #1 (Figure 5.5, in yellow), which was relatively larger than the other cells, had cell wall surfaces that appeared punctured after 1 h from the beginning of the period of intensive observation. This suggests earlier cell death compared with normal cells or necrosis by osmotic pressure (Figure 5.5, double arrows, 47 h 53 min). Cell #2 (Figure 5.5, in green) had a wrinkle, which may have been formed by compression within the observation chamber with restricted space, and divided 45 min after monitoring began (Figure 5.5, single arrow, 47 h 38 min). However, their cell walls ruptured shortly thereafter, similar to cell #1 (Figure 5, 48 h 8 min). Cell #3 (Figure 5.5, white) exhibited similar properties to those of cell #2 with respect to doubling and puncture, although death was delayed (Figure 5.5, 48 h 53 min). Cell #4 (Figure 5.5, red) exhibited significant growth, rather than division, as the culture continued, reached a maximum size (Figure 5.5, 48 h 38 min), and its cell wall eventually ruptured at 49 h 38 min. Cell #5 (Figure 5.5, blue) notably showed both size expansion (Figure 5.5, maximum at 48 h 53 min) and division (Figure 5.5, 49 h 8 min), and died 30 min afterwards. It should be noted that several holes, an indicator of death, were detected on the cellular surfaces prior to division (Figure 5.5, 48 h 38 min and 48 h 53 min). Cell #6 (Figure 5.5, orange), which uniquely survived throughout the monitoring period, underwent a volume expansion and surface-hole formation in the middle of the observation period (Figure 5.5, 49 h 38 min).

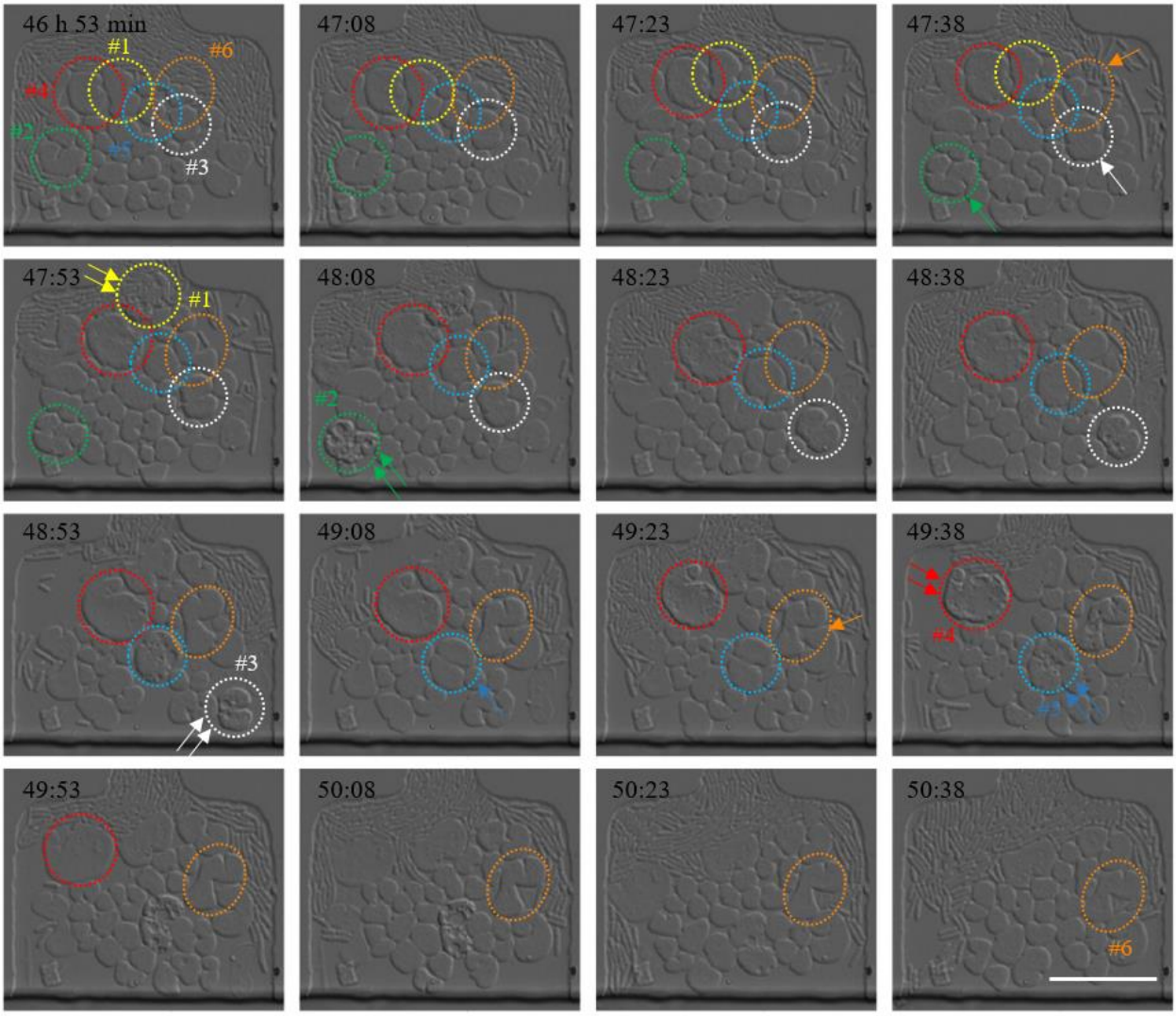

Figure 5.5. Image time series showing the cell life span under stochastic growth within the spatially confined chamber of the microfluidic device. Scale bar indicates 25 μm.

The growth and death of relatively large cells targeted for observation revealed clonal heterogeneity and aging under stochastic culture conditions. Observations of cell wall integrity, an indicator of cell viability, showed that the majority of cells (five out of six) expressed phenotypes consistent with apoptosis. They appeared expanded in volume prior to division, displayed a limited number of divisions before apoptosis, and gave rise to daughter cells with short lifespans. However, it was unclear whether the short lifespan was shared by other larger cells not observed during the predetermined period. This phenotypic variation may have been induced by age differences among the initially confined cells [126]. Normal bacterial cells with much smaller sizes

can quickly reproduce and form dense populations. As these cells were not tightly confined within the structures, they were able to flow out along the main medium flow into the microfluidic device, and the density was consequently variable. These results were consistent with those of a previous study revealing two distinct fates of yeast cells individually isolated within a microfluidic chamber [126, 131]. In this previous study, a single isolated cell proliferated in a typical manner and, in contrast, a confined larger cell exhibited limited cell divisions along with a substantial increase in cell size. Viability tests showed that the majority of cells that divided into dense populations remained viable, while the larger yeast cells displayed hallmarks of apoptosis.

Microscopic observations indicated that the apoptosis of larger cells was accompanied by cell wall rupture, as described earlier, which could be explained by a high osmotic pressure in the cytoplasm. Indeed, gram-negative *E. coli* cells have significantly thinner cell walls (only approximately 3 nm; [129]) than those of gram-positive bacteria (30–40 nm) [138]. The relatively thinner cell walls of *E. coli* do not allow the osmotic pressure to significantly exceed 2–3 atm [139]. This characteristic is associated with high plasticity, the ability to change in response to variable environmental conditions, such as mechanical stress and nutrient availability [125]. Thin cell walls, however, are more vulnerable to damage and, thus, aberrant morphologies can result from defects in cell walls [140]. The cell-wall defects likely formed in the microfluidic channel where *E. coli* underwent local, environmentally induced changes. Additional defects may have formed when the cells were confined within the narrow chamber for an extended time period, leading to the breakdown of peptidoglycan [125]. The mechanical stress may also disrupt the functioning of cytoskeletal proteins of *E. coli* in narrow channels, eventually resulting in cell death.

5.4.4. Stochastic growth of single cells that exhibit typical gene expression patterns

At a late stage in the observation period, a single cell expressed GFP, indicating the induction of the quorum-sensing gene circuit. As shown in the images captured after 59 h from the culture onset in Figure 5.6, a single cell divided into two daughter cells with a doubling time of about 45 min (Figure 5.6, between 59 h 7 min and 59 h 52 min). After 15 min, one of the descendants emitted green fluorescence and divided again in approximately the same doubling

time (Figure 5.6, 60 h 52 min). Both daughter cells displayed fluorescence, and the intensity increased gradually for the next 1.5 h (Figure 5.6, 60 h 52 min and 62 h 22 min). This phenotype was accompanied by an increase in cell size, without division. Thereafter, the fluorescence faded and was finally was lost after about 30 min. This may indicate stochastic quorum sensing as a stress response occurred in the absence of the inducing molecule, as demonstrated in a previous report [68].

Single cells exhibit phenotypic variation in response to local environmental conditions under stressful environments, as mentioned earlier. Cells, like all organisms, continuously adapt to varying conditions through the process of natural selection. Indeed, previous studies have demonstrated a remarkable ability for wild-type *E. coli* to produce a very large and broad array of irregular morphologies [131]. Although the frequency of divisions decreased as cell size increased, the accuracy of this type of division could remain essentially unaffected by the shape and size of the cell. Asymmetrical inheritance of cell properties can also generate phenotypic diversity [124, 141]. For example, striking individual differences resulting from variation among the chemotactic behaviors of individual *E. coli* cells [142] and among fluorescence signals from individual cells expressing a fluorescent protein have been observed [106].

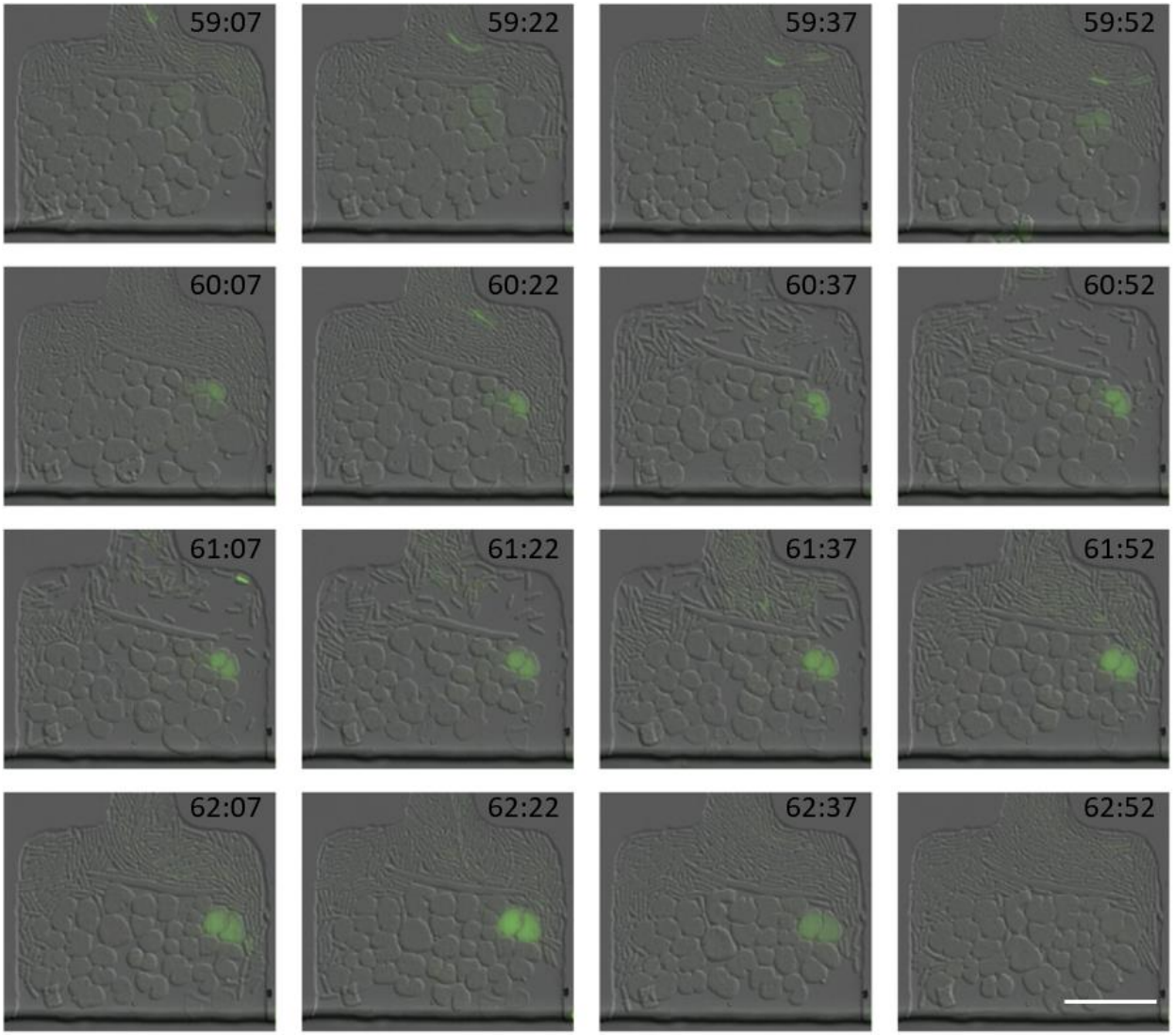

Figure 5.6. Stochastic phenotypic expression of the quorum-sensing signal of bacterial cells and cell division. Scale bar indicates 25 μm.

5.5. Conclusion

A microfluidic channel device that mimics bacterial biofilm structures was developed to grow elastic *E. coli* cells, which eventually displayed stochastic phenotypic expression as a stress response. Significant morphological changes were observed over the culture period, in addition to the expression of a quorum-sensing GFP reporter, without the application of an inducer molecule. The cell capture region for bacteria culture were specifically designed to have limited height of

<0.97 μm such that single cells with a swollen morphology were selectively confined within the channel structure and to provide culture conditions similar to those of natural biofilms. Microscopic observation of the isolated target cells revealed cellular expansion, low rates of cell division, and early apoptosis, which are characteristic patterns of stochastic responses of single cells to stressful conditions. In addition, stochastic quorum sensing in the absence of the AHL signaling molecule was observed from single cells, consistent with previous results. We were able to utilize the microfluidic device as an artificial biofilm model to further characterize the properties of microbial populations, e.g., their chemical resistance to drugs such as antibiotics.

CHAPTER 6.

BACTERIAL BIOFILM FORMATION AT THE INTERFACE OF WATER-IN-OIL DROPLETS SPATIALLY SEGREGATED WITHIN A MICROFLUIDIC DEVICE

6.1. Abstract

Biofilms are both a key research focus in fields spanning from microbial ecology to industrial food processing. They are also an important public health issue owing to the ability of biofilms to form even in harsh environments, including on medical equipment and in hospital settings, and their resistance to conventional antibiotics. Accordingly, efficient and scalable methods to screen biofilm control agents are of considerable practical value. To this end, we developed a water-in-oil droplet-based bioreactor that encapsulates bacterial cells in an aqueous core, with spatial segregation within microfluidic channels. The system was applied to the culture of engineered *Escherichia coli* with quorum sensing genes using the signaling molecule *N*-acyl homoserine lactone for visualizing biofilm consortia. We successfully observed initial bacterial growth and subsequent biofilm formation at the hydrophobic interface based on green fluorescent protein expression within the compartmentalized droplets. The droplet bioreactor developed in the present study has broad applications in future research. This system facilitates the culture of small aggregations of cells under controlled conditions such as the precise introduction of chemical compounds (e.g., AHL and other cell inducing or inhibitory molecules) to assay their effects on bacterial growth, biofilm formation, and visualize other fine-scale culture phenotypes. This system further allows multiplexed assays for drug screening against the bacterial populations comprised within biofilms.

6.2. Introduction

Many microorganisms are able to grow in various environments, which has serious human health consequences, e.g., foods, medical instruments, and drinking water pipelines [143-144]. Even from an initially small inoculum, microorganisms exponentially grow into colonies that continue unabated as long as permissive growth conditions are available. However, populations rapidly approach saturation under various stresses, including nutrient depletion and the accumulation of toxic metabolic compounds. Such conditions can cause epigenetic changes in microorganisms; these modifications have the potential to promote survival and can result in adaptation to the surrounding conditions through epigenetic mechanisms [143]. Repression and induction of genetic programs are activated by epigenetic switching mechanisms that facilitate long-term survival in hostile environments. One typical example is the formation of bacterial biofilms, which are mostly comprised of an extracellular matrix consisting of polysaccharides, cell debris, and nucleotides occurring at interfaces (e.g., liquid–solid, liquid–air, and liquid–liquid interfaces) [145]. As such, consortia of microorganisms are most often metabolically dormant and nonculturable, and they are notoriously difficult to control with traditional chemical compounds, such as antibiotics, which enables cells to persist [146]. Therefore, chemicals used to control bacterial growth in these unique bacterial habitats require further investigation in order to validate their efficacy for controlling biofilms. In order to screen appropriate effectors, conventional procedures based on microtiter plates or test tubes are inefficient with respect to cost and labor [146]. These conventional procedures used to screen for compounds and surfaces with favorable properties include the alamarBlue assay [146], adenosine triphosphate-driven luminescent assays [146], the Calgary biofilm device [147], and the crystal violet assay [148].

Conventional microbial tests have been conducted on the macro-scale, but these tests can be improved through the utilization of microfluidic technology. A micro-bioreactor for microbial culture can be produced that immobilizes or entraps cells in polymer matrices [149-150], e.g., polydimethylsiloxane. Immobilized cell technology has advanced to utilize cell encapsulation, in particular, by entrapping cells in an alginate gel matrix [151], spray drying (commonly used in the

food industry) [152], and extrusion, which involves the projection of an emulsion core and coating material via flow through a nozzle at high pressure [153]. Recently, water-in-oil compartmentalization has been introduced to retain microbial cells in the aqueous core for cultivation [154-155]. This cell capture method was accomplished using droplet microfluidic technology. Briefly, a cell-containing aqueous medium is injected into the oil phase environment. Nano- to micro-sized droplets form and are used to cultivate various bacterial cells. A similar droplet-based platform was used to examine communication between quorum signaling components located in spatially isolated droplets [154]. Genetic constructs were designed using an inducible P_{lux} promoter attached to a reporter gene as the receiver and a constitutive PLtet0 promoter fused to the *luxI* gene as the signaling molecule. The cell-containing droplets were placed within a micro-compartment under a moderate flow and maintained to observe quorum signaling [154]. As microfluidic devices can be constructed to have parallel assay channels, similar experiments can be conducted to test various chemical conditions, e.g., antibiotics, with a simultaneous control [156].

Bacteria primarily exist in surface-associated multicellular communities, and the term biofilm describes a matrix-enclosed bacterial population of cells adherent to each other and/or substrates [144, 157]. Bacterial biofilms undergo several stages of development, from the initial attachment of bacteria to the ultimate detachment and colonization of new interfaces [158]. The effectiveness of biofilm formation is dependent on cell-surface hydrophobicity, since hydrophobicity is important in the initial attachment process of bacteria to hydrophobic surfaces. Although the viscoelastic matrix of biofilms can be composed of extracellular DNA, polysaccharides, and proteins, the precise structure, chemistry, and physiology depend on the characteristics of the resident microbes and the local environment. Such phenotypic variability may be an important strategy for bacterial survival in an unpredictable environment [124, 134-135]. For example, the stochastic development of persister cells enables lineages of pathogens to survive antibiotic treatment and accordingly has serious clinical consequences [133]. Furthermore, as biofilms are adherent aggregates of bacterial cells that form on biotic and abiotic surfaces, including human tissues, they also play a role in resistance to antibiotic treatment and bacterial persistence in chronic infections [159].

To establish a multiplexed biofilm assay system, in this study, we developed a droplet-based bioreactor in a spatially segregated configuration, which we inoculated with a bacterium (i.e., *E. coli*) for culture. The droplet approach enabled relatively convenient control over the culture and also allowed the spatial segregation of bacterial cells within the microfluidic channels, providing the ability to perform multiple fine-scale assays in parallel. As hydrophobic surfaces are preferable for primary cell adhesion, the cells were encapsulated in a water-in-oil droplet to promote cell aggregate adherence at the interface [160]. In this technique, droplets are captured and maintained within a compartment of a microfluidic device through which oil continuously flows. Cell aggregate formation was monitored using synthetic gene networks in *E. coli* that express green fluorescent protein (GFP) upon induction with AHL, which was used to better visualize biofilm-like structures. Bacterial growth was measured using a fluorescent microscope and images were captured at preset time intervals.

6.3. Materials and Methods

6.3.1. Manufacture of microfluidic device

Master mold fabrication for water-in-oil bioreactor. All master molds were fabricated in the Virginia Tech Micro & Nano Fabrication Laboratory (MICRON). Photomasks were drawn in AutoCAD (Autodesk, San Rafael, CA, USA), printed onto transparency film by CAD/Art Services, Inc. (Output City, Poway, CA, USA), and mounted onto glass plates (McMaster-Carr, Los Angeles, CA, USA) maintaining the print side facing the silicon wafer. All silicon wafers were cleaned prior to using by rinsing with acetone, isopropyl alcohol and deionized water and dried on a hot plate (120°C) for 10 min. The master mold was created by first spin-coating with SU-8 2010 negative photoresist (MicroChem Corp., Newton, MA, USA) onto clean silicon wafers to 15 µm in height using a WS-650-8B programmable spinner (Laurell Technologies Corp., North Wales, PA, USA). The photoresist was first cured on a hot plate (120°C) for 2 min and exposed to UV radiation using a MA/BA6 UV contact mask aligner (MicroTec, Garching, Germany). After being exposed to UV radiation, the exposed photoresist was cured on a hot plate (120°C) for 3 min and

the unexposed photoresist was rinsed away using developer (MicroChem Corp.). The final master mold was cured on a hot plate (120°C) for 1 hr.

Master mold fabrication for water-in-oil homogeneous droplet. All master molds were fabricated using SU-8 2050 negative photoresist to yield 50 μm in height. Deposited photoresist was cured on a hot plate for 3 and 5 min, prior and subsequent to UV exposure, respectively. All other details follow the process mentioned above.

PDMS device fabrication. Replica molds were created from master molds by mixing PDMS/Sylgard 184 (Dow Corning, Midland, MI, USA) with a 10:1 ratio of the elastomer base to curing agent, degassing in a vacuum desiccator for 1 h, and curing in an oven at 90°C for 2 h. Following removal of the PDMS, devices were cut, holes were punched for ports, and the cell was cleaned with filtered DI water and then permanently bonded to clean coverslips (Thermo Fisher Scientific, Waltham, MA, USA) via exposure to O_2 plasma for 1 min in a PDC-32G plasma cleaner (Harrick Scientific, Ithaca, NY, USA).

Fluidics. A syringe pump (PHD 2000, Harvard Apparatus, Holliston, MA, USA) was used to generate and manoeuvre droplets along the microfluidic channel. The pump was used at a rate of 5 μl/ml to generate LB medium droplets that subsequently merged with the mother droplet and HFE-7500 oil containing 0.0018% Krytox® 157 FSL (DuPont, Wilmington, DE, USA) as the surfactant was gravity-driven in the main flow channel at a rate of 10 μl/ml.

6.3.2. Construction and characterization of the quorum sensing receiver circuit

Cloning details. The receiver circuit (pSP035) used in this study was constructed using six components, pKE1-MCS as the vector, P_{lux}, luxR T1T2, rbs027 and GFPmut3b as inserts (Figure 3.1). The desired restriction sites were added to the 5′ and 3′ ends of each construct using overhang PCR (Table 3.1). For each insertion, both the insert construct and vector were uniquely double digested using appropriate enzymes. Followed by gel purification, the fragments were then ligated and transformed, and the resulting clones were screened against carbenicillin (Cb) resistance.

Induction conditions. To characterize the performance of the receiver circuit we conducted a series of experiments. The cells were first grown overnight in LB media with 100 μg/ml Cb from a frozen stock. At the beginning of the experiment, overnight grown cells were diluted 1:1000 in fresh LB media and once again grown and kept at exponential growth density. The receiver cells were then either non-induced or induced with of AHL to yield final concentrations 1 mM. The fluorescent intensity was measured after 5 hr of induction using a plate reader (Biotek Instruments, Inc., Vermont, USA). Cell were maintained at 37°C before analysis.

6.3.3. Maintenance and monitoring of cell growth in microfluidic channels

Microfluidic cell culture. After filling the entire chamber with oil, the recombinant *E. coli* cells suspended in LB media supplemented with 0.1 mM AHL were loaded into the trapping channels of the microfluidic device by directing the flow in the direction from the inlet port to the outlet port. Upon trapping a few cells in each region and creating a droplet, the oil flow was controlled to a steady flow rate of 10 μl/ml to prevent the loaded droplet from escaping the chamber.

Cell microscopy. Cell images were acquired using an inverted epifluorescent microscope (Ti-E; Nikon Instruments Inc., Tokyo, Japan). DIC and fluorescent images were captured every 15 min, and focus was maintained automatically using Nikon Elements software.

6.4. Results and Discussion

6.4.1. Utilization of quorum sensing bacteria for monitoring biofilm formation in droplets

A synthetic receiver circuit was designed to test quorum sensing signals based on communication between AHL and receiver cells [102]; we used this system to visualize bacterial

biofilm formation in a hostile environment. To this end, *E. coli* was engineered to contain a quorum sensing (P_{lux}-driven) circuit that expresses GFP upon induction with a chemical signaling molecule, AHL. The amphiphilic molecule, encapsulated prior to use, can be manually added to the aqueous medium or synthesized by sender cells encapsulated upstream, located within the same device (Figure 6.1). In this system, receiver cells were utilized to quantitatively monitor the metabolic status of bacteria under cultivation in the droplet-based micro-bioreactor.

When the density of cells in a culture exceeds a threshold, many bacterial populations create biofilms as a stress response to nutrient and spatial limitations. Although the mode of quorum sensing activation was used to study a particular cellular status [161], the fluorescent signal can be produced at any time by the addition of the inducing molecule in the medium. This allowed us to monitor the cells, regardless of growth status, and eventually to monitor the metabolic state, represented by GFP expression, within the biofilm after the exponential phase. Since biofilms usually demonstrate resistance to hostile environments, even in the presence of drugs such as antibiotics [8], the bacterial response could further be used to screen therapeutic drugs added to the culture. When a chemical added to the medium effectively inhibits metabolic activity, the biofilm cells are inactivated compared to the control without the chemical additive. In this case, the fluorescent signal can be turned off, enabling the identification of drug candidates. Thus, rapid, parallel, quantitative screening of multiple drugs based on signal intensity may be carried out using the droplet reactors with spatially segregated microfluidic channels.

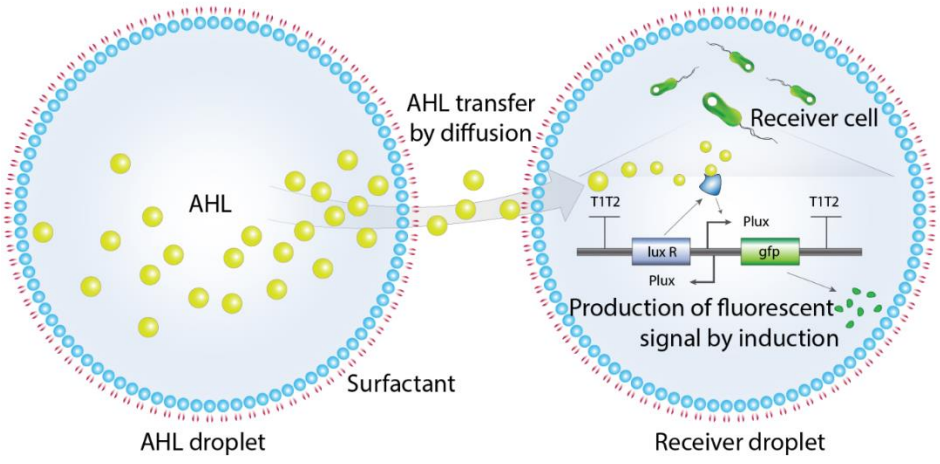

Figure 6.1. Response of a quorum sensing receiver bacterium to the presence of an inducer that diffuses from the main medium**.**

We demonstrated in this study the production of water-in-oil droplets and the utilization of the droplets as spatially isolated micro-bioreactors inoculated with recombinant *E. coli* containing quorum sensing gene circuits.

6.4.2. Producing droplets that retain the receiver cells

Standard photolithographic fabrication processes were used to first generate a microfluidic system capable of producing droplets [154]. A photolithographic mask was initially designed using AutoCad 2013 (AutoDesk, San Rafael, CA, USA) (Figure 6.2a). The design was then used to fabricate the microfluidic device, providing a junction where an aqueous medium containing bacterial cells was injected into the oil phase (Figure 6.2b). This was conducted by constructing the device so that the aqueous medium (e.g., LB medium) flowed through the central channel and oil supplemented with a surfactant was supplied at the junction (e.g., HFE 7500 with 0.0018% Krytox® 157 FSL) from the both sides, originating from an identical supply port. After constructing this device, the aqueous medium was supplied at a volumetric rate of 200 µL/min, and the oil was pumped at a speed of 400 µL/min to produce homogeneous micro-sized droplets (Figure 6.2c). Each can be used as a single bioreactor encapsulating the engineered cells within the aqueous phase.

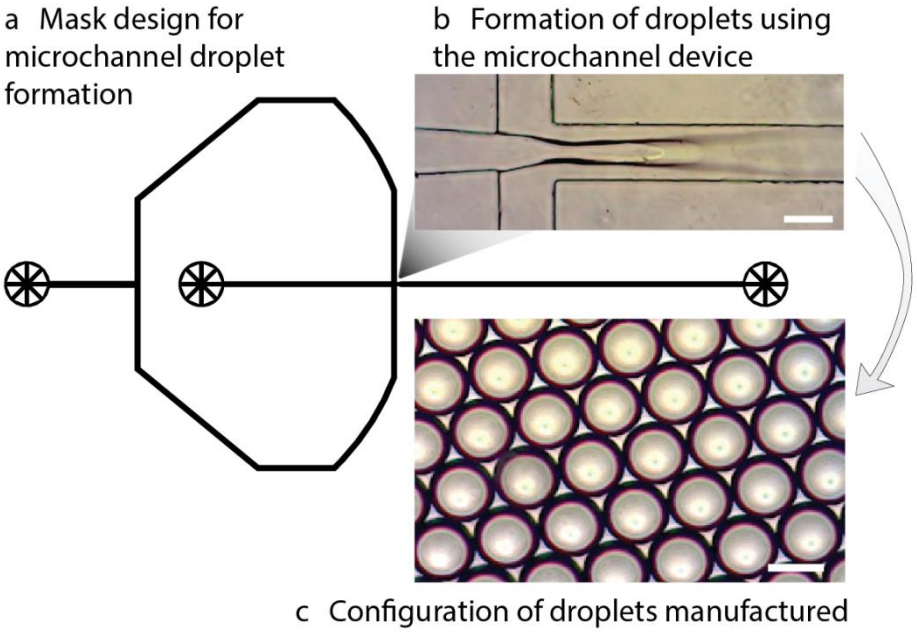

Figure 6.2. Manufacture of homogeneous, micrometer-sized water-in-oil droplets using a microfluidic device. The scale bar shown in b and c represents 100 μm.

To monitor quorum signaling, we constructed a synthetic bacterial cell line, referred to as the 'receiver', which generated visible GFP signals upon induction with AHL, as mentioned previously. The receiver contained the transcription factor *luxR* and a *gfp* gene with a bidirectional P_{lux} promoter (Figure 6.3a, left panel) [162]. The gene construct for quorum sensing was tested by activating the receiver system through the manual addition of AHL into receiver cultures in 96-well plates, and monitoring the GFP signals via the plate reader (Figure 6.3a, left panel). Subsequently, the induced receiver cells were encapsulated in droplets (average diameter = 100 μm), as described in Figure 6.2, and transferred to an observation channel (2 × 4 mm) by simply bridging the two ports extended from the outlet of the droplet-producing microfluidic device, for further characterization (Figure 6.3b). The induced receiver cell-containing droplets where cultured overnight for 12 h (average diameter = 100 μm; Figure 6.3b, upper panel). Images of the receiver cell fluorescence were captured at a predetermined time to observe the cell behavior and viability (lower panel). Even after encapsulation of the recombinant cells, the receiver system remained intact, permitting visualization of the quorum-induced cells. It should be noted that the oil, HFE 7500, used as the ambient environment is Fluorinert™, i.e., an inert fluid normally used to cool circuit boards [163].

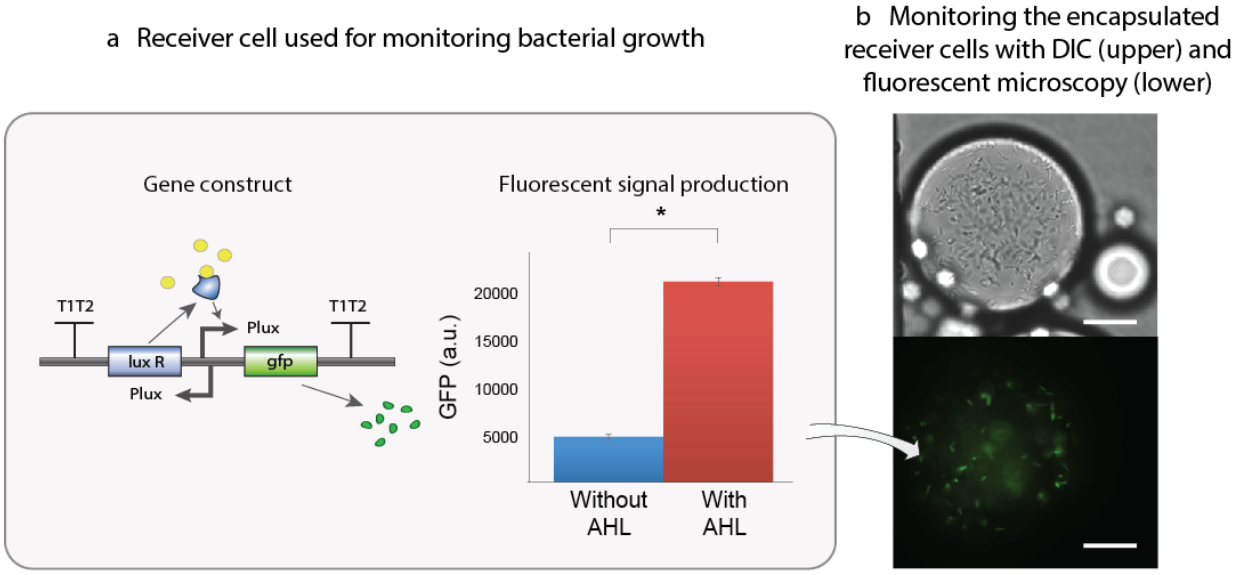

Figure 6.3. Characterization of the receiver system in *E. coli* cells. The error bars in the graph indicate standard deviation of triple measurements at each condition. The scale bar in b represents 50 μm.

6.4.3. Bacterial cell culture in a single-droplet microfluidic bioreactor

Although colonies of the same engineered receiver cells contain the same gene circuit, these cells may express a heterogeneous behavior in response to the inducer, complicating parallel processing. Therefore, a microfluidic device allowing the spatial segregation of colonies was developed in order to visualize induction of quorum sensing signals within micro-compartments. First, a microcfluidic device was manufactured using standard microfabrication technology based on soft-photolithography (Figure 6.4, left panel). The device comprised a single tortuous channel for the flow of the fluorocarbon oil and a central compartment for maintaining a water-in-oil droplet, i.e., a mother droplet, as a bioreactor for bacterial cultivation (Figure 6.4, right panel). The compartment was constructed with one inlet and an outlet combined with gates to allow the medium to flow through and a main physical support to hold the mother droplet within the designated space. Subsequently, small aqueous droplets were maneuvered to flow in through a single inlet (width = 70 μm) and out through an outlet (width = 50 μm), with significantly decreased pressure towards the mother droplet, with the help of supporting pillars functioning as a soft valve. This configuration can hold an aqueous droplet within the surrounding fluorocarbon medium and further maintain the culture of the bacterial cells encapsulated within the mother droplet.

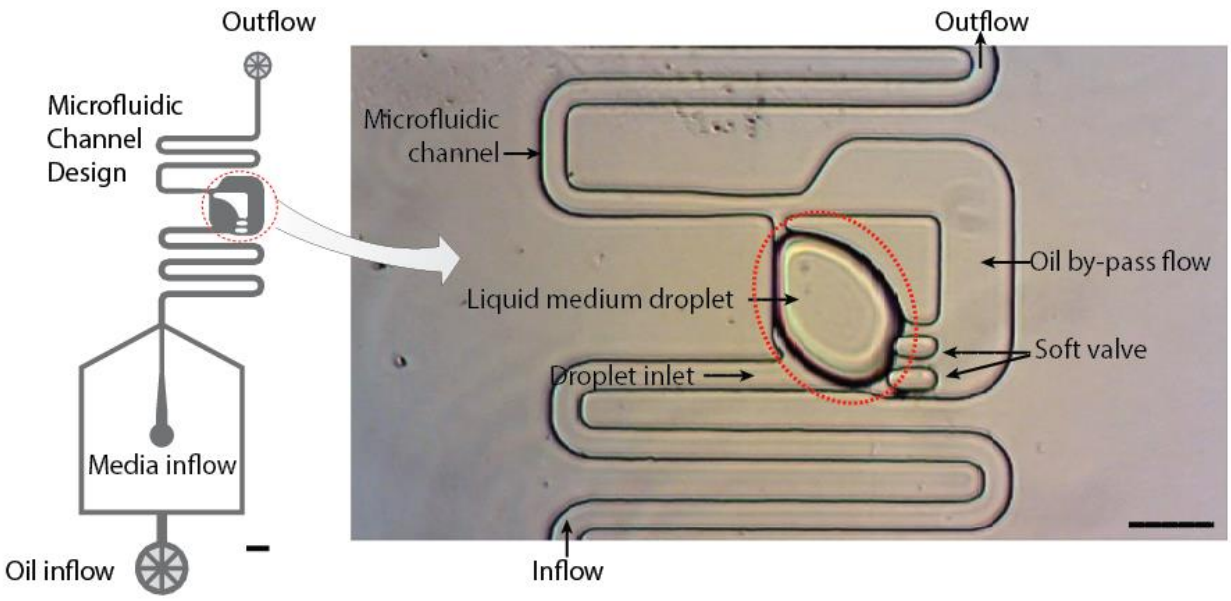

Figure 6.4. Spatial segregation of the droplet-based bacterial culture system using a microfluidic device. The scale bar represents 200 µm.

To further investigate the proper functionality of the device we maneuvered small droplets through the channel (Figure 6.5a). Upon entering the inlet region of the holding compartment, the small aqueous droplet subsequently went in contact with the mother droplet held in the in the chamber, inducing coalescence caused by surface tension (Figure 6.5b). The droplet volume exceeding the holding capacity of the chamber was drawn from the chamber by generating a daughter droplet in the downstream channel of the device (Figure 6.5c). In further sections of our research, the sequence of droplet maneuver, coalescence, and generation of daughter droplet will facilitate the supply of nutrients to the cells cultivated within the mother droplet. The same approach can also be used for the supply of the signaling molecule, AHL, and other chemical compounds, e.g., antibiotics, by its inclusion in the aqueous medium of the small droplets.

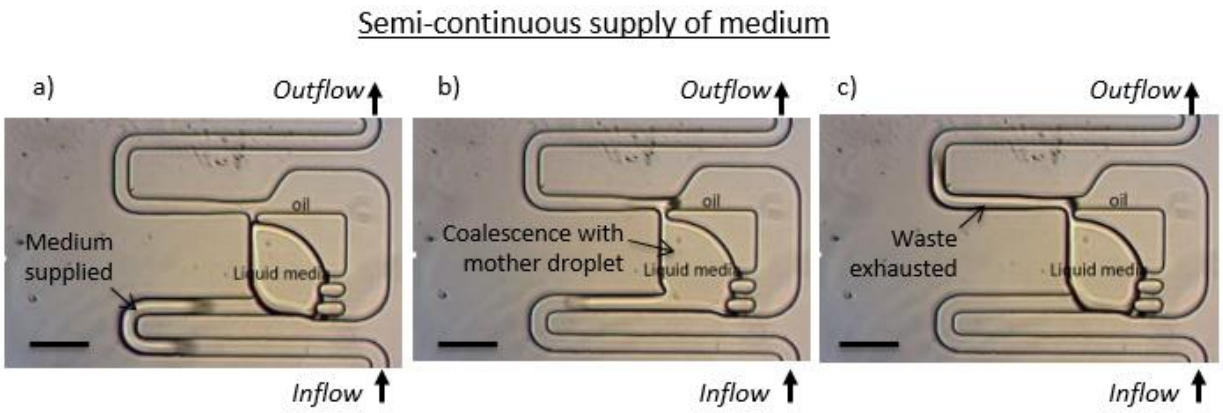

Figure 6.5. Maintenance of the droplet-based bioreactor for cultivating engineered *E. coli* cells in a semi-continuous manner. The scale bar represents 200 µm.

6.4.4. Formation of a bacterial biofilm at the water–oil interface

With our modified approach from previous investigations [164], we were able to grow and maintain bacteria cells within the holding compartment of the device by semi-continuously providing nutrients to the mother droplet. First, a water-in-oil droplet retaining the quorum sensing receiver cells as well as AHL was placed in the holding compartment of the microfluidic device (Figure 6.6). For subsequent input droplets, the oil phase was HFE 7500 with 0.0018% Kyrtox while the other, aqueous phase consisted of the LB medium supplemented with AHL. Although the droplet was relatively small in size (diameter = ~100 µm; Figure 6.6, 0 h) at the initial time point, it gradually grew as the LB medium containing AHL was supplied. This indicated that the input droplets merged with the mother droplet by coalescence to maintain an ultimate size determined by the compartment capacity. A steady-state droplet size was reached after about 3 h and, thereafter, the droplet was approximately constant in size for the study duration, up to 18 h.
To monitor bacterial growth behavior, we utilized the GFP expression within the quorum sensing receiver cell activated by an amphiphilic inducer molecule, AHL. During the cell culture in the mother droplet bioreactor, the GFP signal was not detected within the droplet at the initial time point, but was detected after 1.5 h. The signal became significant after 3 h and seemed to be limited to local areas within the droplet proximate to the medium inlet after 6 h. The maximum observed brightness, suggesting bacterial biofilm formation, was maintained until the end of the culture period (18 h).

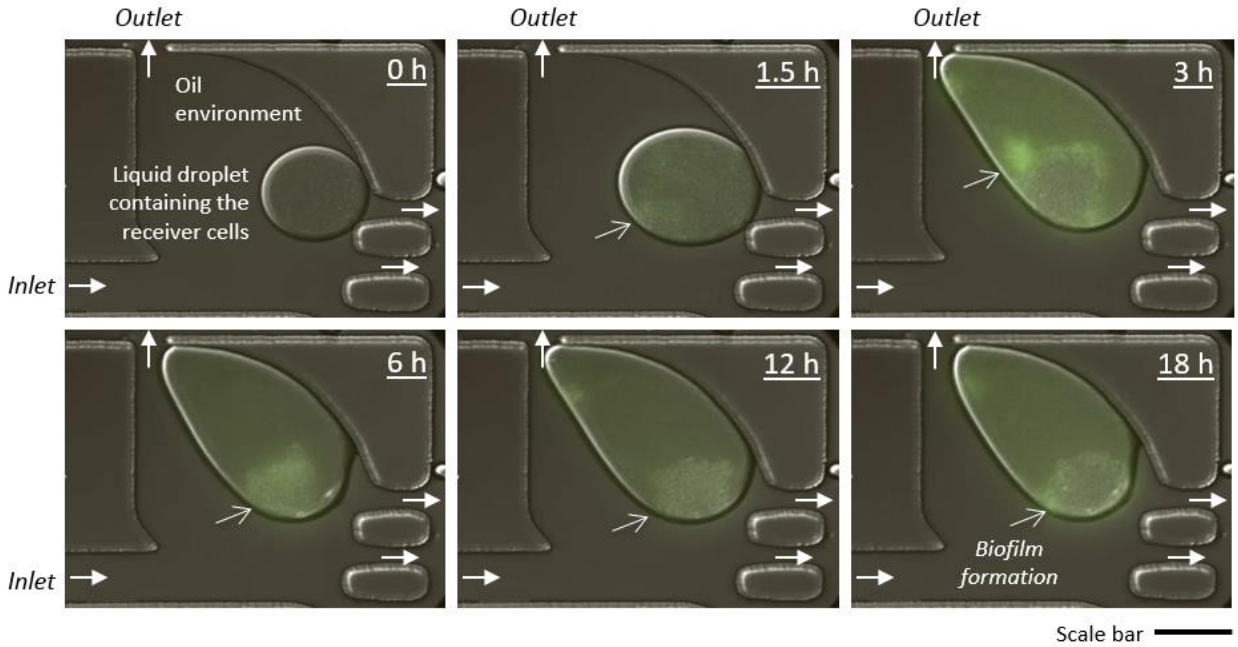

Figure 6.6. Long-term culture of engineered receiver *E. coli* cells in a spatially isolated droplet bioreactor used to monitor biofilm formation. The scale bar represents 100 μm.

The rapid increase in signal intensity during the initial period, i.e., the first 3 h, could be related to the growth in droplet size. As the size expansion indicated the immersion of fresh LB medium nutrients into the mother droplet containing the cell inoculum, the cell culture was provided with sufficient nutrients, fulfilling the conditions for growth and metabolism. Therefore, cells within the mother droplet were able to achieve exponential growth, which was particularly apparent in proximity to the entrance of the holding compartment. Since the engineered *E. coli* cell maintained a doubling time of around 45 min [165], the cells can ideally expand up to 16 times in density after 3 h and 256 times after 6 h. This may be sufficient to support growth of the bacterial population beyond the stationary phase, eventually resulting in biofilm formation near the water–oil interface after 6 h from the onset of cell cultivation. While this aspect of cellular community was kept until the end of the culture, microscopic observations interestingly revealed the rotation of biofilm formed within the mother droplet. Such cell aggregate rotation may result from the fluorocarbon oil flow and can thus be controlled by manipulating the water–oil phase interface according to the flow direction. Also, the *E. coli* cells grew within the droplet in three-dimensional multicellular assemblies, rather than in a planar arrangement at the interface, consistent with previous findings [158].

Bacterial adsorption at various interfaces (e.g., liquid–solid, liquid–air, and liquid–liquid) is a key factor in biofilm formation [158]. Bacteria can initially adhere to interfacial surfaces via unspecific binding by means of electrostatic, short range Lewis acid–base, and hydration interactions [166]. The electrostatic interactions under most physiological conditions are repulsive, as both the bacteria and most surfaces are net negatively charged. However, owing to the hydrophobicity of the complex and the heterogeneity of the cell surface containing flagella, fimbriae, pili, proteins, and surface polysaccharides, this repulsion is overcome. Numerous factors influence bacterial adhesion, including pH, ionic strength, bacterial mobility, state of growth, and growth factors in the medium [167]. Therefore, biofilm formation and development can vary according to bacterial species under different culture, nutritional, and environmental conditions.

To establish methods for the control of stable bacterial habitats, it may be critical to construct a multiplex bacterial cell culture system permitting reproducible biofilm formation at hydrophobic interfaces. In this study, bacterial attachment and biofilm growth over time at the water–oil interface were monitored by microscopy. We were able to observe the initial bacterial growth in segregated droplets using microfluidic channels and also biofilm formation at the liquid–liquid interface. The recombinant *E. coli* cells were eventually allowed to adsorb at the water–oil interface, particularly in their non-growing, stationary state. To minimize labor and time involved in testing a number of potential control candidates, it is essential to reproducibly generate biofilms in the small droplet spaces in a spatially segregated fashion. This could be advantageous for constructing parallel, multiple experimental setups to accelerate the screening of substances that efficiently inhibit bacterial metabolism in the biofilm structure. Biofilms are known to be difficult to treat with antibiotics, to be associated with food poisoning outbreaks and clinical infections [167], and to even clog industrial pipes [157, 168-170]; accordingly, methods for the formation of biofilms in spatially-segregated droplets have medical, industrial, and ecological relevance.

6.5. Conclusion

We demonstrated reproducible generation of biofilm structures in the small droplet spaces in a spatially segregated fashion, which could be advantageous for constructing parallel, multiple experimental setups to conduct biofilm assays in high throughput. A device such as this is essential to minimizing the labor and time required to testing a large number of parameters that may influence the formation and function of microbial consortia. One typical application of this system is the screening of substances that efficiently inhibit bacterial metabolism in the biofilm structure. In the future, this new technology can be extended to enable parallel assays using segregated colonies within a single system. This system has broad potential applications across a range of fields in which microbial cellular pattern formation and signal propagation are critical, such as biophysics, developmental biology, and tissue engineering.

CHAPTER 7.

CONCLUSIONS

As a ubiquitous and naturally occurring form of bacteria, the most abundant type of organism worldwide, biofilms are an essential target of microbiological research. Limitations to the study of bacterial biofilms are one of the greatest obstacles to understanding this common bacterial form as well as overcoming the challenges that biofilms present to human health and economic activities. Accordingly, the microfluidic devices described in this thesis will be an essential tool for exploring the biology of biofilms and devising control methods that can prevent the negative impacts of biofilms. In conjunction with bacterial strains developed using genetic engineering tools such as genetic circuits, these microfluidic devices provide a powerful approach to dissecting the molecular mechanisms underlying biofilms.

The main microfluidic device utilized throughout this research is a flow cell instrument that permits the culture of bacteria in artificial conditions that mimic the nutrient stress that bacteria endure in their biofilm form. Experimental cultures have confirmed that this device has broad potential for the study of bacterial biofilms based on several of its strengths. First and foremost, the device PDMS device is small, relatively inexpensive, and designed to maximize the ability to visualize individual cells using real-time epifluorescent microscopy under fluorescent. These features enable high-throughput assays of chemical compounds with real-time imaging—the former permitting large experiments with high statistical power and the latter permitting confirmation of effects, especially in conjunction with genetic constructs that utilize fluorescent reporter proteins such as GFP or mCherry.

The study of biofilms at the level of individual cells is impractical because cells are, by definition, tightly aggregated within biofilms. For this reason, it is extremely difficult to visualize a cell that is within a three-dimensional mass of neighboring cells. The biofilm-mimicking microfluidic device eliminates this issue by only having physical space for a single layer of cells to develop. The flow channels of the microfluidic device are just 0.97 μm in height, which is

slightly smaller than the typical 1-μm diameter of *E. coli* at their thinnest point. Importantly, this flow cell can be redesigned to accommodate cell of sizes that are smaller or larger than *E. coli*. In addition to trapping cells within a one-cell-thick plane, which enables the straightforward visualization of individual cells, this restricted flow channel height also prevents cell motility. This added benefit also facilitates the continuous tracking of cell lineages. As a mother cell divide into two daughter cells, which in turn divide into four daughter cells as well, and so on, continuous imaging of all cells divisions can be captured using microscopy. This enables viewing of the entire time course of an experiment in great detail, especially when used in conjunction with *E. coli* cells lines that contain reporter constructs.

In the first set of experiments utilizing this device, the ability of the microfluidic device to induce biofilm-like stress was confirmed (proof of the first hypothesis presented in Chapter 1). The *E. coli* cultured in this experiment were contained a simple genetic circuit—specifically, a receiver construct containing the bidirectional P_{lux} promoter and a GFP reporter regulated by a luxR transcription factor. When induced with AHL, a quorum sensing signaling molecule, this cell line expresses its GFP signal. However, under the stressful culture conditions of the microfluidic device, the GFP signal was expressed even in the absence of AHL. This spontaneous expression of the GFP quorum sensing reporter suggests that the biomimetic structures of the microfluidic device impose conditions similar to those of natural biofilms, thus triggering stochastic gene expression pathways.

Spontaneous expression of stress-induced responses in bacterial cells cultured in the biofilm-mimicking device were also supported by a similar experiment utilizing an *E. coli* strain containing a genetic toggle switch. The simple toggle switch constitutively expressed one of two states determined by an initial stimulus, essentially acting as a simple ON/OFF switch. After receiving the initial signal of aTc, nearly all cells remained in that expression state. However, induction with IPTG, was stochastically reversed over the course of the 5-day culture period; by the end of this time, more than 5% of cells had spontaneously reverted to the alternative toggle switch state. This asymmetry was unexpected. However, the stochastic change in toggle switch state indicates that the stressful conditions of the microfluidic cell overcame the bistability of this system as predicted by previous theoretical [120] and empirical research [118].

The stress induction of the microfluidic system was further confirmed in a series of experiments that utilized the facilitation of continuous cell tracking in the system (proof of the second hypothesis). Specifically, an aberrant, enlarged cell morphology was observed within the stressful environment of the microfluidic cell. Moreover, this phenotype was observed to be inherited by daughter cells, suggesting that an epigenetic switch had been induced by the nutrient deficient conditions.

The final series of experiments utilized an entirely different type of microfluidic cell that may also be used to examine group phenotypes of small numbers of bacterial cells, such as may occur within small portions of biofilms (proof of the third hypothesis). This microfluidic device enabled the continuous culture of a small number of cells within a bubble of aqueous medium suspended within a flow of oil. This water-in-oil droplet bioreactor was able to both continuous culture a small population of cells as well as permit the precise introduction of chemical compounds while generating biofilms. Under these culture conditions, AHL was successfully introduced into the cultured cells, which then expressed their GFP quorum sensing reporter.

Both of the devices explored in this thesis will continue to be useful tools of the study of *E. coli* cells within biofilms, and with minor design modifications, may be applied to other microbial systems. Future research should be focused on the application of these devices to large panels of chemical compounds for their inhibitory or cell-killing effects. This specific line of research would be especially useful in identifying next-generation antibiotics that are able to overcome the inherent defenses of bacterial biofilms.

REFERENCES

1. Mattila-Sandholm, T.; Wirtanen, G., Biofilm formation in the industry: a review. *Food Reviews International* 1992**, 8** (4), 573-603.
2. Peters, B. M.; Jabra-Rizk, M. A.; Graeme, A.; Costerton, J. W.; Shirtliff, M. E., Polymicrobial interactions: impact on pathogenesis and human disease. *Clinical microbiology reviews* 2012**, 25** (1), 193-213.
3. Socransky, S. S.; Haffajee, A. D., Dental biofilms: difficult therapeutic targets. *Periodontology 2000* 2002**, 28** (1), 12-55.
4. Momba, M.; Kfir, R.; Venter, S. N.; Cloete, T. E., An overview of biofilm formation in distribution systems and its impact on the deterioration of water quality. 2000.
5. Wang, X.; Wood, T. K., Toxin-antitoxin systems influence biofilm and persister cell formation and the general stress response. *Applied and environmental microbiology* 2011**, 77** (16), 5577-5583.
6. Costerton, J. W.; Stewart, P. S.; Greenberg, E. P., Bacterial biofilms: a common cause of persistent infections. *Science* 1999**, 284** (5418), 1318-1322.
7. Høiby, N.; Bjarnsholt, T.; Givskov, M.; Molin, S.; Ciofu, O., Antibiotic resistance of bacterial biofilms. *International journal of antimicrobial agents* 2010**, 35** (4), 322-332.
8. Stewart, P. S.; Costerton, J. W., Antibiotic resistance of bacteria in biofilms. *The lancet* 2001**, 358** (9276), 135-138.
9. Stewart, P. S.; Franklin, M. J., Physiological heterogeneity in biofilms. *Nature Reviews Microbiology* 2008**, 6** (3), 199-210.
10. Ruder, W. C.; Lu, T.; Collins, J. J., Synthetic biology moving into the clinic. *Science* 2011**, 333** (6047), 1248-52.
11. Khalil, A. S.; Collins, J. J., Synthetic biology: applications come of age. *Nature reviews. Genetics* 2010**, 11** (5), 367-79.
12. Anderson, J. C.; Clarke, E. J.; Arkin, A. P.; Voigt, C. A., Environmentally controlled invasion of cancer cells by engineered bacteria. *J Mol Biol* 2006**, 355** (4), 619-27.
13. Duan, F.; March, J. C., Engineered bacterial communication prevents Vibrio cholerae virulence in an infant mouse model. *Proc Natl Acad Sci U S A* 2010**, 107** (25), 11260-4.
14. Ye, H.; Daoud-El Baba, M.; Peng, R. W.; Fussenegger, M., A synthetic optogenetic transcription device enhances blood-glucose homeostasis in mice. *Science* 2011**, 332** (6037), 1565-8.
15. Chen, Y. Y.; Jensen, M. C.; Smolke, C. D., Genetic control of mammalian T-cell proliferation with synthetic RNA regulatory systems. *Proc Natl Acad Sci U S A* 2010**, 107** (19), 8531-6.
16. Gardner, T. S.; Cantor, C. R.; Collins, J. J., Construction of a genetic toggle switch in *Escherichia coli*. *Nature* 2000**, 403** (6767), 339-42.
17. Elowitz, M. B.; Leibler, S., A synthetic oscillatory network of transcriptional regulators. *Nature* 2000**, 403** (6767), 335-8.
18. Danino, T.; Mondragon-Palomino, O.; Tsimring, L.; Hasty, J., A synchronized quorum of genetic clocks. *Nature* 2010**, 463** (7279), 326-30.

19. Ellis, T.; Wang, X.; Collins, J. J., Diversity-based, model-guided construction of synthetic gene networks with predicted functions. *Nat Biotechnol* 2009**, 27** (5), 465-71.
20. Friedland, A. E.; Lu, T. K.; Wang, X.; Shi, D.; Church, G.; Collins, J. J., Synthetic gene networks that count. *Science* 2009**, 324** (5931), 1199-202.
21. Fung, E.; Wong, W. W.; Suen, J. K.; Bulter, T.; Lee, S. G.; Liao, J. C., A synthetic gene-metabolic oscillator. *Nature* 2005**, 435** (7038), 118-22.
22. Rinaudo, K.; Bleris, L.; Maddamsetti, R.; Subramanian, S.; Weiss, R.; Benenson, Y., A universal RNAi-based logic evaluator that operates in mammalian cells. *Nat Biotechnol* 2007**, 25** (7), 795-801.
23. Tabor, J. J.; Salis, H. M.; Simpson, Z. B.; Chevalier, A. A.; Levskaya, A.; Marcotte, E. M.; Voigt, C. A.; Ellington, A. D., A synthetic genetic edge detection program. *Cell* 2009**, 137** (7), 1272-81.
24. You, L.; Cox, R. S., 3rd; Weiss, R.; Arnold, F. H., Programmed population control by cell-cell communication and regulated killing. *Nature* 2004**, 428** (6985), 868-71.
25. Qi, H.; Blanchard, A.; Lu, T., Engineered genetic information processing circuits. *Wiley Interdisciplinary Reviews: Systems Biology and Medicine* 2013**, 5** (3), 273-287.
26. Berthiaume, F.; Maguire, T. J.; Yarmush, M. L., Tissue Engineering and Regenerative Medicine: History, Progress, and Challenges. *Annual Review of Chemical and Biomolecular Engineering* 2011**, 2** (1), 403-430.
27. Forbes, N. S., Engineering the perfect (bacterial) cancer therapy. *Nat Rev Cancer* 2010**, 10** (11), 785-794.
28. Levskaya, A.; Chevalier, A. A.; Tabor, J. J.; Simpson, Z. B.; Lavery, L. A.; Levy, M.; Davidson, E. A.; Scouras, A.; Ellington, A. D.; Marcotte, E. M.; Voigt, C. A., Synthetic biology: engineering *Escherichia coli* to see light. *Nature* 2005**, 438** (7067), 441-2.
29. Bashor, C. J.; Helman, N. C.; Yan, S.; Lim, W. A., Using engineered scaffold interactions to reshape MAP kinase pathway signaling dynamics. *Science* 2008**, 319** (5869), 1539-43.
30. Xia, B.; Bhatia, S.; Bubenheim, B.; Dadgar, M.; Densmore, D.; Anderson, J. C., Developer's and user's guide to Clotho v2.0 A software platform for the creation of synthetic biological systems. *Methods in enzymology* 2011**, 498**, 97-135.
31. Bilitchenko, L.; Liu, A.; Cheung, S.; Weeding, E.; Xia, B.; Leguia, M.; Anderson, J. C.; Densmore, D., Eugene--a domain specific language for specifying and constraining synthetic biological parts, devices, and systems. *PLoS One* 2011**, 6** (4), e18882.
32. Egbert, R. G.; Klavins, E., Fine-tuning gene networks using simple sequence repeats. *Proceedings of the National Academy of Sciences* 2012**, 109** (42), 16817-16822.
33. Salis, H. M.; Mirsky, E. A.; Voigt, C. A., Automated design of synthetic ribosome binding sites to control protein expression. *Nat Biotech* 2009**, 27** (10), 946-950.
34. Callura, J. M.; Dwyer, D. J.; Isaacs, F. J.; Cantor, C. R.; Collins, J. J., Tracking, tuning, and terminating microbial physiology using synthetic riboregulators. *Proc Natl Acad Sci U S A* 2010**, 107** (36), 15898-903.
35. Isaacs, F. J.; Dwyer, D. J.; Ding, C.; Pervouchine, D. D.; Cantor, C. R.; Collins, J. J., Engineered riboregulators enable post-transcriptional control of gene expression. *Nat Biotechnol* 2004**, 22** (7), 841-7.
36. Gallivan, J. P., Toward reprogramming bacteria with small molecules and RNA. *Current opinion in chemical biology* 2007**, 11** (6), 612-9.
37. Topp, S.; Gallivan, J. P., Guiding bacteria with small molecules and RNA. *Journal of the American Chemical Society* 2007**, 129** (21), 6807-11.

38. Babiskin, A. H.; Smolke, C. D., A synthetic library of RNA control modules for predictable tuning of gene expression in yeast. *Mol Syst Biol* 2011**, 7**, 471.
39. Win, M. N.; Smolke, C. D., Higher-order cellular information processing with synthetic RNA devices. *Science* 2008**, 322** (5900), 456-60.
40. Siuti, P.; Yazbek, J.; Lu, T. K., Synthetic circuits integrating logic and memory in living cells. *Nat Biotechnol* 2013**, 31** (5), 448-52.
41. Lutz, R.; Bujard, H., Independent and tight regulation of transcriptional units in *Escherichia coli* via the LacR/O, the TetR/O and AraC/I1-I2 regulatory elements. *Nucleic acids research* 1997**, 25** (6), 1203-10.
42. Xie, Z.; Wroblewska, L.; Prochazka, L.; Weiss, R.; Benenson, Y., Multi-input RNAi-based logic circuit for identification of specific cancer cells. *Science* 2011**, 333** (6047), 1307-11.
43. Tamsir, A.; Tabor, J. J.; Voigt, C. A., Robust multicellular computing using genetically encoded NOR gates and chemical 'wires'. *Nature* 2011**, 469** (7329), 212-5.
44. Anderson, J. C.; Voigt, C. A.; Arkin, A. P., Environmental signal integration by a modular AND gate. *Mol Syst Biol* 2007**, 3**, 133.
45. Daniel, R.; Rubens, J. R.; Sarpeshkar, R.; Lu, T. K., Synthetic analog computation in living cells. *Nature* 2013**, 497** (7451), 619-23.
46. Stricker, J.; Cookson, S.; Bennett, M. R.; Mather, W. H.; Tsimring, L. S.; Hasty, J., A fast, robust and tunable synthetic gene oscillator. *Nature* 2008**, 456** (7221), 516-9.
47. Wong, W. W.; Tsai, T. Y.; Liao, J. C., Single-cell zeroth-order protein degradation enhances the robustness of synthetic oscillator. *Mol Syst Biol* 2007**, 3**, 130.
48. Tigges, M.; Marquez-Lago, T. T.; Stelling, J.; Fussenegger, M., A tunable synthetic mammalian oscillator. *Nature* 2009**, 457** (7227), 309-12.
49. Tigges, M.; Denervaud, N.; Greber, D.; Stelling, J.; Fussenegger, M., A synthetic low-frequency mammalian oscillator. *Nucleic acids research* 2010**, 38** (8), 2702-11.
50. Simpson, M. L.; Cox, C. D.; Sayler, G. S., Frequency domain analysis of noise in autoregulated gene circuits. *Proceedings of the National Academy of Sciences of the United States of America* 2003**, 100**, 4551-6.
51. Austin, D. W.; Allen, M. S.; McCollum, J. M.; Dar, R. D.; Wilgus, J. R.; Sayler, G. S.; Samatova, N. F.; Cox, C. D.; Simpson, M. L., Gene network shaping of inherent noise spectra. *Nature* 2006**, 439**, 608-11.
52. McGinness, K. E.; Baker, T. a.; Sauer, R. T., Engineering controllable protein degradation. *Molecular cell* 2006**, 22**, 701-7.
53. Banaszynski, L. a.; Chen, L.-C.; Maynard-Smith, L. a.; Ooi, a. G. L.; Wandless, T. J., A rapid, reversible, and tunable method to regulate protein function in living cells using synthetic small molecules. *Cell* 2006**, 126**, 995-1004.
54. Auslander, D.; Fussenegger, M., Optogenetic therapeutic cell implants. *Gastroenterology* 2012**, 143** (2), 301-6.
55. Bacchus, W.; Fussenegger, M., The use of light for engineered control and reprogramming of cellular functions. *Current opinion in biotechnology* 2012**, 23** (5), 695-702.
56. Tabor, J. J.; Levskaya, A.; Voigt, C. A., Multichromatic control of gene expression in *Escherichia coli*. *J Mol Biol* 2011**, 405** (2), 315-24.
57. Antunes, M. S.; Morey, K. J.; Smith, J. J.; Albrecht, K. D.; Bowen, T. A.; Zdunek, J. K.; Troupe, J. F.; Cuneo, M. J.; Webb, C. T.; Hellinga, H. W.; Medford, J. I., Programmable ligand detection system in plants through a synthetic signal transduction pathway. *PLoS One* 2011**, 6** (1), e16292.

58. Thompson, K. E.; Bashor, C. J.; Lim, W. A.; Keating, A. E., SYNZIP protein interaction toolbox: in vitro and in vivo specifications of heterospecific coiled-coil interaction domains. *ACS synthetic biology* 2012**, 1** (4), 118-29.
59. Bashor, C. J.; Horwitz, A. A.; Peisajovich, S. G.; Lim, W. A., Rewiring cells: synthetic biology as a tool to interrogate the organizational principles of living systems. *Annual review of biophysics* 2010**, 39**, 515-37.
60. Bhattacharyya, R. P.; Remenyi, A.; Good, M. C.; Bashor, C. J.; Falick, A. M.; Lim, W. A., The Ste5 scaffold allosterically modulates signaling output of the yeast mating pathway. *Science* 2006**, 311** (5762), 822-6.
61. Deans, T. L.; Cantor, C. R.; Collins, J. J., A tunable genetic switch based on RNAi and repressor proteins for regulating gene expression in mammalian cells. *Cell* 2007**, 130** (2), 363-72.
62. Kramer, B. P.; Viretta, A. U.; Daoud-El-Baba, M.; Aubel, D.; Weber, W.; Fussenegger, M., An engineered epigenetic transgene switch in mammalian cells. *Nat Biotechnol* 2004**, 22** (7), 867-70.
63. Nevozhay, D.; Zal, T.; Balazsi, G., Transferring a synthetic gene circuit from yeast to mammalian cells. *Nature communications* 2013**, 4**, 1451.
64. Duan, F.; Curtis, K. L.; March, J. C., Secretion of insulinotropic proteins by commensal bacteria: rewiring the gut to treat diabetes. *Appl Environ Microbiol* 2008**, 74** (23), 7437-8.
65. Rao, S.; Hu, S.; McHugh, L.; Lueders, K.; Henry, K.; Zhao, Q.; Fekete, R. A.; Kar, S.; Adhya, S.; Hamer, D. H., Toward a live microbial microbicide for HIV: commensal bacteria secreting an HIV fusion inhibitor peptide. *Proc Natl Acad Sci U S A* 2005**, 102** (34), 11993-8.
66. Farrar, M. D.; Whitehead, T. R.; Lan, J.; Dilger, P.; Thorpe, R.; Holland, K. T.; Carding, S. R., Engineering of the gut commensal bacterium Bacteroides ovatus to produce and secrete biologically active murine interleukin-2 in response to xylan. *J Appl Microbiol* 2005**, 98** (5), 1191-7.
67. Xiang, S.; Fruehauf, J.; Li, C. J., Short hairpin RNA-expressing bacteria elicit RNA interference in mammals. *Nat Biotechnol* 2006**, 24** (6), 697-702.
68. Paek, S. H.; Ruder, W. C., Stochastically induced quorum sensing. *Submitted* 2017.
69. Chmielewski, R.; Frank, J., Biofilm formation and control in food processing facilities. *Compr Rev Food Sci Food Saf* 2003**, 2** (1), 22-32.
70. Wood, T. K.; Hong, S. H.; Ma, Q., Engineering biofilm formation and dispersal. *Trends Biotechnol.* 2011**, 29** (2), 87-94.
71. Karimi, A.; Karig, D.; Kumar, A.; Ardekani, A., Interplay of physical mechanisms and biofilm processes: review of microfluidic methods. *Lab on a Chip* 2015**, 15** (1), 23-42.
72. Gao, G.; Lange, D.; Hilpert, K.; Kindrachuk, J.; Zou, Y.; Cheng, J. T.; Kazemzadeh-Narbat, M.; Yu, K.; Wang, R.; Straus, S. K., The biocompatibility and biofilm resistance of implant coatings based on hydrophilic polymer brushes conjugated with antimicrobial peptides. *Biomaterials* 2011**, 32** (16), 3899-3909.
73. Davey, M. E.; O'toole, G. A., Microbial biofilms: from ecology to molecular genetics. *Microbiol. Mol. Biol. Rev.* 2000**, 64** (4), 847-867.
74. Baehni, P.; Takeuchi, Y., Anti-plaque agents in the prevention of biofilm-associated oral diseases. *Oral Dis.* 2003**, 9** (s1), 23-29.
75. Wingender, J.; Neu, T. R.; Flemming, H.-C., *Microbial extracellular polymeric substances: characterization, structure and function*. Springer Science & Business Media: 2012.

76. Weber, M. M.; French, C. L.; Barnes, M. B.; Siegele, D. A.; McLean, R. J., A previously uncharacterized gene, yjfO (bsmA), influences *Escherichia coli* biofilm formation and stress response. *Microbiology* 2010**, 156** (1), 139-147.
77. Wen, Z. T.; Suntharaligham, P.; Cvitkovitch, D. G.; Burne, R. A., Trigger factor in Streptococcus mutans is involved in stress tolerance, competence development, and biofilm formation. *Infection and immunity* 2005**, 73** (1), 219-225.
78. Rachid, S.; Ohlsen, K.; Witte, W.; Hacker, J.; Ziebuhr, W., Effect of subinhibitory antibiotic concentrations on polysaccharide intercellular adhesin expression in biofilm-forming Staphylococcus epidermidis. *Antimicrob. Agents Chemother.* 2000**, 44** (12), 3357-3363.
79. O'Toole, G.; Kaplan, H. B.; Kolter, R., Biofilm formation as microbial development. *Annual Reviews in Microbiology* 2000**, 54** (1), 49-79.
80. Davies, D. G. In *Physiological events in biofilm formation*, Symposia-society for General Microbiology, Cambridge; Cambridge University Press; 1999: 2000; pp 37-52.
81. Patel, R., Biofilms and antimicrobial resistance. *Clin. Orthop. Relat. Res.* 2005**, 437**, 41-47.
82. Helloin, E.; Jänsch, L.; Phan-Thanh, L., Carbon starvation survival of Listeria monocytogenes in planktonic state and in biofilm: a proteomic study. *Proteomics* 2003**, 3** (10), 2052-2064.
83. Webster, N. S.; Smith, L. D.; Heyward, A. J.; Watts, J. E.; Webb, R. I.; Blackall, L. L.; Negri, A. P., Metamorphosis of a scleractinian coral in response to microbial biofilms. *Appl. Environ. Microbiol.* 2004**, 70** (2), 1213-1221.
84. Parsek, M. R.; Greenberg, E., Sociomicrobiology: the connections between quorum sensing and biofilms. *Trends Microbiol.* 2005**, 13** (1), 27-33.
85. Stewart, P. S., Diffusion in biofilms. *J. Bacteriol.* 2003**, 185** (5), 1485-1491.
86. Dunne, W. M., Bacterial adhesion: seen any good biofilms lately? *Clin. Microbiol. Rev.* 2002**, 15** (2), 155-166.
87. Di Bonaventura, G.; Pompilio, A.; Picciani, C.; Iezzi, M.; D'Antonio, D.; Piccolomini, R., Biofilm formation by the emerging fungal pathogen Trichosporon asahii: development, architecture, and antifungal resistance. *Antimicrob. Agents Chemother.* 2006**, 50** (10), 3269-3276.
88. Whitchurch, C. B.; Tolker-Nielsen, T.; Ragas, P. C.; Mattick, J. S., Extracellular DNA required for bacterial biofilm formation. *Science* 2002**, 295** (5559), 1487-1487.
89. Picioreanu, C.; Van Loosdrecht, M. C.; Heijnen, J. J., Two-dimensional model of biofilm detachment caused by internal stress from liquid flow. *Biotechnol. Bioeng.* 2001**, 72** (2), 205-218.
90. Donlan, R. M., Biofilms: microbial life on surfaces. *Emerg. Infect. Dis.* 2002**, 8** (9).
91. De Beer, D.; Stoodley, P.; Roe, F.; Lewandowski, Z., Effects of biofilm structures on oxygen distribution and mass transport. *Biotechnol. Bioeng.* 1994**, 43** (11), 1131-1138.
92. Picioreanu, C.; Van Loosdrecht, M. C.; Heijnen, J. J., Effect of diffusive and convective substrate transport on biofilm structure formation: a two-dimensional modeling study. *Biotechnol. Bioeng.* 2000**, 69** (5), 504-515.
93. Bishop, P. L.; Zhang, T. C.; Fu, Y.-C., Effects of biofilm structure, microbial distributions and mass transport on biodegradation processes. *Water Sci. Technol.* 1995**, 31** (1), 143-152.
94. Bennett, M. R.; Hasty, J., Microfluidic devices for measuring gene network dynamics in single cells. *Nature Rev Genet* 2009**, 10** (9), 628-638.
95. Gravesen, P.; Branebjerg, J.; Jensen, O. S., Microfluidics-a review. *J. Micromech. Microeng.* 1993**, 3** (4), 168.

96. Zheng, Y.; Nguyen, J.; Wei, Y.; Sun, Y., Recent advances in microfluidic techniques for single-cell biophysical characterization. *Lab on a Chip* 2013**, 13** (13), 2464-2483.
97. Zhu, Y.; Fang, Q., Analytical detection techniques for droplet microfluidics—A review. *Anal. Chim. Acta* 2013**, 787**, 24-35.
98. Danino, T.; Mondragón-Palomino, O.; Tsimring, L.; Hasty, J., A synchronized quorum of genetic clocks. *Nature* 2010**, 463** (7279), 326-330.
99. Longo, D.; Hasty, J., Dynamics of single-cell gene expression. *Mol. Syst. Biol.* 2006**, 2** (1), 64.
100. Drescher, K.; Shen, Y.; Bassler, B. L.; Stone, H. A., Biofilm streamers cause catastrophic disruption of flow with consequences for environmental and medical systems. *Proc. Natl. Acad. Sci.* 2013**, 110** (11), 4345-4350.
101. Khalil, A. S.; Collins, J. J., Synthetic biology: applications come of age. *Nature Reviews Genetics* 2010**, 11** (5), 367-379.
102. Litcofsky, K. D.; Afeyan, R. B.; Krom, R. J.; Khalil, A. S.; Collins, J. J., Iterative plug-and-play methodology for constructing and modifying synthetic gene networks. *Nature methods* 2012**, 9** (11), 1077-1080.
103. Shadel, G.; Baldwin, T., The Vibrio fischeri LuxR protein is capable of bidirectional stimulation of transcription and both positive and negative regulation of the luxR gene. *Journal of bacteriology* 1991**, 173** (2), 568-574.
104. Waters, C. M.; Bassler, B. L., Quorum sensing: cell-to-cell communication in bacteria. *Annu. Rev. Cell Dev. Biol.* 2005**, 21**, 319-346.
105. Lopez, D.; Vlamakis, H.; Kolter, R., Generation of multiple cell types in Bacillus subtilis. *FEMS microbiology reviews* 2009**, 33** (1), 152-163.
106. Raj, A.; van Oudenaarden, A., Nature, nurture, or chance: stochastic gene expression and its consequences. *Cell* 2008**, 135** (2), 216-226.
107. Bjedov, I.; Tenaillon, O.; Gerard, B.; Souza, V.; Denamur, E.; Radman, M.; Taddei, F.; Matic, I., Stress-induced mutagenesis in bacteria. *Science* 2003**, 300** (5624), 1404-1409.
108. Marks, L. R.; Reddinger, R. M.; Hakansson, A. P., High levels of genetic recombination during nasopharyngeal carriage and biofilm formation in Streptococcus pneumoniae. *MBio* 2012**, 3** (5), e00200-12.
109. Banas, J. A.; Miller, J. D.; Fuschino, M. E.; Hazlett, K. R.; Toyofuku, W.; Porter, K. A.; Reutzel, S. B.; Florczyk, M. A.; McDonough, K. A.; Michalek, S. M., Evidence that accumulation of mutants in a biofilm reflects natural selection rather than stress-induced adaptive mutation. *Applied and environmental microbiology* 2007**, 73** (1), 357-361.
110. Voigt, C. A., Genetic parts to program bacteria. *Curr. Opin. Biotechnol.* 2006**, 17** (5), 548-557.
111. Gardner, T. S.; Cantor, C. R.; Collins, J. J., Construction of a genetic toggle switch in *Escherichia coli*. *Nature* 2000**, 403** (6767), 339-342.
112. Ruder, W. C.; Lu, T.; Collins, J. J., Synthetic biology moving into the clinic. *Science* 2011**, 333** (6047), 1248-1252.
113. McDaniel, R.; Weiss, R., Advances in synthetic biology: on the path from prototypes to applications. *Curr. Opin. Biotechnol.* 2005**, 16** (4), 476-483.
114. Prigent-Combaret, C.; Brombacher, E.; Vidal, O.; Ambert, A.; Lejeune, P.; Landini, P.; Dorel, C., Complex regulatory network controls initial adhesion and biofilm formation in *Escherichia coli* via regulation of thecsgD gene. *J. Bacteriol.* 2001**, 183** (24), 7213-7223.

115. Fox, E. P.; Bui, C. K.; Nett, J. E.; Hartooni, N.; Mui, M. C.; Andes, D. R.; Nobile, C. J.; Johnson, A. D., An expanded regulatory network temporally controls Candida albicans biofilm formation. *Mol. Microbiol.* 2015**, 96** (6), 1226-1239.
116. Schuster, M.; Greenberg, E. P., A network of networks: quorum-sensing gene regulation in Pseudomonas aeruginosa. *Int. J. Med. Microbiol.* 2006**, 296** (2), 73-81.
117. Ng, W.-L.; Bassler, B. L., Bacterial quorum-sensing network architectures. *Annu. Rev. Genet.* 2009**, 43**, 197-222.
118. Wang, J.; Zhang, J.; Yuan, Z.; Zhou, T., Noise-induced switches in network systems of the genetic toggle switch. *BMC Syst. Biol.* 2007**, 1** (1), 50.
119. Bokes, P.; King, J. R.; Wood, A. T.; Loose, M., Transcriptional bursting diversifies the behaviour of a toggle switch: hybrid simulation of stochastic gene expression. *Bull. Math. Biol.* 2013**, 75** (2), 351-371.
120. Kim, K.-Y.; Wang, J., Potential energy landscape and robustness of a gene regulatory network: toggle switch. *PLoS Comput. Biol.* 2007**, 3** (3), e60.
121. Elowitz, M. B.; Leibler, S., A synthetic oscillatory network of transcriptional regulators. *Nature* 2000**, 403** (6767), 335-338.
122. Brosius, J.; Erfle, M.; Storella, J., Spacing of the-10 and-35 regions in the tac promoter. Effect on its in vivo activity. *Journal of biological chemistry* 1985**, 260** (6), 3539-3541.
123. Vogel, J.; Wagner, E. G. H., Target identification of small noncoding RNAs in bacteria. *Current opinion in microbiology* 2007**, 10** (3), 262-270.
124. Mullineaux, C. W., Bacteria in solitary confinement. *J. Bacteriol.* 2015**, 197** (4), 670-671.
125. Männik, J.; Driessen, R.; Galajda, P.; Keymer, J. E.; Dekker, C., Bacterial growth and motility in sub-micron constrictions. *Proceedings of the National Academy of Sciences* 2009**, 106** (35), 14861-14866.
126. Iyer-Biswas, S.; Wright, C. S.; Henry, J. T.; Lo, K.; Burov, S.; Lin, Y.; Crooks, G. E.; Crosson, S.; Dinner, A. R.; Scherer, N. F., Scaling laws governing stochastic growth and division of single bacterial cells. *Proceedings of the National Academy of Sciences* 2014**, 111** (45), 15912-15917.
127. Halldorsson, S.; Lucumi, E.; Gómez-Sjöberg, R.; Fleming, R. M., Advantages and challenges of microfluidic cell culture in polydimethylsiloxane devices. *Biosens. Bioelectron.* 2015**, 63**, 218-231.
128. Sackmann, E. K.; Fulton, A. L.; Beebe, D. J., The present and future role of microfluidics in biomedical research. *Nature* 2014**, 507** (7491), 181-189.
129. Yao, X.; Jericho, M.; Pink, D.; Beveridge, T., Thickness and elasticity of gram-negative murein sacculi measured by atomic force microscopy. *J. Bacteriol.* 1999**, 181** (22), 6865-6875.
130. Wu, F.; Van Schie, B. G.; Keymer, J. E.; Dekker, C., Symmetry and scale orient Min protein patterns in shaped bacterial sculptures. *Nature nanotechnology* 2015**, 10** (8), 719-726.
131. Männik, J.; Wu, F.; Hol, F. J.; Bisicchia, P.; Sherratt, D. J.; Keymer, J. E.; Dekker, C., Robustness and accuracy of cell division in *Escherichia coli* in diverse cell shapes. *Proceedings of the National Academy of Sciences* 2012**, 109** (18), 6957-6962.
132. Avery, S. V., Microbial cell individuality and the underlying sources of heterogeneity. *Nature Reviews Microbiology* 2006**, 4** (8), 577-587.
133. Davidson, C. J.; Surette, M. G., Individuality in bacteria. *Annu. Rev. Genet.* 2008**, 42**, 253-268.
134. Veening, J.-W.; Smits, W. K.; Kuipers, O. P., Bistability, epigenetics, and bet-hedging in bacteria. *Annu. Rev. Microbiol.* 2008**, 62**, 193-210.

135. Lidstrom, M. E.; Konopka, M. C., The role of physiological heterogeneity in microbial population behavior. *Nat. Chem. Biol.* 2010**, 6** (10), 705-712.
136. Maheshri, N.; O'Shea, E. K., Living with noisy genes: how cells function reliably with inherent variability in gene expression. *Annu. Rev. Biophys. Biomol. Struct.* 2007**, 36**, 413-434.
137. Harper, J. C.; Brozik, S. M.; Brinker, C. J.; Kaehr, B., Biocompatible microfabrication of 3D isolation chambers for targeted confinement of individual cells and their progeny. *Anal. Chem.* 2012**, 84** (21), 8985-8989.
138. Matias, V. R.; Beveridge, T. J., Cryo-electron microscopy reveals native polymeric cell wall structure in Bacillus subtilis 168 and the existence of a periplasmic space. *Mol. Microbiol.* 2005**, 56** (1), 240-251.
139. Koch, A. L., The surface stress theory of microbial morphogenesis. *Adv. Microb. Physiol.* 1983**, 24**, 301-366.
140. Huang, K. C.; Mukhopadhyay, R.; Wen, B.; Gitai, Z.; Wingreen, N. S., Cell shape and cell-wall organization in Gram-negative bacteria. *Proceedings of the National Academy of Sciences* 2008**, 105** (49), 19282-19287.
141. Kulasekara, B. R.; Kamischke, C.; Kulasekara, H. D.; Christen, M.; Wiggins, P. A.; Miller, S. I., c-di-GMP heterogeneity is generated by the chemotaxis machinery to regulate flagellar motility. *Elife* 2013**, 2**, e01402.
142. Sourjik, V.; Wingreen, N. S., Responding to chemical gradients: bacterial chemotaxis. *Curr. Opin. Cell Biol.* 2012**, 24** (2), 262-268.
143. Garrett, T. R.; Bhakoo, M.; Zhang, Z., Bacterial adhesion and biofilms on surfaces. *Prog. Nat. Sci.* 2008**, 18** (9), 1049-1056.
144. Pratt, L. A.; Kolter, R., Genetic analysis of *Escherichia coli* biofilm formation: roles of flagella, motility, chemotaxis and type I pili. *Mol. Microbiol.* 1998**, 30** (2), 285-293.
145. Martí, S.; Rodríguez-Baño, J.; Catel-Ferreira, M.; Jouenne, T.; Vila, J.; Seifert, H.; Dé, E., Biofilm formation at the solid-liquid and air-liquid interfaces by Acinetobacter species. *BMC Res. Notes* 2011**, 4** (1), 5.
146. Trask Jr, O. J.; Davies, A.; Haney, S.; Peng, F.; Hoek, E. M.; Damoiseaux, R., High-content screening for biofilm assays. *Journal of biomolecular screening* 2010**, 15** (7), 748-754.
147. Olson, M. E.; Ceri, H.; Morck, D. W.; Buret, A. G.; Read, R. R., Biofilm bacteria: formation and comparative susceptibility to antibiotics. *Can. J. Vet. Res.* 2002**, 66** (2), 86-92.
148. Flick, D. A.; Gifford, G. E., Comparison of in vitro cell cytotoxic assays for tumor necrosis factor. *J. Immunol. Methods* 1984**, 68** (1-2), 167-175.
149. Stricker, J.; Cookson, S.; Bennett, M. R.; Mather, W. H.; Tsimring, L. S.; Hasty, J., A fast, robust and tunable synthetic gene oscillator. *Nature* 2008**, 456** (7221), 516-519.
150. Kailasapathy, K., Microencapsulation of probiotic bacteria: technology and potential applications. *Curr. Issues Intest. Microbiol.* 2002**, 3** (2), 39-48.
151. Champagne, C. P.; Lacroix, C.; Sodini-Gallot, I., Immobilized cell technologies for the dairy industry. *Crit. Rev. Biotechnol.* 1994**, 14** (2), 109-134.
152. F. Gibbs, S. K., Inteaz Alli, Catherine N. Mulligan, Bernard, Encapsulation in the food industry: a review. *Int. J. Food Sci. Nutr.* 1999**, 50** (3), 213-224.
153. Madene, A.; Jacquot, M.; Scher, J.; Desobry, S., Flavour encapsulation and controlled release–a review. *Int. J. Food Sci. Technol.* 2006**, 41** (1), 1-21.
154. Weitz, M.; Mückl, A.; Kapsner, K.; Berg, R.; Meyer, A.; Simmel, F. C., Communication and computation by bacteria compartmentalized within microemulsion droplets. *J. Am. Chem. Soc.* 2013**, 136** (1), 72-75.

155. Zhang, Y.; Ho, Y.-P.; Chiu, Y.-L.; Chan, H. F.; Chlebina, B.; Schuhmann, T.; You, L.; Leong, K. W., A programmable microenvironment for cellular studies via microfluidics-generated double emulsions. *Biomaterials* 2013**, 34** (19), 4564-4572.
156. Groisman, A.; Lobo, C.; Cho, H.; Campbell, J. K.; Dufour, Y. S.; Stevens, A. M.; Levchenko, A., A microfluidic chemostat for experiments with bacterial and yeast cells. *Nature methods* 2005**, 2** (9), 685-689.
157. Costerton, J. W.; Lewandowski, Z.; Caldwell, D. E.; Korber, D. R.; Lappin-Scott, H. M., Microbial biofilms. *Annu. Rev. Microbiol.* 1995**, 49** (1), 711-745.
158. Rühs, P.; Böcker, L.; Inglis, R.; Fischer, P., Studying bacterial hydrophobicity and biofilm formation at liquid–liquid interfaces through interfacial rheology and pendant drop tensiometry. *Colloids Surf., B.* 2014**, 117**, 174-184.
159. Hoffman, L. R.; D'argenio, D. A.; MacCoss, M. J.; Zhang, Z.; Jones, R. A.; Miller, S. I., Aminoglycoside antibiotics induce bacterial biofilm formation. *Nature* 2005**, 436** (7054), 1171-1175.
160. Macedo, A. J.; Kuhlicke, U.; Neu, T. R.; Timmis, K. N.; Abraham, W.-R., Three stages of a biofilm community developing at the liquid-liquid interface between polychlorinated biphenyls and water. *Appl. Environ. Microbiol.* 2005**, 71** (11), 7301-7309.
161. Miller, M. B.; Bassler, B. L., Quorum sensing in bacteria. *Annu. Rev. Microbiol.* 2001**, 55** (1), 165-199.
162. Pearson, B.; Lau, K. H.; Allen, A.; Barron, J.; Cool, R.; Davis, K.; DeLoache, W.; Feeney, E.; Gordon, A.; Igo, J., Bacterial hash function using DNA-based XOR logic reveals unexpected behavior of the LuxR promoter. *Interdisciplinary Bio Central* 2011**, 3** (3), 10.1-10.8.
163. Fabian, J.-H.; Hartmann, S.; Hamidi, A. In *Analysis of insulation failure modes in high power IGBT modules*, Industry Applications Conference, 2005. Fourtieth IAS Annual Meeting. Conference Record of the 2005, IEEE: 2005; pp 799-805.
164. Niu, X.; Gielen, F.; Edel, J. B., A microdroplet dilutor for high-throughput screening. *Nat. Chem.* 2011**, 3** (6), 437-442.
165. Hiraga, S.; Ichinose, C.; Niki, H.; Yamazoe, M., Cell Cycle–Dependent Duplication and Bidirectional Migration of SeqA-Associated DNA–Protein Complexes in *E. coli*. *Mol. Cell* 1998**, 1** (3), 381-387.
166. Poortinga, A. T.; Bos, R.; Norde, W.; Busscher, H. J., Electric double layer interactions in bacterial adhesion to surfaces. *Surf. Sci. Rep.* 2002**, 47** (1), 1-32.
167. Van Houdt, R.; Michiels, C. W., Biofilm formation and the food industry, a focus on the bacterial outer surface. *J. Appl. Microbiol.* 2010**, 109** (4), 1117-1131.
168. Hoyle, B. D.; Costerton, J. W., Bacterial resistance to antibiotics: the role of biofilms. In *Progress in Drug Research/Fortschritte der Arzneimittelforschung/Progrès des recherches pharmaceutiques*, Springer: 1991; pp 91-105.
169. Lawrence, J.; Korber, D.; Hoyle, B.; Costerton, J.; Caldwell, D., Optical sectioning of microbial biofilms. *J. Bacteriol.* 1991**, 173** (20), 6558-6567.
170. Finlay, B. B.; Falkow, S., Common themes in microbial pathogenicity revisited. *Microbiol. Mol. Biol. Rev.* 1997**, 61** (2), 136-169.